EXPERIMENTALLY GROWN FORAMINIFERA AND THEIR RESPONSE TO HEAVY METAL (ARSENIC, CADMIUM, NICKEL, AND ZINC) CONTAMINATION

by

CHRISTOPHER W. SMITH

(Under the Direction of Susan T. Goldstein)

ABSTRACT

Benthic foraminifera have a long history as environmental indicators of heavy-metal contaminants in marine environments. This study compares the effects of selected heavy metal contaminants (arsenic, cadmium, nickel, and zinc) on benthic foraminifera, grown experimentally from propagules (small juveniles) collected from two coastal sites: Sapelo Island, Georgia, and Little Duck Key, Florida.

Surface sediment was collected from both locations and sieved immediately after collection. The propagules were then used to experimentally grow assemblages with each assemblage exposed to a different heavy metal. The goal here was to compare the effects of these heavy metals on the abundance, diversity, and possible test deformities in benthic foraminifera while also comparing possible different responses of rotalid, miliolid, as well as monothalamid foraminifera. Samples of the two most common species from each location (*Ammonia tepida* (Cushman) and *Haynesina germanica* (Ehrenberg) from Sapelo Island and *Quinqueloculina sabulosa* (Cushman) and *Triloculina oblonga* (Montagu) from Little Duck Key) were then selected for trace element analysis using LA-ICP-MS to quantify possible heavy-metal incorporation among the foraminifera. Finally, additional experimental foraminiferal assemblages were grown under different

temperature and salinity regimes, including intermediate (22°C, 32 psu), elevated temperature (30°C, 32 psu), reduced temperature (18°C, 32 psu), elevated salinity (22°C, 40 psu), and reduced salinity (22°C, 12 psu) in an attempt to identify possible effects of salinity and temperature change on heavy-metal impact on foraminifera.

Increasing concentrations of the trace elements led to decreases in abundance and diversity for the foraminifera. Elevated concentrations above a certain threshold, especially with zinc, resulted in an increase of deformed tests among the foraminifera. However, test deformities did not consistently occur in different salinities and temperatures. Differences exist between the rotalid and miliolid species in their incorporation of the heavy metals. Rotalid species incorporated more cadmium as its concentration in the surrounding water increased, whereas miliolid species incorporated more of the metals zinc and nickel. These results underscore the importance of foraminifera as bioindicators, but also show that several factors, such as interspecific variation and environmental variability must be considered in using foraminifera in pollution studies.

INDEX WORDS: benthic foraminifera, heavy metals, biomonitoring, arsenic, cadmium, nickel, zinc, LA-ICP-MS

EXPERIMENTALLY GROWN FORAMINIFERA AND THEIR RESPONSE TO HEAVY METAL (ARSENIC, CADMIUM, NICKEL, AND ZINC) CONTAMINATION

by

CHRISTOPHER W. SMITH

B.S., University of North Carolina at Chapel Hill, 2011

M.S., Auburn University, 2015

A Dissertation Submitted to the Graduate Faculty of The University of Georgia in Partial Fulfillment of the Requirements for the Degree

DOCTOR OF PHILOSOPHY

ATHENS, GEORGIA

2019

EXPERIMENTALLY GROWN FORAMINIFERA AND THEIR RESPONSE TO HEAVY METAL (ARSENIC, CADMIUM, NICKEL, AND ZINC) CONTAMINATION

by

CHRISTOPHER W. SMITH

Major Professor:	Susan T. Goldstein
Committee:	Steven Holland
	Anthony Rathburn
	Paul A. Schroeder

Electronic Version Approved:

Ron Walcott
Interim Dean of the Graduate School
The University of Georgia
December 2019

DEDICATION

This is for my parents, Wayne and Kathy Smith, my fiancée, Samra Ward, and my supportive friends and family.

ACKNOWLEDGEMENTS

I would first like to thank my advisor Dr. Susan Goldstein providing me with the opportunity to pursue my doctorate at the University of Georgia. I have learned an incalculable amount from Sue in these past four and a half years and I will be forever grateful to her for all that she has taught me about not only foraminifera, but also every single facet of higher education and academia.

I would also like to thank my dissertation committee, Dr. Steven Holland, Dr. Anthony Rathburn, and Dr. Paul Schroeder for all of their help along the way. Steve has always been available with advice on statistical approaches and R coding. It has also been an absolute privilege to take his Data Analysis, Sequence Stratigraphy, and Sapelo Island Geology courses. It is not hyperbole to say that Steve is one of the best teachers I have ever had, and he has been an inspiration and model for me on how I would like to teach in my future career. I have also enjoyed the wealth of comic book movie discussions over the years. Dr. Rathburn has been a key resource for me on foraminifera. While the timing of our meetings through Skype have always been challenging, Tony has always gone out of his way to be available and helpful. Paul has been a great help to me with mineralogy and instrumentation. He has assumed the responsibility of Department Chair this past year and despite that, he has always remained available to me and I sincerely appreciate that. I had the pleasure of taking his Clay Mineralogy course and it proved invaluable when attempting to better understand the Sapelo Island and Little Duck Key sediments.

I also need to thank Dr. Jennifer Fehrenbacher, Dr. Chris Russo, and Theresa Fritz-Endres at Oregon State University for their help with chapter 3 of this dissertation. They were extraordinarily accommodating in my two trips there for LA-ICP-MS analysis. Jennifer was my coauthor on my second paper and her knowledge and experience with using laser ablation on foraminifera were key. Chris was a life saver, particularly with his aid in utilizing the LA-ICP-MS machinery. Theresa helped me greatly with not only cleaning my samples, but also LA-ICP-MS data analysis and management. Thanks also to Dr. John Shields and Dr. Eric Formo of the Georgia Electron Microscopy (GEM) Lab for their aid in electron microscopy and Dr. Sayed Hassan of the University of Georgia Center for Applied Isotope Studies (CAIS) for aid in ICP-MS analysis of residual water samples.

This research was funded by the Joseph A. Cushman Award for Student Research (Cushman Foundation for Foraminiferal Research), the Bernold M. “Bruno” Hanson Memorial Environmental Grant (American Association of Petroleum Geologists Foundation), the Garry Jones and Brian O’Neill Memorial Grant (North American Micropaleontology Section), the Levy Award for Marine Geology, and the Watts-Wheeler Fund (Department of Geology, University of Georgia).

Pursuing a doctorate can be enormously stressful and I would not have made it through without the help of my fellow graduate students. I would like to thank Erik Alberts, Garett Brown, Melanie Callihan, Kelly Cronin, Alex Edwards, Matt Hess, Cullen LaPointe, Pedro Monarrez, Rachel Rotz, Sierra Swenson, Devon Verellen, Kelsey Warden, and Sarah Wright for their friendship, laughs, and group therapy sessions. A special thank you to Cullen for helping me collect samples in the field. Another special

thank you to Pedro for being a constant source of valuable advice and guidance from the second I arrived in Athens. One last special thanks to Garett, Kelly, and Kelsey, for their friendship and for being a sounding board for ideas, problems, and all manner of issues.

I lastly want to thank my friends and family for supporting my long journey to this point. My best friend Cameron VanIderstine has always been available for a chat at times when it seemed like my sanity was ebbing away. I thank him for making me laugh and remember that there is life beyond the classroom. I would also be remiss if I did not thank my fiancée Samra Ward for all of her love and support. There were times that I thought of quitting and I can honestly say that without her, I do not know if I would have made it through. I also want to thank my parents, Wayne and Kathy Smith, for always being there when I needed them no matter what, whether it be a supportive phone call, a thoughtful surprise card in the mail, or even a field assistant on an emergency sampling trip to the Florida Keys.

TABLE OF CONTENTS

Page

LIST OF TABLES

Page

LIST OF FIGURES

Page

CHAPTER 1

INTRODUCTION

Foraminifera as Biomonitors

Environmental change has become one of the key problems of the 21st century. Anthropogenic pollution and its deleterious effect on the environment have become especially important and have been the subject of an enormous upswing in scientific research. Identification of so-called bioindicator species or biomonitors has been one of the cornerstones of this research (James & Evison, 1979; Gerhardt, 2002) Bioindicators are defined as species of organisms that are used to gather important information about the overall ecosystem in which they live (Gerhardt, 2002). Marine protists such as foraminifera are known for their key role in the marine ecosystem and their sensitivity to environmental change, and thus are well suited to acting as bioindicators (Haynes, 1981; Anderson, 1988; Yanko et al., 1999).

Benthic foraminifera have long been used as biomonitors in marine environments (e.g., Alve, 1995; Yanko et al., 1998; Nigam et al., 2006; Martinez-Colon et al., 2009; Martins et al., 2013). They are abundant and diverse in marine settings, making them easy to use and cost effective in environmental studies (Alve, 1995; Yanko et al., 1999). Their effectiveness in this manner primarily derives from their great sensitivity to environmental changes (e.g., Resig, 1960; Schafer, 1970; Boltovskoy & Wright, 1976; Alve, 1991). Foraminifera respond to changes based on a multitude of factors, including temperature, salinity, solubility of CaCO3, water depth, wave action, light intensity,

nutrition, substrate, and dissolved oxygen (e.g., Murray, 1991; Boltovskoy et al., 1991). At first, the effects of sewage pollution on foraminifera were the primary focus of research (Resig, 1960; Watkins, 1961; Bandy et al., 1964; Schafer, 1970; Boltovskoy & Wright, 1976; Alve, 1991), but later, research expanded to include other types of human impacts as well as natural occurrences of contaminants (e.g., Yanko et al., 1994; Scott et al., 2001; McCloskey, 2009; Hart et al., 2014).

The use of foraminifera as environmental monitors centers on documenting and correlating certain foraminiferal characteristics, such as overall abundance, species relative abundances, species diversity, relative abundances of shell types (calcareous perforate, calcareous imperforate, agglutinated, organic), and the occurrence of shell deformities with the presence and abundance of contaminants in the environment (reviewed by Boltovskoy & Wright, 1976; Boltovoskoy et al., 1991; Yanko et al., 1994; 1999; Alve, 1995; Scott et al., 2001; Olugbode et al., 2005; Nigam et al., 2006; Martinez-Colon et al., 2009; Hart et al., 2014). Foraminiferal environmental sensitivity can become a problem when attempting to carry out analysis. It can be difficult to distinguish the effects of various factors on foraminiferal abundance, diversity, and test deformities (Geslin et al., 2000; Lee et al., 2015).

Heavy Metal Contamination

In the context of environmental micropaleontology, the term “heavy metals” is used to describe any metallic element that is potentially toxic (Frontalini & Coccioni, 2008). While they occur naturally, heavy metals are among the most prominent byproducts of anthropogenic pollution, often introduced into marine environments via industrial pollution, agricultural waste, or urban runoff (e.g., Alloway, 2013; Alve, 1991;

Julian II, 2015; Tansel & Rafiuddin, 2016). Heavy metals differ from one another in various important ways, including chemical speciation, solubility, and metabolic utility (Rainbow, 2016). The metabolic utility, or essentiality, of heavy metals relates to their requirement in biological activities (Mertz, 1981; Adriano, 2001; Martinez-Colon et al., 2009; Maret, 2016; Desideri et al., 2016). This topic is controversial as the relative essentiality of some elements is the subject of much debate (Mertz, 1981; Maret, 2016).

Benthic foraminifera have unique potential as indicators for heavy metals, with their abundance and diversity clearly affected by exposure to heavy metals (Boltovoskoy et al., 1991; Yanko et al., 1994; 1999; Alve, 1995; Scott et al., 2001; Olugbode et al., 2005; Nigam et al., 2006; Martinez-Colon et al., 2009; Hart et al., 2014; Brouillette Price et al., 2019). Further, benthic foraminifera have long been known to take up heavy metals from the marine environment and incorporate them into their test structure (e.g., Boyle, 1981; Rosenthal et al., 1997; Dissard et al., 2010a; Dissard et al., 2010b; Munsel et al., 2010; Nardelli et al., 2016; Frontalini et al., 2018). Several factors complicate understanding the relationships between metal occurrences in the environment and benthic foraminifera, including sediment type and the diverse fine structure and test construction of different foraminiferal clades (e.g., Angell, 1979; Angell, 1980; Elderfield et al., 1996; Hansen, 1999; de Noojier et al., 2009a; de Noojier et al., 2009b; de Noojier et al., 2014).

Propagule Method

The propagule method provides a valuable way to better understand the relationship between foraminifera and their surrounding environments. Propagules are juvenile foraminifera collected from sediment samples, which can lay dormant for long

periods of time before eventually maturing under the right conditions (Goldstein & Alve, 2011; Alve & Goldstein, 2014). The propagule method involves growing experimental assemblages of foraminifera in the laboratory from propagules present in the fine sediment (Alve & Goldstein, 2002; 2003; 2010). This allows for control of the environment during foraminiferal growth, including the many factors that can potentially influence foraminiferal assemblages. Using this technique, research studies can be designed that allow better analysis of foraminiferal response to various factors, including the presence of heavy metals in seawater.

Purpose of Study

The purpose of this dissertation is to test the impact of heavy-metal contaminants on benthic foraminifera using the propagule method. The heavy metals chosen for this study include arsenic, cadmium, nickel, and zinc. These metals were selected because they are common heavy-metal contaminants in coastal marine settings and in most cases are known to severely impact marine organisms (Alve, 1995; Neff, 1997; Weber & Casazza, 2006). These metals also represent a spectrum of metabolic function for organisms. Arsenic is a dark gray metalloid that commonly occurs in the –III, 0, III, and V oxidation states (Adriano, 2001). Arsenic, well known for its toxicity in most organisms, was long considered non-essential, but now arsenic is known to have limited metabolic utility (Uthus, 2003; Zeng et al., 2005). Cadmium is a soft white metal that occurs naturally in the II oxidation state, commonly produced as a by-product of zinc refinement (Adriano, 2001). Cadmium is non-essential for almost all living things save for a select organism (e.g. a planktonic diatom) in a special ecological niche (Maret, 2016). Nickel and zinc are both metals that occur in nature commonly in the II state

(Adriano, 2001). Nickel is more essential in plants and bacteria than animals, playing a key role in enzymatic functions and seed germination, while zinc is broadly essential to enzymatic functions in all life (Mertz, 1981; Anke et al., 1984; Poonkothai & Vijayavathi, 2012; Maret, 2016).

Each part of this dissertation involves experimental foraminiferal assemblages and their exposure to these heavy metals in varying concentrations. United States Environmental Protection Agency's National Recommended Water Quality Criteria for Saltwater Criteria Maximum Concentration (CMC) was used to determine how much of each metal should be added to the assemblages. The CMC is the amount of a potentially harmful element that can occur in a marine setting before "resulting in an unacceptable effect" (U.S. EPA, 2006). Using the CMC as a starting point, a group of experimental assemblages were grown with exposure to a range of concentrations for each individual heavy metal.

The propagules for this study were collected from two locations: Sapelo Island, Georgia and Little Duck Key, Florida. Sapelo Island is a tidally dominated barrier island along the southeastern Georgia coast that was selected primarily because of its abundance of several species of rotalid foraminifera (Goldstein & Frey, 1986; Goldstein & Alve, 2011; Brouillette Price et al., 2019). Little Duck Key is a small key located in the middle Florida Keys chosen because of its abundance of miliolid foraminifera (Weinmann & Goldstein, 2016). The dichotomy of foraminifera present in each location allows for effective comparison of the impact of heavy metals on each clade respectively.

The second chapter of this dissertation focuses on the varying concentrations of arsenic, cadmium, nickel, and zinc and how they affect the abundance, diversity, and test

deformities of benthic foraminifera grown from propagules gathered from each location. The specific objectives are to (a) identify and compare different impacts of the selected heavy metals on the assemblages; (b) record the potentially different effects that each heavy metal has on rotalid and miliolid foraminifera; and (c) identify effective bioindicator species for environmental monitoring research.

The third chapter of this dissertation examines the incorporation of heavy metals in the calcite tests of selected benthic foraminifera. This is accomplished using laser ablation inductively coupled plasma mass spectrometry (LA-ICP-MS), which provides concentrations (Me/Ca) of each heavy metal of interest within selected foraminiferal chambers. The objective is to identify differences in incorporation between clades, species, and individuals, including intra-individual variation. Because of the difficulties that often occur when parsing the effect of pollutants on foraminiferal abundance and diversity (e.g., Geslin et al., 2000; 2002; Lee et al., 2015), it is helpful to look at incorporation in foraminifera as an additional biomonitoring tool (Alve, 1995; Yanko et al., 1998; 1999; Nigam et al., 2006; Martinez-Colon et al., 2009; Martins et al., 2013). This information will improve the overall application of foraminifera as bioindicators of heavy-metal pollution.

Finally, the fourth chapter of this dissertation examines the effect of varying salinity and temperature on heavy-metal effects on foraminifera. As mentioned previously, the sensitivity of foraminifera can make distinguishing the effects of multiple factors difficult (e.g., Geslin et al., 2000; 2002; Lee et al., 2015). For foraminifera to be used effectively as bioindicators in natural marine settings, we must better understand how environmental factors can change the effect of pollutants. Foraminifera in higher or

lower salinities or temperatures might be more or less resistant to the impacts of contaminants. Because they caused a higher percentage of test deformities in the previous chapters, nickel and zinc were selected for this study. Abundance, diversity, and potential test deformities were analyzed for experimentally grown foraminifera exposed to nickel and zinc, but this time the salinity and temperature of the growth chamber environment were varied. Five temperature and salinity regime were used: intermediate (22°C, 32 psu), high temperature (30°C, 32 psu), low temperature (18°C, 32 psu), high salinity (22°C, 40 psu), and low salinity (22°C, 12 psu). A better understand of potential nuances of temperature and salinity variation will improve the use of bioindicator foraminifera in the future.

CHAPTER 2

THE EFFECTS OF SELECTED HEAVY METAL ELEMENTS (ARSENIC, CADMIUM, NICKEL, ZINC) ON EXPERIMENTALLY GROWN FORAMINIFERAL ASSEMBLAGES FROM SAPELO ISLAND, GEORGIA AND LITTLE DUCK KEY, FLORIDA, U.S.A.[1]

[1] Smith, C.W., Goldstein, S.T. 2019. Journal of Foraminiferal Research. 49: 303–318. Reprinted here with permission of publisher.

Abstract

Benthic foraminifera are valuable environmental indicators of heavy-metal contaminants in marine environments. To broaden their effectiveness as bioindicators, this study com- pares individually the effects of selected heavy-metal contaminants, including both metabolically essential and non-essential elements, on temperate rotalids and subtropical miliolids, as well as associated monothalamid foraminifera. To accomplish these aims, assemblages of foraminifera were grown experimentally from propagules (small juveniles) collected from two coastal sites: Sapelo Island, Georgia, and Little Duck Key, Florida, that provide an effective comparison between environments and types of foraminifera. Surface sediment was collected from both locations and sieved immediately after collection. Using the propagule method, assemblages of foraminifera were grown in the laboratory from propagules in the sediment samples. Two metabolically essential trace elements, nickel, and zinc, and two non-essential elements, arsenic and cadmium were used to represent both types of heavy metal. Experimental conditions were held constant while varying only the metal concentrations.

In treatments from both origins, increasing concentrations of cadmium, nickel, and zinc led to decreases in abundance and diversity for the foraminifera. In addition, zinc, and to a lesser extent cadmium and nickel above certain concentrations, resulted in an increase of deformed tests among the foraminifera. Deformities occurred amongst the most common calcareous species from Sapelo island: *Ammonia tepida* and *Haynesina germanica*. Fewer deformities were observed in common calcareous species from Little Duck Key, the miliolids *Quinqueloculina sabulosa* and *Quinqueloculina bosciana* featured few deformities. Notably, monothalamid species such as *Psammophaga sapela*

remained present at high metal concentrations. These results support previous research and reinforce the usefulness of rotalids such as *A. tepida* and *H. germanica* as bioindicators of heavy-metal contamination as well as suggesting a possible use of monothalamids such as *P. sapela* in this manner.

Introduction

Benthic foraminifera have a long history as environmental bioindicators of various contaminants in marine and transitional marine settings (e.g., Alve, 1995; Yanko et al., 1998; Nigam et al., 2006; Martinez-Colon et al., 2009; Mar- tins et al., 2013). Specifically, they have been widely applied in research on heavy metals for decades (Alve, 1991; Carnahan et al., 2008; Frontalini & Coccioni, 2008; Brouillette & Goldstein, 2008; Brouillette Price et al., 2019; Foster et al., 2012; Linshy et al., 2013). However, our knowledge of how foraminiferal populations and assemblages are impacted by these heavy metals is limited. For example, uncertainty exists in how essential and non-essential elements affect foraminifera. Essential elements are required in some capacity for metabolism whereas non-essential elements have no metabolic function (Mertz, 1981; Adriano, 2001; Martinez-Colon et al., 2009; Desideri et al., 2016). Could essential elements be more readily bioavailable and thus cause a greater effect on foraminiferal populations? In addition, do miliolid and rotalid foraminifera respond to heavy-metal exposure differently? Previous research has suggested a link between heavy-metal pollution and foraminiferal test deformities (Yanko et al., 1998; Brouillette Price et al., 2019; Foster et al., 2012). Do such deformities occur in all calcareous foraminifera? This study addresses these questions by examining the effects of a suite of heavy-metal contaminants, tested individually, on the abundance, diversity, and potential shell

deformities in experimentally grown assemblages (EGAs) of foraminifera. These EGAs were grown from propagules collected from two shallow-water sites: Sapelo Island, Georgia, and the Little Duck Key, Florida. The in situ foraminiferal assemblages of these two sites are distinct, reflecting environmental and climatic differences (e.g., Weinmann & Goldstein, 2016). The objectives are to (1) identify and compare the different impacts of selected essential and non- essential elements on experimentally grown foraminiferal assemblages, (2) record the potentially different effects that these contaminants have on representative rotalid, miliolid, and monothalamid foraminifera, so that (3) the best bioindicator species for each lineage and location might be identified. As shown in previous research, an ideal bioindicator foraminiferal species will be an easily identifiable one that is clearly affected by heavy-metal contamination, in abundance, diversity, or test structure (Alve, 1991; Carnahan et al., 2008; Carnahan et al., 2009; Frontalini et al., 2009). This study builds on previous work by Brouillette Price et al. (2019), in which EGAs (also from Sapelo Island) of foraminifera were exposed to varying concentrations of cadmium, lead, and zinc. That study found that increased exposure to these metals resulted in decreased abundances and species richness. Exposure to zinc also produced test deformities.

Regional Setting

Sapelo Island (Fig. 2.1A) is a tidally dominated barrier island along the southeastern Georgia coast that contains isolated, rare mudflats (Roychoudhury, 2007). The sampling site, located north of Doboy Sound near the Sapelo Lighthouse on the southern end of the island, is a mudflat adjacent to prominent oyster beds and a low marsh that hosts *Spartina alterniflora* Loisel. The sediment is heterogeneous, consisting

of mostly clays with silt and sand. Surficial mudflat sediments appear brownish gray in color but transition to black a few millimeters below the surface. This black layer is known to be sulfide-rich (Roychoudhury, 2007). The hydrography of Sapelo Island waters is heavily tied to the seasons. Water temperature recorded in the Doboy Sound ranged from just above 10°C in January 2016 to 32°C in August 2016 while salinity ranged from 11 psu in January 2016 to 32 psu in August 2016 (http://gcelter.marsci.uga.edu/, accessed 5 December 2017).

Little Duck Key is a small key located just west of Marathon in the middle Florida Keys (Fig. 2.1B). The sample site is a back-reef area on the southern shore of the key. The sediment is heterogeneous, generally fine calcareous mud with sparse sand and silt sized grains present along with abundant shell debris (Weinmann & Goldstein, 2016). The sediment is whitish gray to light brown, with small intertidal sediment mounds ranging from 20–30 cm in diameter dotting the location. Sparse short blades of *Thalassia* are also present, but most appear to be either dead or in poor condition (Weinmann & Goldstein, 2016). The seasonal variation in hydrography at Little Duck Key is much less pronounced. The water temperature recorded at nearby Vaca Key (15 km away) ranged from 21°C in January 2016 to 32°C in August 2016 while the salinity at nearby Sombrero Key (12 km away) ranged between 29 and 38 psu in 2008 (http://www.ndbc.noaa.gov, Station-IDs VCAF1 and SMKF1).

Materials and Methods

Sediment samples were taken from Sapelo Island (31° 23′ 24.7704″ N81° 17′ 5.8164″ W) and Little Duck Key (24° 40′ 51.114″ N) during the summer of 2016 (Fig. 2.1). At both locations, surface sediment (the upper few mm) was collected within a ~1

square meter area of the mudflat. A 2- liter container was used to gather 1 liter of surface sediment. This sediment was then sieved immediately after collection using 53- and 850-micron stainless steel sieves. The 850- micron sieve removed larger debris such as plant material or gastropod shells and allowed for more efficient sieving of the <53-micron fraction, which was transported back to the University of Georgia and used as the source of propagules.

Using the propagule method (Goldstein & Alve, 2011; Alve & Goldstein, 2014), assemblages of foraminifera were grown in the laboratory from propagules present in the fine sediment (Alve & Goldstein, 2002; 2003; 2010). During growth, experimentally grown assemblages (EGAs) were each exposed to a selected heavy metal that is either essential or non-essential for metabolic functions. Two essential elements, nickel, and zinc, and two non-essential elements, arsenic and cadmium were used. Cadmium, nickel, and zinc were selected because they are among the most common heavy-metal contaminants in coastal marine settings (Alve, 1995). Arsenic was selected because it severely impacts marine organisms (Neff, 1997; Weber & Casazza, 2006; McCloskey, 2009).

The EGAs were grown in 118 mL polypropylene culture containers using the propagule-bearing sediment collected at each location. Each culture container contained 20 mL of the < 53-micron sediment fraction, and 40 mL of Instant Ocean adjusted to the salinity at the time of collection (32 psu for both locations). Following Brouillette (2009), a set concentration of one heavy metal was then added to the mixture in each container. The concentrations added were based upon the United States Environmental Protection Agency's National Recommended Water Quality Criteria for Saltwater Criteria

Maximum Concentration (Ni 0.074 mgL^{-1}; Zn 0.090 mgL^{-1}; As 0.069 mgL^{-1}; and Cd 0.033 mgL^{-1}; see https://www.epa.gov/ wqc/national-recommended-water-quality-criteria-aquatic-life-criteria-table). The Criteria Maximum Concentration (CMC) is the amount of heavy metal that can occur in an aquatic setting briefly before "resulting in an unacceptable effect" (U.S. EPA, 2006). Using the CMC as a starting point, the added concentrations increased by an order of magnitude for four additional levels for a total of five treatments. Heavy metals were added as dissolved chlorides except for arsenic, which was added as a dissolved oxide. Each growth chamber was exposed to a different concentration of each element during growth. Two treatments were made for each concentration level of all five metals along with two controls consisting of solely Instant Ocean, for a total of 104 treatments, 52 from each location.

Starting on May 24, 2016, containers were kept at a constant temperature and illuminated on a 12-hour cycle. The samples from Sapelo Island were incubated at 20°C, while the samples from Little Duck Key were incubated at 24°C. The containers were rotated twice a week in the incubator to provide equal access to the light source. After one month, on June 24, 2016, the containers were harvested by sieving over a 63-micron sieve, and the contents fixed using a 10% formalin mixture, buffered with sodium carbonate to a pH of around 8.0, containing 1 g/L rose Bengal added as a vital stain (Walton, 1952; Murray & Bower, 2000). The salinity and pH of the water in all treatments remained the same (32 psu and 8.1 respectively) as it was pre-experiment.

After approximately one week, the fixative/stain mixture was removed, and samples were rinsed with tap water and preserved in 50% ethanol. The contents were then picked wet for foraminifera, which were identified, and counted. All foraminifera

harvested were counted. In each EGA, complete assemblage abundance and the abundance of individual species were recorded, with stained and non-stained foraminifera noted. Diversity was calculated as species richness (S) and as Fisher's α. Finally, the Berger-Parker index was calculated as a measure of dominance (Berger & Parker, 1970; Hayek et al., 2010; Hayek & Buzas, 2013). Additionally, any shell deformities that occurred were recorded, and standardized as the percentage deformed of the total assemblage. Assemblage abundance was plotted against the heavy-metal concentration in solution of each treatment.

The dissolved heavy-metal concentration in each treatment was measured using ICP-MS at the termination of the experiment (e.g. Brouillette Price et al., 2019). SEM micrographs of the foraminifera were taken using a Zeiss 1450EP SEM (Georgia Electron Microscopy) (Figs. 2.2–2.3). Images were captured of the most abundant species at each location along with examples of deformed tests. Using R software, species abundance was plotted logarithmically against the heavy-metal content of each treatment for the two most common calcareous species at each location, as well as the most common monothalamid at each location (R Core Team 2018). The percentage of deformed tests was also plotted against heavy-metal content when applicable, along with the percentage of deformed tests among certain species.

Results

Cadmium, nickel, and zinc caused a decline in foraminiferal abundance as concentration increased over the CMC in EGAs from both locations. In most cases, this decline was exponential (Fig. 2.4). In the Little Duck Key EGAs, arsenic also caused an exponential decline in foraminiferal abundance as concentration increased over the CMC.

In almost all cases, there were discrepancies between the amount of metal added and the amount measured in solution after the experiment. This is consistent with previous work using these techniques (Brouillette Price et al. 2019). Because of this, the post-experiment measurement was used exclusively throughout. However, in the Sapelo Island EGAs, there were noticeably large discrepancies between the amount of arsenic added and the amount recorded in residual water by ICP-MS after the experiment. For example, in one EGA, 690 mgL^{-1} of arsenic was added to mixture, but only 0.0804 mgL^{-1} of arsenic was detected in the residual water by ICP-MS after the experiment.

The two most abundant calcareous species in the EGAs from Sapelo Island were *Haynesina germanica* (Ehrenberg) and *Ammonia tepida* (Cushman) (Fig. 2.2), while the two most abundant calcareous species in the EGAs from Little Duck Key were *Quinqueloculina sabulosa* Cushman and *Quinqueloculina bosciana* d'Orbigny (Fig. 2.3). The abundance of all four species declined in response to increased concentrations of cadmium, nickel, and zinc, yet were among the hardiest calcareous species, as they grew even at higher concentrations (Figs. 2.5–2.6). In addition, the abundance of both *Q. sabulosa* and *Q. bosciana* declined in response to increased arsenic in the Little Duck Key EGAs (Fig. 2.6).

The most abundant monothalamid species in the EGAs from Sapelo Island was *Psammophaga sapela* Altin-Ballero, Habura, Goldstein (Fig. 2.2) and from Little Duck Key was *Ovammina opaca* Dahlgren (Fig. 2.3) though this species also grew in the Sapelo EGAs. For the most part, *P. sapela* remained present as heavy-metal concentrations of cadmium, nickel, and zinc increased (Fig. 2.7). While abundance declined in response to higher concentrations of cadmium and zinc, *P. sapela* was still

present at extremely high concentrations of both metals. Species abundance even appeared to increase slightly in response to elevated nickel concentrations. In contrast, the species abundance of *O. opaca* decreased exponentially as heavy-metal concentrations of arsenic, cadmium, nickel, and zinc increased (Fig. 2.7), more similar to the trends seen with calcareous species.

Test deformities occurred in EGAs exposed to all five metals (Tables 2.1 and 2.2), but only occurred in consistently high percentages with a large sample size in Sapelo Island EGAs exposed to zinc (Fig. 2.8). The percentage of deformed tests in these Sapelo Island EGAs spikes heavily at zinc concentrations of 0.0597 and 0.0545 mgL^{-1} respectively, reaching 37% and 51% respectively (Table 2.1). In addition, the vast majority of deformed tests belonged to the rotalid species *Ammonia tepida* and *Haynesina germanica*, with no deformed tests recorded among miliolids or monothalamids (Fig. 2.9).

Diversity of the assemblages, when measured in species richness, tended to decrease as cadmium, nickel, and zinc concentrations increased at both locations (Tables 2.1 and 2.2). In the Sapelo Island EGAs, species richness decreased at cadmium concentrations above 149 mgL^{-1}, nickel concentrations above 0.4094 mgL^{-1}, and zinc concentrations above 0.0545 mgL^{-1}. In the Little Duck Key EGAs, species richness decreased at cadmium concentrations above 0.148 mgL^{-1}, nickel concentrations above 0.4075 mgL^{-1}, and zinc concentrations above 0.263 mgL^{-1}. Species richness also decreased in response to arsenic concentrations above 5.512 mgL^{-1} in the Little Duck Key EGAs. When measured in Fisher's α, this decrease in diversity is not as consistent, with diversity increasing in some cases in response to larger concentrations of cadmium

(182 mgL^{-1} in the Sapelo Island EGAs; 0.137 mgL^{-1} in the Little Duck Key EGAs), nickel (0.4094 mgL^{-1} in the Sapelo Island EGAs; 0.5585 mgL^{-1} in the Little Duck Key EGAs), and zinc (4.14 mgL^{-1} in the Sapelo Island EGAs; 0.221 mgL^{-1} in the Little Duck Key EGAs) at both locations. In contrast, dominance tended to increase as cadmium (149 mgL^{-1}), nickel (1.2794 mgL^{-1}), and zinc (4.14 mgL^{-1}) concentrations increased in Sapelo Island EGAs. This was especially true of the Sapelo Island EGAs where *Psammophaga sapela* tended to be the sole remaining species at the highest concentrations (Table 2.1). In the Little Duck Key EGAs, dominance increases at higher concentrations of the metals at first, but then decreases as abundances decline at the largest concentrations of arsenic, cadmium, nickel, and zinc.

Discussion

Because of their sensitivity to environmental changes, foraminifera have been used in pollution research for decades (e.g., Alve, 1995; Yanko et al., 1998; Nigam et al., 2006; Martinez-Colon et al., 2009; Martins et al., 2013). Historically, the use of foraminifera as bioindicators began with documenting and correlating certain foraminiferal characteristics, such as overall abundance, species relative abundances, species diversity, relative abundances of shell types (calcareous perforate, calcareous imperforate, agglutinated, organic), and the occurrence of shell deformities with the presence and abundance of contaminants in the environment (reviewed by Boltovoskoy et al., 1991; Boltovskoy & Wright, 1976; Yanko et al., 1994; 1999; Alve, 1995; Scott et al., 2001; Olugbode et al., 2005; Nigam et al., 2006; Martinez-Colon et al., 2009; Hart et al., 2014; Mar- tins et al., 2018). While at first the effects of sewage pollution on foraminifera were the initial focus (Resig, 1960; Watkins, 1961; Bandy et al., 1964;

Schafer, 1970; Boltovskoy & Wright, 1976; Alve, 1991), later the list expanded to include all manner of human impacts as well as natural occurrences of heavy metals (e.g., Yanko et al., 1994; Scott et al., 2001; Hart et al., 2014; Martins et al., 2018).

The very sensitivity that makes foraminifera so valuable can also prove to be a detriment in some cases. Distinguishing the effects of pollution from responses to naturally fluctuating environmental conditions can prove difficult (e.g. Geslin et al., 2000; Lee et al., 2015). Foraminiferal assemblages have been shown to change based on a multitude of factors, including temperature, salinity, solubility of CaCO3, water depth, wave action, light intensity, nutrition, substrate, and dissolved oxygen (e.g., Boltovskoy et al., 1991). The propagule method provides a helpful avenue around this complication by allowing experimental control of the foraminiferal growth environment and parsing of the effects of various factors on foraminiferal assemblages (Alve & Goldstein, 2002, 2003, 2010, 2014; Goldstein & Alve, 2011; Duffield et al., 2014, 2015; Brouillette Price et al., 2019).

The lower population densities and diversities in response to heavy-metal treatments seen in this study are consistent with previous field-based studies (Alve, 1995; Yanko et al., 1998; Linshy et al., 2013; Brouillette Price et al., 2019). As concentrations of cadmium, nickel, and zinc increase, the overall abundance, species abundance, and diversity decreased, for the most part in an exponential pattern in both the Sapelo Island and Little Duck Key EGAs. Arsenic caused a similar pattern in the Little Duck Key EGAs. This matches closely the pattern observed in previous work done on Sapelo Island foraminiferal EGAs (Brouillette Price et al., 2019).

Bioavailability, an important factor to consider, is the potential of living organisms to take up elements either from food or the environment (Adriano, 2001; Rainbow, 2007). Dissolved substances in solution tend to be more bioavailable than solids (Traina & Laperche, 1999). ICP-MS showed that each metal persisted in solution at the conclusion of the experiment. Consequently, foraminifera grown in this study were exposed to a single dissolved metal in solution for a month of growth time. Adsorption of metals onto the sediment and even the container wall probably occurred, making these metals less bioavailable to most foraminifera. However, some foraminifera are deposit feeders, which means the metal adsorbed could still be bioavailable to deposit feeding species. Nevertheless, it was vital that we measure the metal content in solution post-experiment rather than immediately upon addition of the metal content to better reflect the bioavailable concentration of the metals.

Both essential and non-essential elements can be taken up metabolically (Rainbow, 2007). However, our results show no discernable differences in the effects of essential and non-essential elements on abundance or diversity. Zinc and nickel, both metals that occur in nature commonly in the II state, are essential elements for all organisms due to their key role in various enzymatic functions (Adriano, 2001; Martinez-Colon et al., 2009). Arsenic, a metalloid that commonly occurs in the –III, 0, III, and V oxidation states, and cadmium, a soft metal that occurs naturally in the II oxidation state, are both considered non-essential, with no known metabolic function (Adriano, 2001; Martinez-Colon et al., 2009; Desideri et al., 2016). However, it should be noted that arsenic may have some use in the microbial metabolism (Nielsen, 1998; Tawfik & Viola, 2011). Despite their varying use in metabolic processes, all of these metals, essential and

non-essential, caused the same negative effects on abundance and diversity of foraminiferal assemblages (Figs. 2.4–2.5). Metals, regardless of essentiality, can be toxic at high concentrations (Rainbow, 2007).

Unlike the Little Duck Key EGAs, there was no discernable pattern to the effect of arsenic on the Sapelo Island EGAs (Fig. 2.4). This reflects a disparity between the amount of arsenic initially added in each treatment and the amount measured via ICP-MS after the experiment. It should be noted that in all cases, the amount of heavy-metal content measured post-experiment was substantially less than the amount added (Tables 2.1 and 2.2). This has occurred in previous studies of this type as well and could be a result of several factors, including adsorption of metal to the polypropylene container or supersaturation of metal in extremely high concentrations (Brouillette Price et al., 2019). Despite this, in most cases, the metal content measured still proved effective as a tool of comparison. The exceptions were the Sapelo Island treatments exposed to arsenic, where the discrepancy between metal added and measured was especially striking. The most likely explanation for this discrepancy lies in the differences between the sediments at the two sampling locations. Arsenic is more likely to be adsorbed in the clay-rich Sapelo Island sediment, resulting in lower concentrations in the residual water. Arsenic was added as As3+, which is commonly adsorbed by clays in environments like Sapelo Island (Ladeira et al., 2004; Roychoudhury, 2007), whereas the other elements that were added had a +2 charge. Additionally, arsenic is commonly adsorbed by the iron mineral goethite, which exists in considerable quantities in Sapelo island sediments (Ladeira et al., 2004; Roychoudhury, 2007). A similar effect has been shown in experiments

involving lead, where a decrease in lead concentration of the water is mirrored by the corresponding increase in concentration of lead in the sediment (Frontalini et al., 2018).

In contrast to other factors, the connection between heavy-metal contaminants and abnormal tests can be much more tenuous. Numerous studies have reported a connection between pollution and test abnormalities (e.g., Alve, 1995; Yanko et al., 1998; Nigam et al., 2006; Weber & Casazza, 2006; Martinez-Colon et al., 2009; Hart et al., 2014; Abu-Zied et al., 2016). There is also evidence suggesting that abnormalities could be explained by the stress of natural fluctuations in temperature, salinity, sediment movement, and dissolved oxygen (Locklin & Maddocks, 1982). Abnormal tests can make up more than 50% of the individuals grown in hypersaline conditions as opposed to just 1% in normal conditions (Stouff, 1998; Geslin et al., 2000; Lee et al., 2015). This is another situation where the propagule method proves invaluable in analysis of effects on foraminiferal assemblages. In this study as well as previous propagule experiments on Sapelo Island foraminifera, test deformities in response to zinc are common (Brouillette Price et al. 2019). However, the deformities become numerous well below the CMC of zinc (0.09 mgL^{-1}). Only zinc caused substantial (~50%) deformities in this study, and while this is supported by Brouillette Price et al. (2019) and others (Stubbles et al., 1996; Stubbles, 1999; Hart et al., 2014), a field study by Weber and Casazza (2006), however, reported a significant correlation between high concentrations of arsenic and test deformation. No such correlation was found in this current study. In addition, no connection between zinc and test abnormalities appeared in EGAs from Little Duck Key. Because miliolids were more common in Little Duck Key EGAs, this could reflect fundamental differences in test morphogenesis and calcification between miliolids and

rotalids (e.g., Angell, 1979; Angell, 1980; Elderfield et al., 1996; Erez, 2003; de Noojier et al., 2014).

Notably, the vast majority of deformed tests seen in this study belonged to rotalids. Previous research on this is mixed. Nardelli et al. (2013) reported that specimens of the species *Pseudotriloculina rotunda* grew new chambers more slowly when exposed to high concentrations of zinc, however they found no evidence of test deformities. In contrast, in propagule experiments, increased exposure to zinc resulted in a decrease in abundance and species diversity as well as test deformity (Brouillette Price et al., 2019). *Ammonia tepida* and *Haynesina germanica* were particularly prone to deformed test morphologies with exposure to elevated concentrations of zinc (Brouillette Price et al., 2019). The lack of deformed miliolids in the Little Duck Key EGAs is notable, because previous research has reported that miliolid test deformities can occur in response to increased heavy-metal concentrations (e.g. Yanko et al., 1998; Brouillette Price et al., 2019).

In the Sapelo Island EGAs, *Psammophaga sapela* showed remarkable stability in high-concentrations of all five heavy metals. This is in contrast with previous work by Brouillette Price et al. (2019) where *P. sapela* was not present in the highest concentrations of metals such as cadmium, lead, and zinc. Like other species of this genus, *P. sapela* ingests mineral grains and retains them within the cell body (Altin-Ballero et al., 2013). X-ray diffraction indicates that this species prefers heavy minerals such as anatase, ilmenite, orthoclase, zircon, basaluminite, pseudobrookite, and pyrrhotite; quartz, which is considerably abundant in the Sapelo Island environment, was almost entirely absent from the *P. sapela* cell body (Altin-Ballero et al., 2013). This

preference for heavier minerals may explain the resistance of *P. sapela* to the heavy-metal treatments used in this study. In contrast, *Ovammina opaca*, the most common monothalamid in the Little Duck Key EGAs, lacking any such mineral ingestion habit, revealed a severe population decline as heavy-metal concentration increased.

Conclusions

Arsenic, cadmium, nickel, and zinc each has a profoundly negative effect on foraminiferal population abundance and diversity at concentrations above the U.S. EPA's Criteria Maximum Concentration. There is no discernable difference between essential and non-essential elements in their effects on the foraminiferal assemblages from both locations.

The most common calcareous species from each location (*Haynesina germanica* and *Ammonia tepida* at Sapelo Island and *Quinqueloculina sabulosa* and *Q. bosciana* at Little Duck Key), while steadily declining as arsenic, cadmium, nickel, and zinc concentrations increased, persisted even at the greater concentrations, making them usable as bioindicators for each location respectively. In the Sapelo Island EGAs, at the highest heavy-metal concentrations, the last foraminiferal species present was usually *Psammophaga sapela*. Because it seemed to be significantly less affected by heavy-metal contamination, *P. sapela* could be an even more effective bioindicator than the common calcareous species at Sapelo Island.

Zinc was more likely to cause major test deformities than arsenic, cadmium, and nickel. Whereas rotalid species such as *Ammonia tepida* and *Haynesina germanica* were more susceptible to test deformities than miliolid foraminifera, specifically in response to

increasing zinc contamination in Sapelo Island EGAs, the comparative lack of deformities seen in the Little Duck Key EGAs indicates a more complicated picture.

Tables

Table 2.1. Diversity data, including number of specimens (N), number of species (S), Fisher's α, Berger-Parker Index, and the percentage of deformed tests for the assemblages grown from Sapelo Island propagules. The symbol N/A denotes an undetectable value.

Sapelo Island							
Expected (mgL^{-1})	**Actual (mgL^{-1})**	***N***	***S***	**Fisher's α**	**Berger-Parker**	**Deformities**	**Percent Deformed**
Arsenic							
(A) 0.069	0.0434	44	11	4.71	0.27	0	0.0%
(B) 0.069	0.1282	75	10	3.10	0.31	2	2. 7%
(A) 0.69	0.0612	284	10	2.02	0.52	3	1.1%
(B) 0.69	0.058	124	10	2.56	0.35	3	2.4%
(A) 6.9	0.0512	177	11	2.59	0.22	3	1.7%
(B) 6.9	0.0538	141	10	2.46	0.37	0	0.0%
(A) 69	0.059	160	9	2.06	0.23	2	1.3%
(B) 69	0.0576	148	10	2.42	0.26	0	0.0%
(A) 690	0.0804	149	7	1.52	0.34	6	4.0%
(B) 690	0.0992	121	8	1.92	0.31	8	6.6%
Cadmium							
(A) 0.04	3.43	156	9	2.08	0.29	0	0.0%
(B) 0.04	3.45	181	7	1.45	0.27	2	1.1%
(A) 0.4	4.34	101	11	3.14	0.22	3	3.0%
(B) 0.4	0.532	210	10	2.18	0.22	0	0.0%
(A) 4	149	29	5	1.74	0.48	0	0.0%
(B) 4	182	27	6	2.39	0.67	0	0.0%
(A) 40	149	37	5	1.56	0.51	5	13.6%
(B) 40	182	31	4	1.22	0.84	0	0.0%
(A) 400	508	15	3	1.12	0.87	1	6.7%
(B) 400	566	4	3	5.45	0.50	1	25.0%
Nickel							
(A) 0.074	0.011	215	11	2.45	0.28	2	0.9%
(B) 0.074	0.0097	187	11	2.55	0.34	2	1.1%
(A) 0.74	0.009	71	9	2.73	0.38	0	0.0%
(B) 0.74	0.0087	125	10	2.55	0.48	4	3.2%
(A) 7.4	0.0106	102	9	2.38	0.36	2	2.0%
(B) 7.4	0.002096	46	9	3.34	0.30	0	0.0%
(A) 74	0.4094	7	4	3.87	0.43	0	0.0%
(B) 74	0.03438	117	10	2.62	0.26	11	9.4%
(A) 740	1.2794	16	4	1.71	0.56	1	6.3%
(B) 740	1.819	8	2	0.85	0.75	0	0.0%
Zinc							

(A) 0.09	0.0195	60	10	3.43	0.42	1	1.7%
(B) 0.09	0.0354	77	8	2.24	0.35	4	5.2%
(A) 0.9	0.0188	135	10	2.49	0.36	26	19.3%
(B) 0.9	0.0165	208	11	2.47	0.25	16	7.7%
(A) 9	0.0597	57	5	1.32	0.37	21	36.8%
(B) 9	0.0545	101	5	1.10	0.46	51	50.5%
(A) 90	11.4	1	1	NA	1.00	0	0.0%
(B) 90	4.14	6	3	2.39	0.67	0	0.0%
(A) 900	328	4	2	1.59	0.50	0	0.0%
(B) 900	246	6	2	1.05	0.67	0	0.0%
Control							
A		218	10	2.16		0.27	0.0%
B		173	10	2.31		0.27	0.0%

Table 2.2. Diversity data, including number of specimens (N), number of species (S), Fisher's α, Berger-Parker Index, and the percentage of deformed tests for the assemblages grown from Little Duck Key propagules. The symbol N/A denotes an undetectable value.

Little Duck Key							
Expected (mgL^{-1})	**Actual (mgL^{-1})**	***N***	***S***	**Fisher's α**	**Berger-Parker**	**Deformities**	**Percent Deformed**
Arsenic							
(A) 0.069	0.116	113	16	5.09	0.34	0	0.0%
(B) 0.069	0.298	121	12	3.31	0.54	0	0.0%
(A) 0.69	0.116	95	12	3.64	0.43	1	1.1%
(B) 0.69	0.147	56	7	2.11	0.54	0	0.0%
(A) 6.9	0.224	107	14	4.30	0.26	0	0.0%
(B) 6.9	0.214	104	13	3.92	0.46	2	1.9%
(A) 69	6.082	2	2	NA	0.50	0	0.0%
(B) 69	5.512	22	5	2.02	0.41	0	0.0%
(A) 690	57.062	3	3	NA	0.33	0	0.0%
(B) 690	51.562	31	12	7.17	0.26	6	19.4%
Cadmium							
(A) 0.04	0.00108	74	15	5.68	0.19	0	0.0%
(B) 0.04	0.00017	145	13	3.46	0.28	0	0.0%
(A) 0.4	0.0119	101	11	3.14	0.36	0	0.0%
(B) 0.4	0.0157	113	12	3.39	0.49	2	1.8%
(A) 4	0.148	56	5	1.33	0.89	0	0.0%
(B) 4	0.05	57	9	3.01	0.23	1	1.8%
(A) 40	0.137	46	15	7.74	0.24	5	10.9%
(B) 40	0.146	23	12	10.12	0.26	2	8.7%
(A) 400	1.08	5	3	3.16	0.40	0	0.0%
(B) 400	1.35	4	3	5.45	0.50	2	50.0%
Nickel							
(A) 0.074	0.0063	168	14	3.63	0.17	1	0.6%
(B) 0.074	0.0096	102	10	2.75	0.30	0	0.0%
(A) 0.74	0.0086	166	12	2.97	0.45	0	0.0%
(B) 0.74	0.0093	102	11	3.13	0.19	1	1.0%
(A) 7.4	0.0535	25	9	5.04	0.32	1	4.0%
(B) 7.4	0.03559	73	9	2.70	0.22	0	0.0%
(A) 74	0.5585	4	3	5.45	0.50	1	25.0%
(B) 74	0.4075	17	5	2.39	0.35	7	41.2%
(A) 740	3.2585	7	4	3.87	0.29	0	0.0%
(B) 740	0.9765	6	4	5.24	0.50	1	16.7%
Zinc							
(A) 0.09	0.0219	142	13	3.48	0.23	0	0.0%

(B) 0.09	0.0262	132	13	3.58	0.53	0	0.0%
(A) 0.9	0.0244	123	15	4.48	0.28	0	0.0%
(B) 0.9	0.0239	109	12	3.44	0.35	2	1.8%
(A) 9	0.0321	105	12	3.49	0.33	1	1.0%
(B) 9	0.0425	109	10	2.68	0.38	1	0.9%
(A) 90	0.263	5	5	NA	0.20	0	0.0%
(B) 90	0.221	28	10	5.56	0.29	4	14.3%
(A) 900	3.61	6	4	5.24	0.50	0	0.0%
(B) 900	6.09	14	5	2.78	0.29	3	21.4%
Control							
A		107	12	3.47	0.40	0	0.0%
B		123	16	4.91	0.24	0	0.0%

Figures

Figure 2.1. Aerial views of the sampling sites in both study areas: **A** Sapelo Island, Georgia (31° 23' 24.7704" N81° 17' 5.8164" W), and **B** Little Duck Key, Florida (24° 40' 51.114" N) (Google Earth).

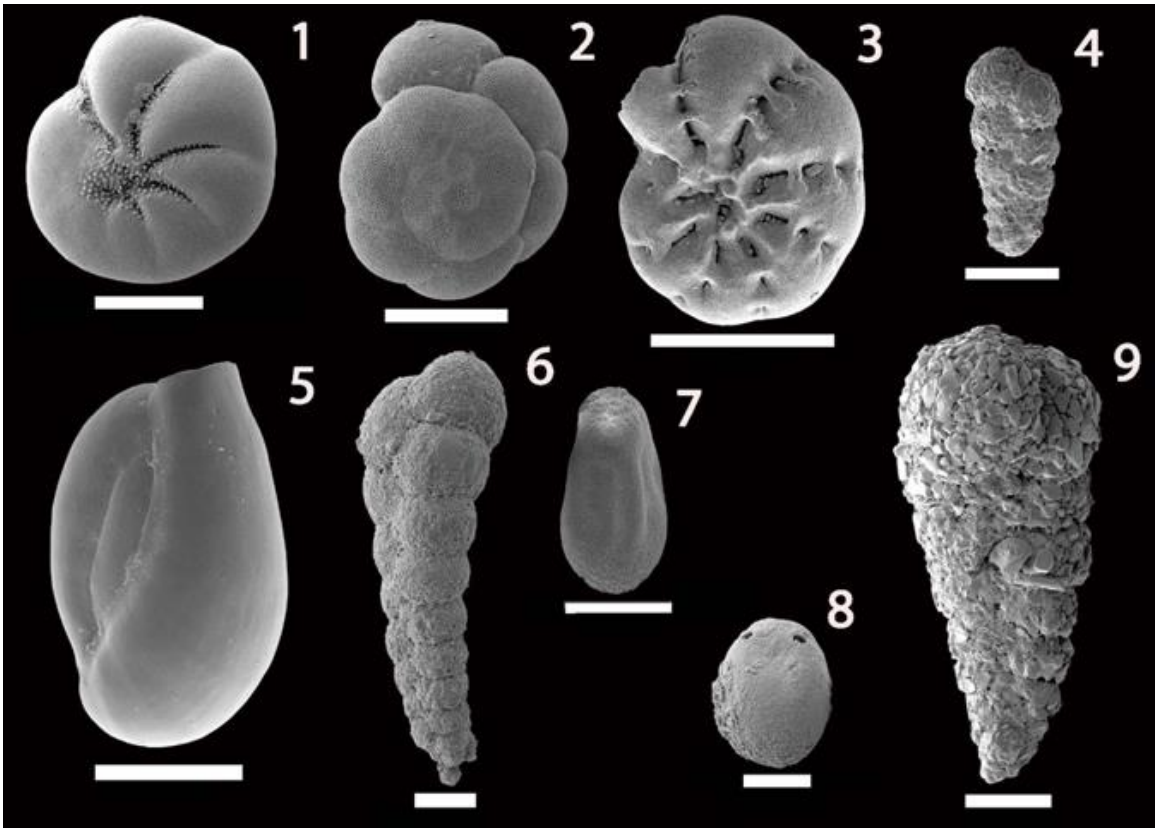

Figure 2.2. SEM micrographs of the most common foraminifera species found in the assemblages grown from Sapelo Island propagules: **1** *Haynesina germanica* (Ehrenberg), **2** *Ammonia tepida* (Cushman), **3** *Elphidium excavatum* (Terquem), **4** *Textularia earlandi* (Parker), **5** *Quinqueloculina dimidiata* (Terquem), **6** *Textularia palustris* (Warren), **7** *Psammophaga sapela* (Altin-Ballero, Habura, and Goldstein), **8** *Ovammina opaca* (Dahlgren), **9** *Textularia pseudogramen* (Chapman & Parr). All scale bars = 100 μm.

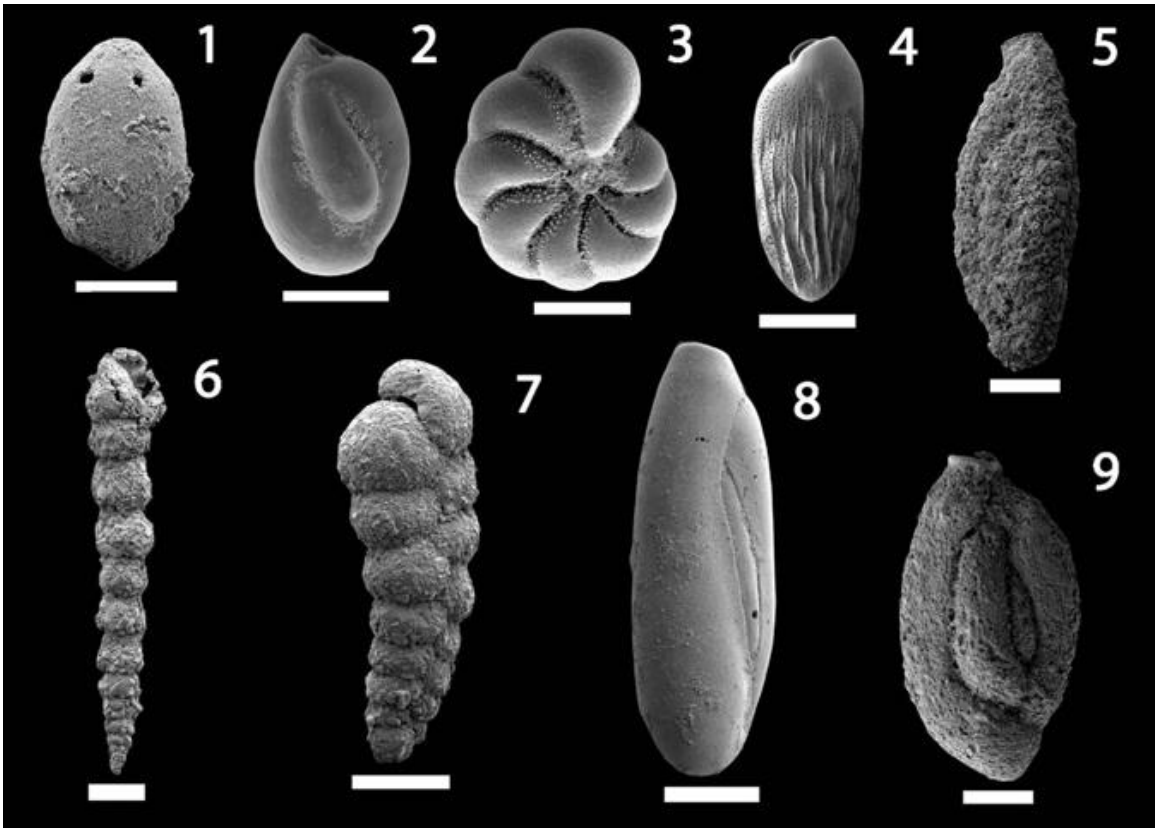

Figure 2.3. SEM micrographs of the most common foraminifera species found in the assemblages grown from Little Duck Key propagules: **1** *Ovammina opaca* (Dahlgren), **2** *Quinqueloculina dimidiata* (Terquem), **3** *Elphidium mexicanum* (Kornfeld), **4** *Bolivina striatula* (Cushman), **5** *Quinqueloculina sabulosa* (Cushman), **6** *Reophax gaussicus* (Rhumbler), **7** *Textularia earlandi* (Parker), **8** *Quinqueloculina bosciana* (d'Orbigney), **9** *Quinqueloculina agglutinans* (d'Orbigney). All scale bars = 100 μm.

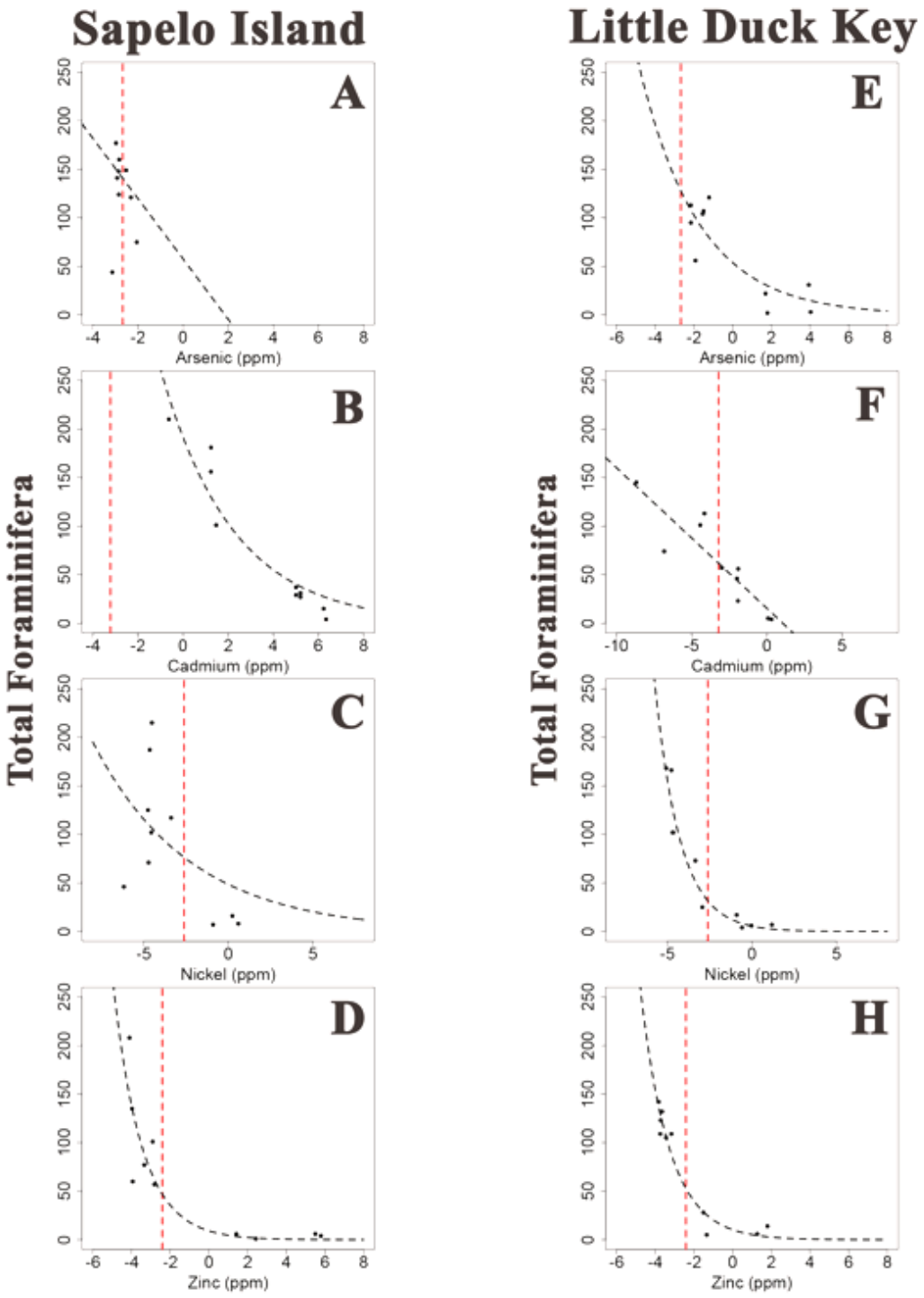

Figure 2.4. Entire foraminiferal abundance in response to the natural log of the concentration of a specific heavy metal: Sapelo Island (left), **A** arsenic, **B** cadmium, **C** nickel, and **D** zinc, and Little Duck Key (right), **E** arsenic, **F** cadmium, **G** nickel, and **H** zinc. The vertical dashed lines indicate the U.S. EPA's CMC (Criteria Maximum Concentration) of each respective metal. The curved and diagonal dashed lines represent the exponential regression line.

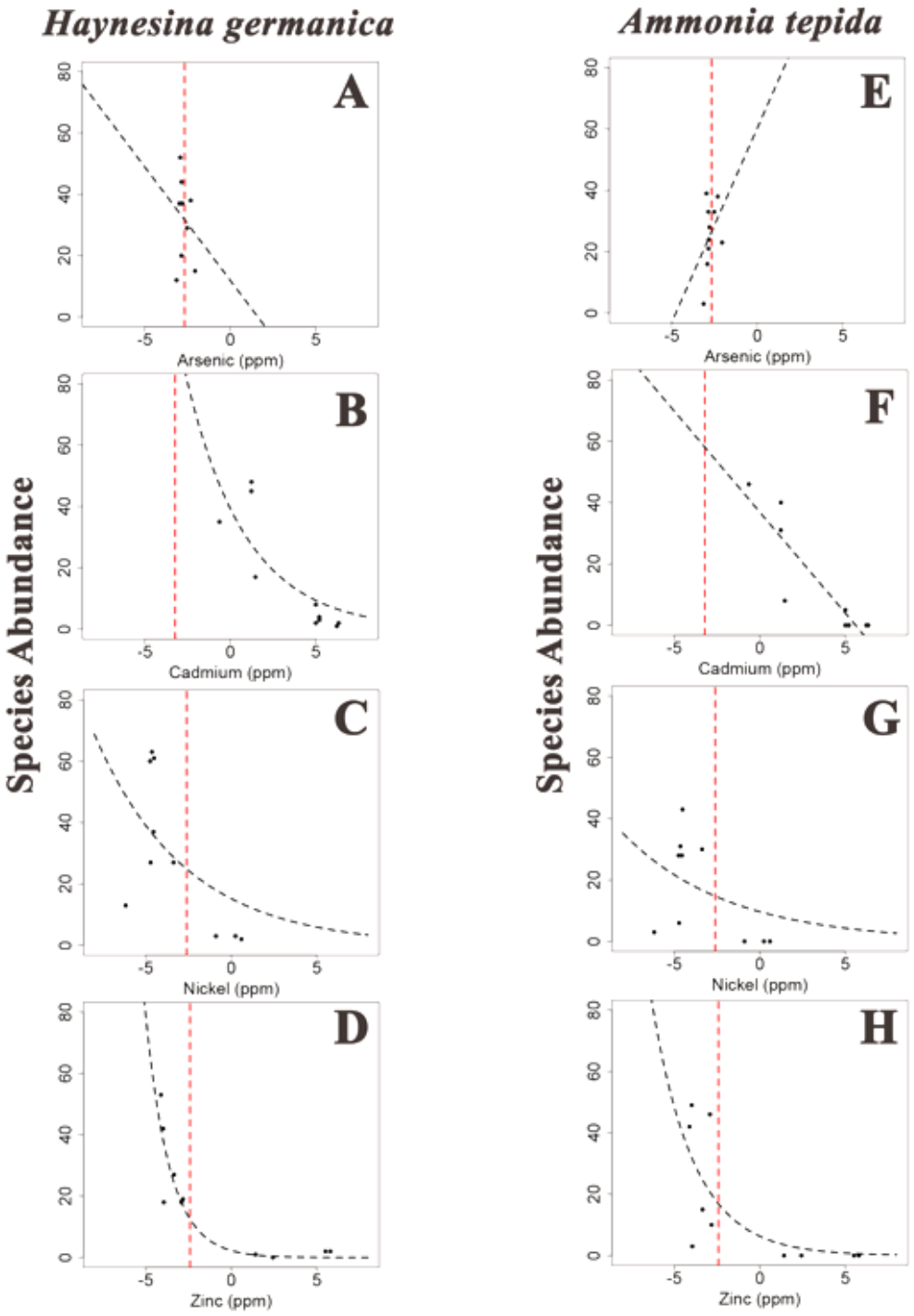

Figure 2.5. Abundance of *Haynesina germanica* (left) in response to the natural log of the concentration of a specific heavy metal: **A** arsenic, **B** cadmium, **C** nickel, and **D** zinc. Abundance of *Ammonia tepida* (right) in response to the natural log of the concentration of a specific heavy metal: **E** arsenic, **F** cadmium, **G** nickel, and **H** zinc. These were grown from propagules collected at Sapelo Island. The vertical dashed lines indicate the U.S. EPA's CMC (Criteria Maximum Concentration) of each respective metal. The curved and diagonal dashed lines represent the exponential regression line.

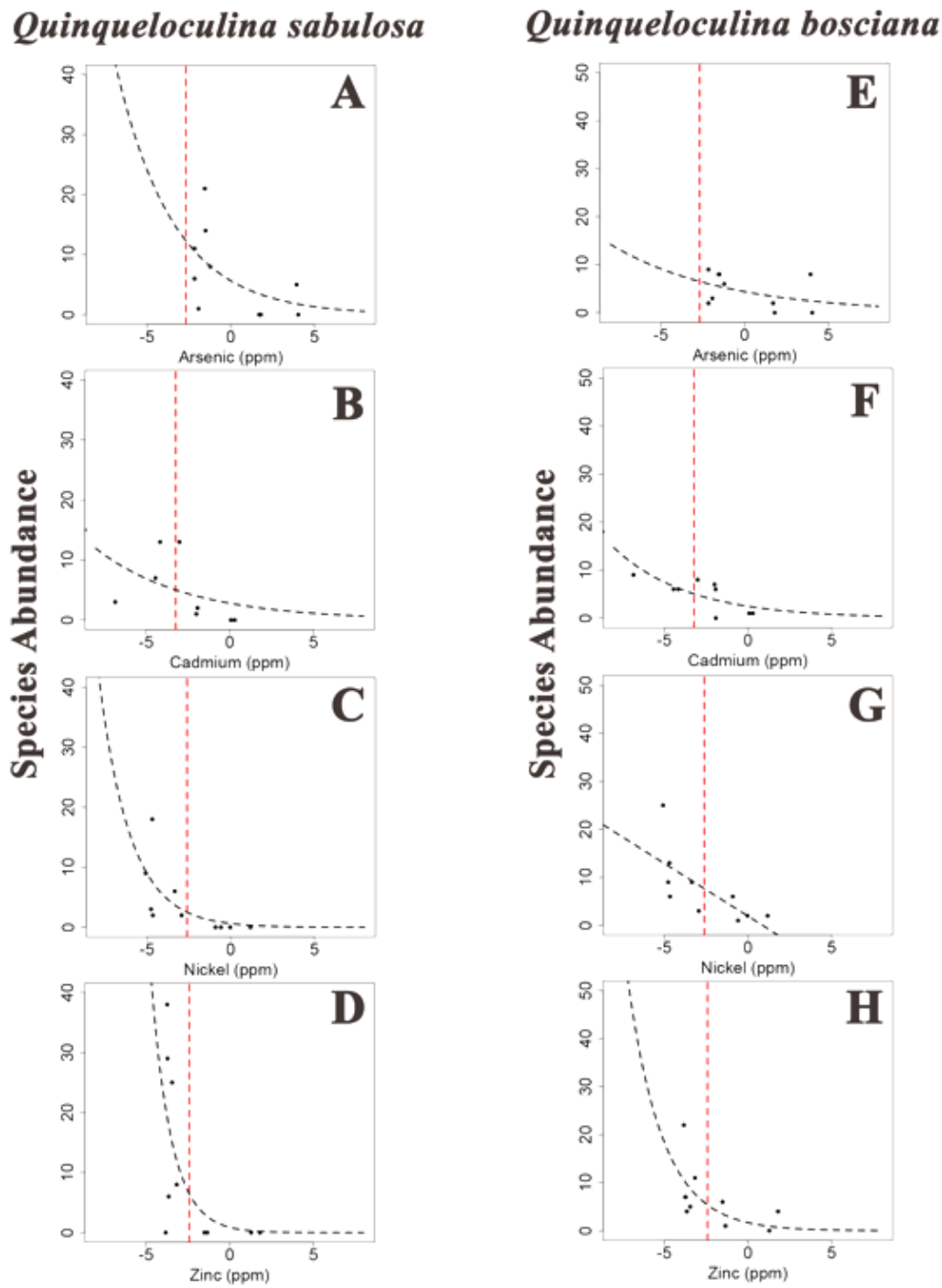

Figure 2.6. Abundance of *Quinqueloculina sabulosa* (left) in response to the natural log of the concentration of a specific heavy metal: **A** arsenic, **B** cadmium, **C** nickel, and **D** zinc. Abundance of *Quinqueloculina bosciana* (right) in response to the natural log of the concentration of a specific heavy metal: **E** arsenic, **F** cadmium, **G** nickel, and **H** zinc These were grown from propagules collected at Little Duck Key. The vertical dashed lines indicate the U.S. EPA's CMC (Criteria Maximum Concentration) of each respective metal. The curved and diagonal dashed lines represent the exponential regression line.

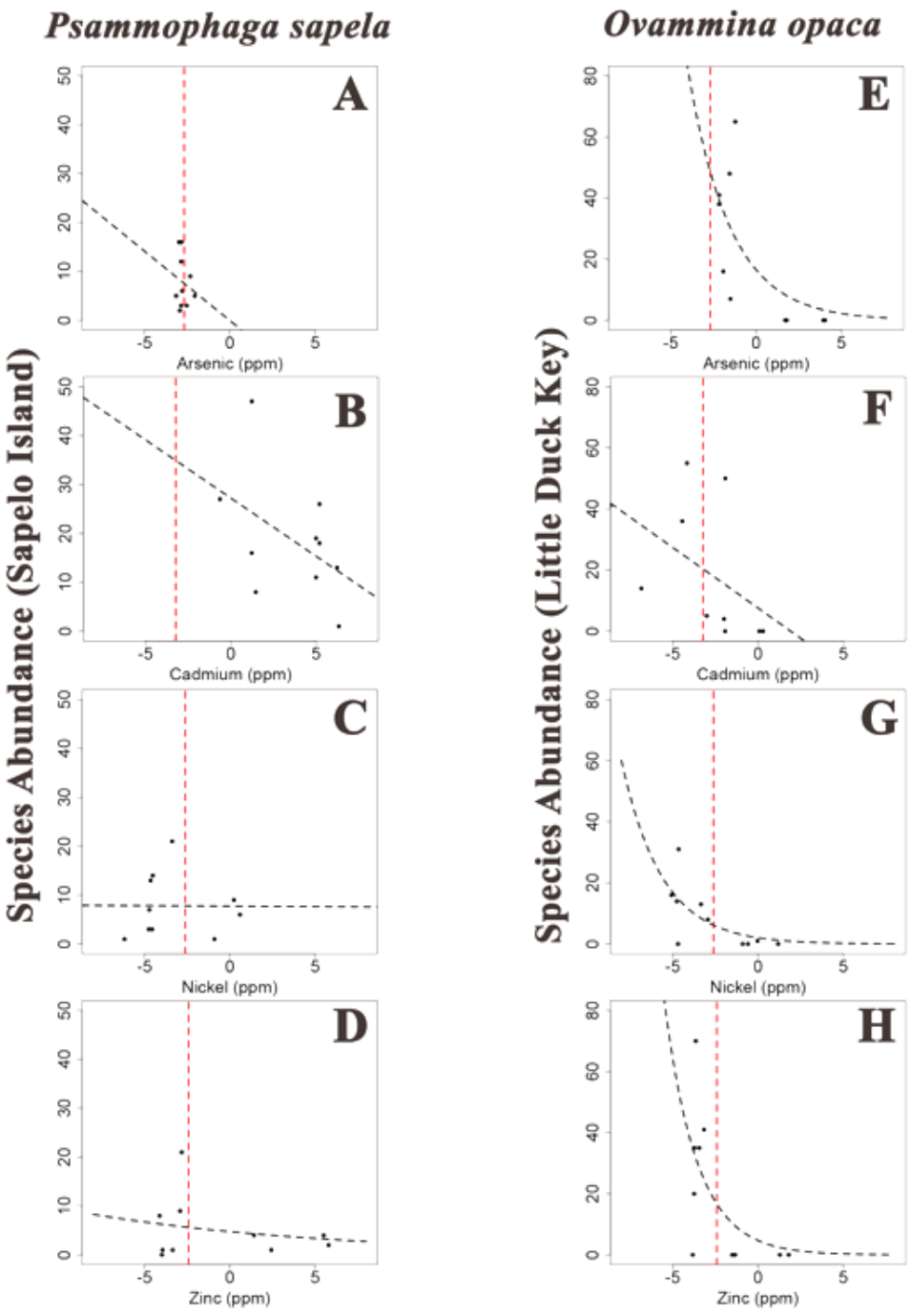

Figure 2.7. Abundance of *Psammophaga sapela* (left) in response to the natural log of the concentration of a specific heavy metal: **A** arsenic, **B** cadmium, **C** nickel, and **D** zinc. These were grown from propagules collected at Sapelo Island. Abundance of *Ovammina opaca* (right) in response to the natural log of the concentration of a specific heavy metal: **A** arsenic, **B** cadmium, **C** nickel, and **D** zinc. These were grown from propagules collected at Little Duck Key. The vertical dashed lines indicate the U.S. EPA's CMC (Criteria Maximum Concentration) of each respective metal. The curved and diagonal dashed lines represent the exponential regression line.

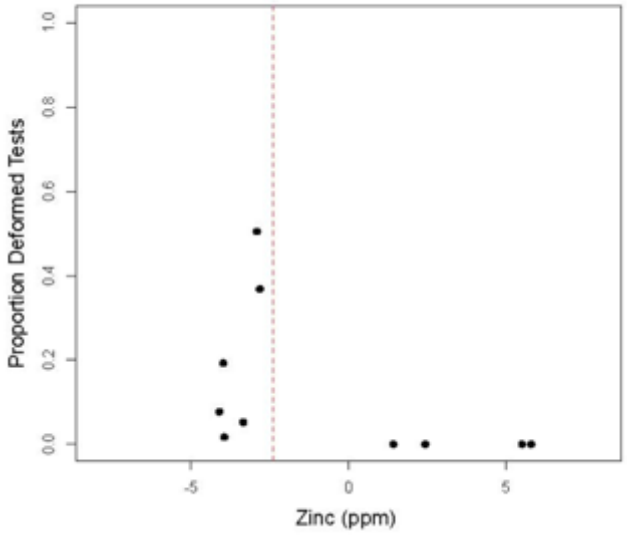

Figure 2.8. Proportion of test deformities in response to the natural log of zinc concentration in assemblages grown from Sapelo Island propagules.

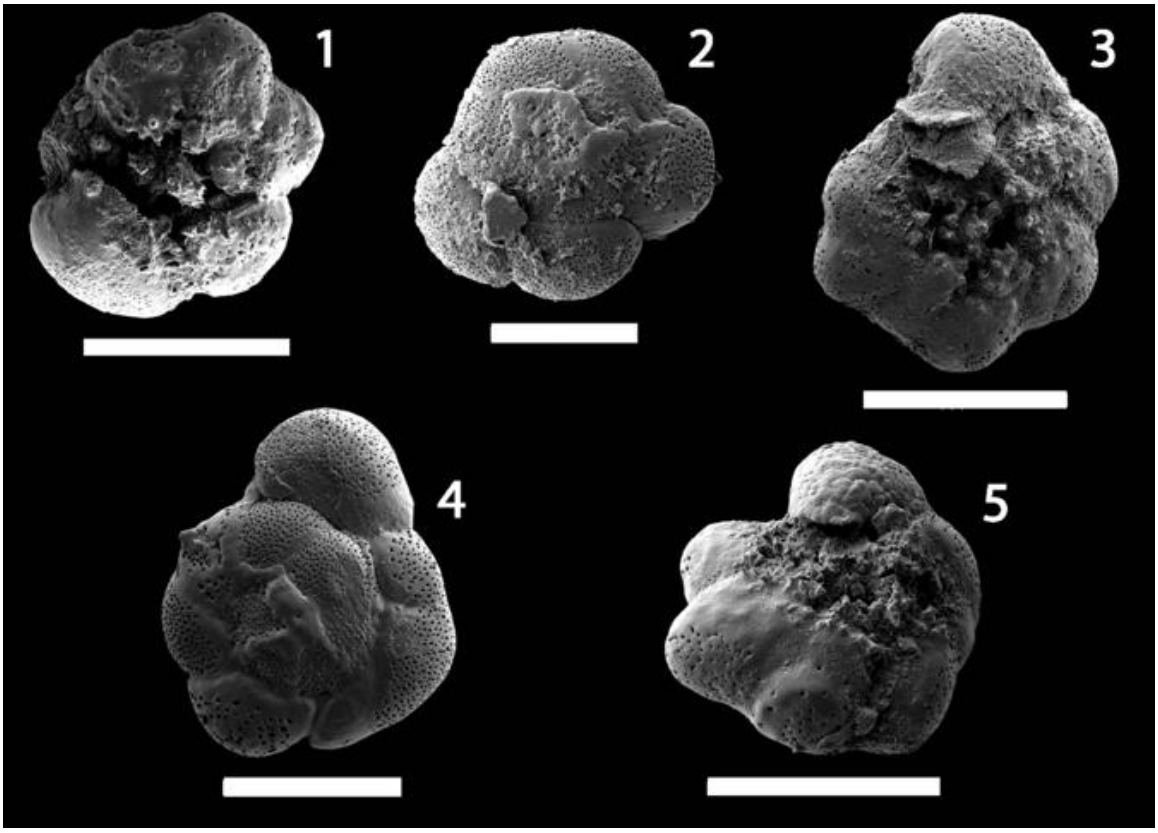

Figure 2.9. SEM micrographs of deformed tests occurring in Sapelo Island assemblages in response to zinc concentrations of 0.0597 and 0.0545 mgL^{-1}. **1–5** is all specimens of either *Ammonia tepida* or *Haynesina germanica*. All scale bars = 100 μm.

CHAPTER 3

INCORPORATION OF HEAVY METALS IN EXPERIMENTALLY GROWN FORAMINIFERA FROM SAPELO ISLAND, GEORGIA AND LITTLE DUCK KEY, FLORIDA, U.S.A.[2]

[2] Smith, C.W., Fehrenbacher, J.S., Goldstein, S.T. Submitted to Marine Micropaleontology.

Abstract

Benthic foraminifera are valuable indicators in environmental studies, including those on marine pollution monitoring. While a great deal of foraminiferal biomonitoring research utilizes abundance and distributional data, further value resides in better understanding the incorporation of heavy-metal pollutants in foraminiferal calcite. By experimentally growing assemblages of foraminifera from propagules (small juveniles) gathered from Sapelo Island, Georgia and Little Duck Key Florida, this study examines foraminiferal incorporation of the heavy metals arsenic, cadmium, nickel, and zinc over a range of concentrations.

Surface sediment was collected and sieved to concentrate the propagules. The propagules were then used to experimentally grow assemblages with each exposed to a different heavy metal. After one month, the experimentally grown foraminifera were harvested and samples of the two most common species from each location (*Ammonia tepida* (Cushman) and *Haynesina germanica* (Ehrenberg) from Sapelo Island and *Quinqueloculina sabulosa* (Cushman) and *Triloculina oblonga* (Montagu) from Little Duck Key) were selected for trace element analysis. Calcite of the tests was analyzed using LA-ICP-MS to quantify the heavy-metal incorporation.

Rotalid species *A. tepida* and *H. germanica* incorporated more cadmium as its concentration in the surrounding water increased, whereas miliolid species *Q. sabulosa* and *T. oblonga* incorporated more of the metals zinc and nickel. This study shows that while foraminiferal incorporation of heavy metals has great potential as a biomonitoring tool, multiple factors (especially inter-clade variation) must be considered carefully. In

future marine environmental research, these factors may help create a more targeted assessment of environmental pollution.

Introduction

Foraminifera have been used as tools for modern and ancient environmental analysis for decades (e.g., Natland, 1935; Hallock & Glenn, 1986; Murray, 2006). Benthic foraminifera in particular have proven effective as pollution monitoring tools reflecting their diversity and sensitivity to environmental changes (e.g., Resig, 1960; Schafer, 1970; Boltovskoy & Wright, 1976; Alve, 1991). Specifically, they have shown great responsiveness to heavy-metal contamination, with it affecting everything from their overall abundance and diversity (Alve, 1991; 1995; Yanko et al., 1994; 1999; Martin, 2000 and papers therein; Scott et al., 2001; Olugbode et al., 2005; Nigam et al., 2006; Martinez-Colon et al., 2009; Foster et al., 2012; Hart et al., 2014; Brouillette Price et al., 2019; Smith & Goldstein, 2019) to their shell chemistry (de Noojier et al., 2007; Frontalini et al., 2009; Munsel et al., 2010; Nardelli et al., 2016; van Dijk et al., 2017; Titelboim et. al, 2018).

Heavy metals are often introduced into marine environments via industrial pollution, agricultural waste, or urban runoff (e.g., Alloway, 2013; Julian II, 2015; Tansel & Rafiuddin, 2016). Foraminifera have remarkable potential as environmental indicators for heavy-metal contamination. Foraminiferal abundance and diversity are clearly affected by exposure to these metals (Boltovoskoy et al., 1991; Yanko et al., 1994; 1999; Alve, 1995; Scott et al., 2001; Olugbode et al., 2005; Nigam et al., 2006; Martinez-Colon et al., 2009; Hart et al., 2014; Brouillette Price et al., 2019; Smith & Goldstein, 2019). However, other environmental changes such as salinity and temperature variation can

have similar effects on foraminiferal assemblages (Geslin et al., 2000; Lee et al., 2015). Because of the difficulty in parsing effects, the shell chemistry of foraminifera can provide an additional approach. The trace element and stable isotope chemistry of foraminiferal tests is used extensively in paleoceanography (e.g., Emiliani, 1955; Erez and Luz, 1983; Erez, 2003; Katz et al., 2010; Schiebel et al., 2018). As others have noted, it follows that incorporation of contaminating heavy metals by foraminifera could act as a valuable environmental biomonitoring tool (Rosenthal et al., 1997; Dissard et al., 2010a; Dissard et al., 2010b; Frontalini et al., 2018; Titelboim et al., 2018; Bergamin et al., 2019).

Benthic foraminifera are known to take up heavy metals from their surrounding environment and incorporate them into the test during calcification (e.g., Boyle, 1981; Rosenthal et al., 1997; Dissard et al., 2010a; Dissard et al., 2010b; Munsel et al., 2010; Nardelli et al., 2016; Frontalini et al., 2018). Understanding relationships between metal occurrences in the environment and metal incorporation in foraminiferal tests will help refine foraminiferal applications in biomonitoring studies. Several factors need to be considered in this regard. Sediment type (e.g. clay mineralogy, presence of carbonates), for example, may affect trace element incorporation. Further, clades of calcareous foraminifera differ with regard to fine structure and test construction (e.g., Angell, 1979; Angell, 1980; Elderfield et al., 1996; Hansen, 1999; de Noojier et al., 2009a; de Noojier et al., 2009b; de Noojier et al., 2014). Miliolid and rotalid foraminifera therefore might incorporate a metal differently based on biological differences and modes of test construction and calcification. Titelboim (2018) found that miliolids tended to incorporate greater concentrations of heavy metals than rotalids, possibly because

miliolids tend to utilize high-Mg calcite in test construction whereas rotalids tend to utilize low-Mg calcite. Seawater is naturally high in Mg concentration. Therefore, when vacuolizing seawater, rotalids must alter the seawater chemistry before calcification can begin, whereas miliolids may not. Incorporation could also vary between species, between individuals, and ontogenetically within a single foraminifer (Rosenthal et al., 2000; Geerken et al., 2018). In addition, exposure to certain heavy metals has been correlated with foraminiferal test deformities (e.g., Alve, 1991; Yanko et al., 1998; Foster et al., 2012; Brouillette Price et al., 2019; Smith & Goldstein, 2019).

Here, we use the propagule method for growing benthic foraminifera under controlled conditions. The propagule method (Goldstein & Alve, 2011; Alve & Goldstein, 2014) provides an effective way to investigate foraminiferal incorporation of heavy metals and how it might be related to environmental variation, test construction, and differences between species and individuals. Propagules are juvenile foraminifera and they are often abundant in fine-grained sediment. They can lie dormant for months to years before eventually maturing if exposed to appropriate conditions (Alve and Goldstein, 2002; 2003; 2010). In this study, foraminifera were grown experimentally from propagules while exposed to an individual heavy metal (arsenic, cadmium, nickel, and zinc) over a range of concentrations and then analyzed using laser ablation inductively coupled plasma mass spectrometry (LA-ICP-MS) to ascertain whether the foraminifera incorporated the metal into the calcite of their test and to further compare concentrations in the test with that of the artificial seawater in which they grew. These metals were chosen because they are amongst the most common sources of marine heavy-metal pollution (Alve, 1995; Martinez-Colon et al., 2009). Results provide insight

into potential differences in incorporation between foraminiferal clades (rotalids and miliolids), species, and individuals, including intra-individual variation, thus improving the application of selected coastal foraminifera as bioindicators of heavy-metal pollution.

Materials and Methods

Sediment samples from Sapelo Island, Georgia and Little Duck Key, Florida (Fig. 3.1) were collected in the summer of 2018. At both locations, the upper few millimeters of sediment were collected within a ~1 square meter area and transferred into a 2-liter container. This sediment was then sieved immediately at the collection site using 53- and 850-micron stainless steel sieves. The 850-micron sieve removed larger material, such as detrital plant material and gastropod shells and allowed smoother sieving. The > 53-micron fraction was discarded while the < 53-micron fraction was transported back to facilities at the University of Georgia and used as the source of propagules. From these sediment samples, experimentally grown assemblages (EGAs) of benthic foraminifera were obtained using the propagule method (Goldstein & Alve, 2011; Alve & Goldstein, 2014). The EGAs were grown in artificial seawater that was spiked with varying concentrations of a heavy metal (arsenic, cadmium, nickel, or zinc) at the onset of the experiment (following Brouillette Price et al., 2019; Smith & Goldstein, 2019). The concentrations used were based upon the United States Environmental Protection Agency's National Recommended Water Quality Criteria for Saltwater Criteria Maximum Concentration (As 0.069 mg/L; Cd 0.033 mg/L; Ni 0.074 mg/L; and Zn 0.090 mg/L). The Criteria Maximum Concentration (CMC) is the amount of heavy metal that can occur in an aquatic setting briefly before "resulting in an unacceptable effect" (U.S. EPA, 2006). Using the CMC as a starting point, the added concentrations increased by an

order of magnitude for four additional levels for a total of five treatments per metal. Heavy metals were added as dissolved chlorides except for arsenic, which was added as a dissolved oxide. Each EGA of foraminifera was exposed to a different concentration of each of the selected metals during growth. Replicates were made for each concentration level of all four metals along with two controls in which no metals were added. The final result was a total of 84 EGAs with 42 representing each sample location. The EGAs were kept at a constant temperature and illuminated on a 12-hour cycle. The samples from Sapelo Island were incubated at 32 psu and 20°C, while the samples from Little Duck Key were incubated at 32 psu and 24°C, reflecting the salinities and ambient water temperatures at the time of collection. The EGAs were rotated twice a week in the incubator to provide equal access to the light source.

After one month, the contents of the EGAs were harvested and fixed using a 10% formalin mixture, buffered with sodium carbonate to a pH of approximately 8.0–9.0, containing 1 g/L rose bengal added as a vital stain (Walton, 1952; Murray & Bowser, 2000). After one week, the fixative/stain mixture was removed, and samples were rinsed using deionized water and preserved in 50% ethanol. The contents were then picked wet for foraminifera. The two most common foraminifera in the Sapelo Island EGAs were *Ammonia tepida* (Cushman) and *Haynesina germanica* (Ehrenberg) while the two most common in the Little Duck Key EGAs were *Quinqueloculina sabulosa* (Cushman) and *Triloculina oblonga* (Montagu) (Smith & Goldstein, 2019) (Fig. 3.2). Where possible, approximately a dozen specimens of each species were picked from each EGA. Sampling was limited in some cases due to low abundance or the absence of foraminifera, especially in EGAs exposed to extremely high concentrations of a metal.

To prepare foraminifera for LA-ICP-MS, specimens were oxidatively cleaned using equal parts of 30% H_2O_2 and 0.1 N NaOH to remove remnant trace organic matter (Fehrenbacher et al., 2015). The objective was to analyze only the calcite component of the test. Around a dozen selected foraminifera from each EGA were placed in 0.6 mL open-top microcentrifuge vials and rinsed thoroughly with Milli-Q water. The contents of each EGA were kept organized and separated with each EGA being assigned a single vial. Each vial was then filled with 150 µl of the cleaning solution and placed in a cleaning rack which was then transferred to a pre-heated (65°C) evaporating dish (large Pyrex crystallizing dish) that was filled with water. The samples were heated for 10 minutes and then removed from the evaporating dish. Each vial was then filled with Milli-Q water and the rack was rapped gently on the counter to remove bubbles and insure the foraminifera remain on the bottom of each vial. The water was then extracted from each vial with a micropipette. This rinsing step was repeated three times to ensure complete removal of the oxidizing agents. The foraminifera were then removed individually from the vials and carefully arranged on strips of carbon tape placed on microscope slides in preparation for laser analysis.

The foraminifera were analyzed via LA-ICP-MS using a Thermo Scientific X-Series II quadruple ICP-MS coupled to a Photon Machine Analyte G2 laser system. During analysis, NIST 610 and NIST 612 glass standards were analyzed every hour to insure proper machine calibration. The glass standards were analyzed at a 5 Hz repetition rate using a 50 µm in diameter spot size and a laser fluence of 3.45 J/cm_3.

When possible, each individual foraminifer was analyzed at least 3 times, once per chamber (Fig. 3.3). The penultimate chamber (F1) was targeted first, with F2 and F3

following. The youngest chamber (F), was avoided in most cases because it tended to be fragile and not ideal for analysis. In some cases, even the older chambers were weak and crumbled quickly. In these cases, additional chambers were analyzed to compensate. For the Sapelo Island foraminifera, the laser diameter was set at 50 μm and the fluence was set to 1.27 J/cm$_3$ with a 4 Hz repetition rate. The Little Duck Key foraminifera tended to be more fragile than their Sapelo Island counterparts. This necessitated operating the laser at a lower fluence (1.04 J/cm$_3$). The laser spot size (50 μm) and frequency (4 Hz) were unchanged from the Sapelo Island foraminiferal analyses. Laser data were processed using LAtools, a Python toolbox used for manipulating and interpreting laser ablation data (Version 0.3.8; Branson, 2019). This process involved a series of data reduction techniques. First the data underwent a signal de-spiking routine to remove physically unrealistic outliers. Background correction was then carried out, followed by normalization to an internal standard ($_{43}$Ca), and the calibration to standard reference materials (SRMs: NIST 610 and 612). This processing provided concentrations (reported as mmol/mol; Me/Ca) of each heavy metal of interest within each foraminiferal chamber. The average concentration and standard deviation of the incorporated heavy metal were calculated for each individual spot analysis (Branson, 2019). Repeat ablations on the same specimen were then averaged to obtain a specimen average ME/Ca value.

While the amount of heavy metal added to each EGA was calculated, it was important to have exact concentration numbers for the heavy-metal content of the water in the EGAs post-experiment. To accomplish this, ICP-MS water analysis was carried out on the residual water remaining from each EGA. For each heavy metal, the concentrations in the water were then plotted against the amount incorporated into each

individual foraminifer (R Core Team, 2019). Concentrations were plotted as ratios (Me/$_{43}$Ca; mmol/mol). This allowed for comparison of the effects of different heavy metals on the foraminiferal incorporation as well as comparison of incorporation between species.

A two-way analysis of covariance (ANCOVA) was run to determine which factors explained the variance in incorporated metals (R Core Team, 2019). One analysis for each metal was run examining the factors of water chemistry and foraminiferal clade. Another analysis for each metal was run for each clade (rotalids and miliolids) examining the factors of water chemistry and foraminiferal species.

Results

Arsenic, cadmium, nickel, and zinc were incorporated into the calcite of the foraminiferal tests examined, but to varying degrees (Figs. 3.4–3.5). The amount of incorporation varied in multiple ways: within individual tests (intra-individual), between individuals of the same species (inter-individual), between species of the same clade (inter-specific), and between rotalids and miliolids. The amount of incorporation was greater in specimens from EGAs exposed to higher concentrations of the metals in many, but not all, cases. In the Sapelo Island EGAs, *Ammonia tepida* and *Haynesina germanica* incorporated more cadmium at increased concentrations of cadmium (Fig. 3.4). Only *A. tepida* incorporated more arsenic when exposed to higher concentrations in the experimental water (Fig. 3.4). In the Little Duck Key EGAs, *Quinqueloculina sabulosa* and *Triloculina oblonga* incorporated greater amounts of nickel and zinc when exposed to higher concentrations of each metal respectively (Fig. 3.5). In specimens from Sapelo Island and Little Duck Key, variation in incorporation of heavy metals occurred within

individual foraminifera (Tables 3.1 and 3.2). In the case of cadmium, a general trend is apparent of larger standard deviation paired with greater amounts of heavy metal in the water. With the other metals, the standard deviation is sporadic with no visible pattern. Incorporation occurred in all of the individual foraminiferal chambers examined (F1, F2, F3, etc.), with no chamber in the sequence showing consistently greater amounts of metal incorporation.

Variation in incorporation occurred between individuals of the same species as well. For example, in the Sapelo Island specimens exposed to a X concentration of arsenic and of nickel, *Ammonia tepida* and *Haynesina germanica* incorporate a range of the heavy metal into their calcite (Fig. 3.4, Table 3.1). While this data spread is not as large in specimens exposed to other metals, variation is still clearly visible between individuals of all four species analyzed (Figs. 3.4–3.5, Tables 3.1 and 3.2).

In most cases, species belonging to the same clade had similar Me/Ca ratios at each experimental seawater concentration. For example, the rotalids *Ammonia tepida* and *Haynesina germanica* incorporated similar amounts of cadmium at 0.0167 mg/L and 0.0714 mg/L, nickel at 0.01634 mg/L and 0.0285 mg/L, and zinc at 0.02026 mg/L (Fig. 3.4). The miliolids *Quinqueloculina sabulosa* and *Triloculina oblonga* incorporated similar amounts of all four metals (Fig. 3.5). However, *A. tepida* and *H. germanica* incorporated arsenic differently, with *A. tepida* incorporating more arsenic with higher concentrations of arsenic in the water (Fig. 3.4).

In the Sapelo Island specimens, the relationship between the amount of heavy metals in the water and the amount incorporated by the foraminifera varied depending on the metal and on the foraminiferal species (Table 3.1). In specimens exposed to arsenic, a

moderately strong correlation exists between arsenic in the water and arsenic incorporated into *Ammonia tepida* (R^2 = 0.588), but not *Haynesina germanica* (R^2 = 0.151; Fig. 3.4). In those exposed to cadmium, *A. tepida* (R^2 = 0.884) and *H. germanica* (R^2 = 0.930) have strong correlations (Fig. 3.4). Of the foraminifera exposed to nickel, *A. tepida* (R^2 = 0.070) and *H. germanica* (R^2 = 0.139) show little correlation (Fig. 3.4). Finally, in EGAs exposed to zinc, *A. tepida* showed little correlation (R^2 = 0.136), while *H. germanica* exhibited a weak relationship (R^2 = 0.278; Fig. 3.4).

The Little Duck Key specimens illustrated different results (Table 3.2). In assemblages exposed to arsenic, the number of data points (N=X) are insufficient to establish a relationship between metal content in the water and incorporation into *Quinqueloculina sabulosa* or *Triloculina oblonga* tests (Fig. 3.5). In assemblages exposed to cadmium, there's a clear difference between the species (*Q. sabulosa* R^2 = 0.119, *T. oblonga* R^2 = 0.520; Fig. 3.5). Unlike in the Sapelo EGAs, a positive correlation exists in Little Duck Key assemblages exposed to nickel (*Q. sabulosa* R^2 = 0.406, *T. oblonga* R^2 = 0.588; Fig. 3.5). Lastly, a strong correlation occurs in Little Duck Key EGAs exposed to zinc, for *Q. sabulosa* (R^2 = 0.890) and *T. oblonga* (R^2 = 0.692; Fig. 3.5).

Results of the ANCOVA analyses reveal more detail on incorporation and which factors are associated with greater variation (Tables 3.3 and 3.4). An F ratio closer to one indicates that the variance between the groups is similar to the variance within the groups, that is, that group membership is not an important source of variation. Higher F ratios indicate that group membership is an increasing source of variation. Foraminiferal clade was not an important source of variance for cadmium (F = 0.007, p = 0.93) and zinc (F = 0.108, p = 0.74), but important for arsenic (F = 5.016, p = 0.032) and nickel (F =

3.579, p = 0.064) (Table 3.3). In the case of foraminiferal species, among the rotalids of Sapelo Island, it was an important source of variance for arsenic (F = 7.953, p = 0.0093), but not for cadmium (F = 0.013, p = 0.91), nickel (F = 120.172, p = 1.3E-13), and zinc (F = 1.408, p = 0.24). Among the miliolids of Little Duck Key, species was a source of variance for nickel (F = 13.340, p = 0.00039), but not for arsenic (F = 0.038, p = 0.86), cadmium (F = 2.071, p = 0.19), and zinc (F = 1.855, p = 0.21) (Table 3.4).

Discussion

Foraminifera grown from both sample locations have clearly incorporated all four of the metals tested (As, Cd, Ni, and Zn) to varying degrees (Figs. 3.4–3.5). Variability in metal incorporation occurs within individuals, between individuals of the same species, between species of the same clade, and between clades. These variations could result from any of a number of factors, including the properties of the metals, differing composition of sediments at Sapelo Island and Little Duck Key, and the vital effects of the foraminifera involved, including the potential different modes of test formation of rotalids and miliolids, and the differing life habits of the species analyzed (e.g., Angell, 1979; Angell, 1980; de Noojier et al., 2014; Nardelli et al., 2016; Frontalini et al., 2018).

Metal Properties

Foraminifera are known to incorporate arsenic, cadmium, nickel, and/or zinc into the calcite of their tests (Boyle, 1981; Rosenthal et al., 1997; de Noojier et al., 2007; Katz et al., 2010; Kramar et al., 2010; Nardelli et al., 2016; Frontalini et al., 2018; Titelboim et al., 2018). These metals differ in many ways including their chemical speciation and their metabolic utility. These factors can affect the bioavailability of the metal, and thus the likelihood of the metal being incorporated into test structures.

One difference of note between the metals in this study was their essentiality, or requirement in biological activities (Mertz, 1981; Adriano, 2001; Martinez-Colon et al., 2009; Maret, 2016; Desideri et al., 2016). Essentiality is a controversial topic and there is much debate regarding the relative essentiality of some elements (Mertz, 1981; Maret, 2016). Even elements known to be toxic such as arsenic are now thought to have important roles as micronutrients in gene silencing and metabolism of the amino acid methionine (Uthus, 2003; Zeng et al., 2005). Essentiality depends also on the organism involved. Nickel, for example, is more essential in plants and bacteria than animals (Anke et al., 1984; Poonkothai and Vijayavathi, 2012; Maret, 2016). The elements in this study span a range of metabolic utility. Zinc is considered broadly essential to all life, while nickel is essential to a slightly more limited group of organisms (Mertz, 1981; Maret, 2016). Cadmium is used by only a select organism (e.g. a planktonic diatom) in a special ecological niche (Maret, 2016). Arsenic for many years was considered non-essential, but now is recognized to have limited utility as well (Uthus, 2003; Zeng et al., 2005). It is also important to point out that the essentiality of elements for foraminifera is not well known compared to other organisms.

Bioavailability of trace elements like the heavy metals in this study is dependent on multiple factors including chemical speciation, the solubility of the metal, potential adsorption of the metal in sediments, metal uptake and the excretion or detoxification of the heavy metals (Rainbow, 2016). Because of their use in biological functions, more essential elements might be more readily bioavailable for foraminifera and therefore more likely to become incorporated in the foraminiferal test. Results of the LA-ICP-MS analysis, however, do not reflect this. Incorporation of less essential metals, arsenic and

cadmium was strongly correlated with arsenic and cadmium content in the water in the Sapelo Island EGAs (Fig. 3.4). More essential metals, zinc and nickel exhibited a similarly strong connection with metal content in the water in the Little Duck Key EGAs (Fig. 3.5). Because the Sapelo species analyzed were both rotalids and the Little Duck Key species analyzed were miliolids, this suggests that clade differences in test construction, calcification, and test composition could influence incorporation (See *Rotalid and Miliolid Test Construction*). However, there is clearly incorporation occurring with all of the metals, even where no correlation exists with trace metal content in the water.

Chemical speciation is also an important consideration. All of the metals tested here have been shown to incorporate into foraminiferal calcite (Boyle, 1981; Rosenthal et al., 1997; de Noojier et al., 2007; Kramar et al., 2010; Nardelli et al., 2016; Frontalini et al., 2018; Titelboim et al., 2018). Metal ions with a 2+ charge might be incorporated more readily than those without due to their similarity to Ca^{2+} ions. Most typically, depending on the type of test structure, Mg^{2+} will often substitute in the place of the calcium cation in calcium carbonate structures (Nurnberg et al., 1996). In this experiment, cadmium, nickel, and zinc were all added to the EGAs as dissolved chlorides in the 2+ form. Arsenic was added as a dissolved oxide in the 3+ form. This did not have much effect as arsenic incorporated just as much as the other metals, especially in the Little Duck Key EGAs. Speciation in sediment is also highly dependent on the pH of the environment (Adriano, 2001). For example, the predominant dissolved species of cadmium depends heavily on pH with Cd^{2+} ions more common at pH values below 7.0 and $CdCO_3$ prevalent at pH values above 7.0 (Adriano, 2001). While it is possible lower pH could

result in more incorporation of certain metals, that was not seen in this experiment, because pH was kept around 8.0 throughout to simulate actual seawater.

Sedimentary Properties

Sediment composition may also influence metal incorporation in foraminiferal tests. Whereas other environmental factors are largely controlled, fine-grained sediment from the collection site is necessarily retained. Sapelo Island, a tidally dominated barrier island, has heterogeneous sediment consisting of clays as well as some siliciclastic silt and sand whereas Little Duck Key, a small key in the Florida Keys chain, has a heterogeneous mix of mostly calcareous mud and sand with scattered shell debris (Roychoudhury, 2007; Weinmann and Goldstein, 2016; Smith & Goldstein, 2019). This could affect incorporation considerably.

Goethite, a common iron mineral in surficial Sapelo Island sediments, has shown a propensity to absorb 3+ ions such as arsenic (Ladeira, 2004; Roychoudhury, 2007). The many clay minerals of Sapelo Island could absorb not only arsenic, but the other metals as well (Ladeira, 2004; Roychoudhury, 2007). This would theoretically lead to lower metal concentrations in the water column and therefore less metal available for possible incorporation. If this were true, there would be greater incorporation overall in Little Duck Key EGAs than in Sapelo Island EGAs. However, the metal concentration in seawater measured in the EGAs was measured post-experiment and represents at least the minimum amount of metal potentially bioavailable in the water at the end of the experiment. While there is evidence that the sediment played a major role in the metal concentration of the residual water post experiment, no great differences exist between

the amount of incorporation between EGAs from each site. Therefore, little evidence of major sedimentary effect on incorporation exists in this experiment.

Rotalid and Miliolid Test Construction

Rotalid and miliolid foraminifera have long been known to exercise different strategies for calcification and test morphogenesis (Angell, 1979; Angell, 1980; Hemleben et al., 1986; Elderfield et al., 1996; Hansen, 1999; de Noojier et al., 2009a; de Noojier et al., 2009b; de Noojier et al., 2014). Rotalids begin chamber construction by surrounding themselves in a protective cyst (Angell, 1979). Inside, some rotalids use low-Mg calcite with a bilamellar method of construction (Angell, 1979; Hansen, 1999). This results in the older, earlier chambers growing gradually thicker over time, with multiple layers of perforate calcite. Miliolids also begin by constructing a surrounding cyst, however, miliolids use high-Mg calcite with a non-lamellar construction that utilizes calcite rods to construct a porcelaneous test wall (Angell, 1980; Hemleben et al., 1986; Erez; 2003).

As reviewed by de Noojier et al. (2014), a crucial factor in potential incorporation of heavy-metal elements is the primary source of Ca^{2+} that foraminifera use in biomineralization and the method by which they obtain it. There is no consensus understanding of the biomineralization pathways of foraminifera and there are several competing models (Erez, 2003; de Noojier et al., 2009a; de Noojier et al., 2009b; Nehrke et al., 2013; de Noojier et al., 2014). One model posits that foraminifera use seawater as a direct source of Ca^{2+} via endocytosis and vacuolization (Erez, 2003; de Noojier et al., 2009a; de Noojier et al., 2009b; de Noojier et al., 2014; Khalifa et al., 2016). A similar model argues that seawater is the primary source of ions, but through direct passive

uptake, not endocytosis (Nehrke et al., 2013; de Noojier et al., 2014) Another model suggests that foraminifera use an internal reservoir of Ca^{2+} as their primary source of material (Ter Kuile et al., 1989; Erez, 2003; de Noojier et al., 2014). The relationship between heavy-metal contamination in the surrounding seawater and incorporation into the test may depend on which of these models is most accurate and how seawater is metabolically processed during calcification. If foraminifera are unable eliminate ions during calcification, it follows that it would lead to more incorporation of contaminating material in that seawater. Crucially, studies leading to these models rely heavily on rotalid species, not miliolids (Nardelli et al., 2016).

In this study, a correlation between incorporation and concentration in the surrounding water was seen in rotalids and miliolids, but with different metals. *Ammonia tepida* and *Haynesina germanica*, rotalids, show a strong relationship with cadmium, which supports previous research involving cadmium and rotalids (Boyle, 1988). *A. tepida* also exhibited a strong relationship with arsenic. For both *A. tepida* and *H. germanica*, there was either no relationship at all, or a weak one for nickel and zinc. In contrast, *Triloculina oblonga* and *Quinqueloculina sabulosa* had a strong correlation between incorporation and water concentration for zinc and an intermediate correlation for nickel, which supports previous research (Titelboim et al., 2018). *T. oblonga* differed in correlation for arsenic and *T. oblonga* and *Q. sabulosa* differed in correlation for cadmium. The variation in incorporation between rotalids and miliolids is also supported by the ANCOVA data, which shows greater variance between clades in samples exposed to arsenic and nickel (Table 3.3).

Overall, the rotalids seemed more likely to incorporate more heavy metal from the surrounding water if they were less essential (arsenic and cadmium) as opposed to more essential (nickel and zinc). This seeming inability for rotalids to take in more zinc and nickel with high concentrations of the metals in the water column has been noted by others (Nardelli et al., 2016; Frontalini et al., 2018). Heavy metals such as zinc have been shown to trigger cytological alterations and organelle degradation in foraminifera (Frontalini et al., 2018). These changes are thought to be a defense mechanism against heavy-metal toxicity and might prohibit the metals from incorporating after a certain threshold in the surrounding water is met (Frontalini et al., 2018). It is possible that in rotalids, these defense mechanisms are either ineffective or not as effective for less essential heavy metals such as arsenic and cadmium, leading to their greater incorporation rates at higher levels of saturation. However, these same defense mechanisms have been noted in miliolids as well (Frontalini et al., 2018).

The strength of the relationship between cadmium in the seawater and cadmium incorporation in rotalids seen in this study is notable, but has been established in prior research (Boyle, 1988). However, the contrasting lack of relationship for cadmium incorporation in miliolids is striking. Likewise, the relationship between zinc content in the seawater and zinc incorporation is particularly strong for miliolids, whereas the opposite is true for rotalids. The results of this study suggest that these elements affect rotalids and miliolids in different ways. Ascertaining why will require further research into miliolids and their biomineralization strategies.

Variation Among Species

In addition to differences between rotalid and miliolid biomineralization, it is becoming increasingly apparent that foraminifera vary in biomineralization even on the species-level (Angell, 1979; Angell, 1980; de Noojier et al., 2014; Nardelli et al., 2016; Frontalini et al., 2018). In this project, the two rotalid species examined, *Haynesina germanica* and *Ammonia tepida*, as well as the two miliolid species, *Quinqueloculina sabulosa* and *Triloculina oblonga* exhibited different results from one another (Table 3.5).

The Sapelo Island specimens exposed to arsenic displayed the largest variation in incorporation between species. *A. tepida* incorporation of arsenic was strongly correlated with arsenic content in the water, but *H. germanica* incorporation was not (Fig. 3.5). This was corroborated by the ANCOVA data which shows a statistically significant variance between the two Sapelo species when exposed to arsenic (Table 3.4). The reason for this difference could reflect the contrasting feeding habits of *A. tepida* and *H. germanica*. *A. tepida* is a deposit feeder, ingesting bacteria, diatoms, and other microbiota along with organic detritus associated with small parcels of sediment consisting largely of clay platelets (Goldstein & Corliss, 1994). *H. germanica* acquires nutrition through sequestration of chloroplasts from diatoms without ingesting sediment aggregates (Lopez, 1979; Goldstein & Richardson, 2018). Because of the tendency for arsenic to be sequestered in the clay minerals and goethite of the Sapelo Island sediment, it seems likely that *A. tepida* is likely to ingest arsenic during feeding. This could have resulted in a higher degree of incorporation of arsenic into tests of *A. tepida*.

Conclusions

Incorporation of arsenic, cadmium, nickel and zinc was recorded in all species analyzed. LA-ICP-MS showed a clear difference between the rotalids and miliolids examined in their tendency to incorporate heavy metals. While *Haynesina germanica* and *Ammonia tepida* readily incorporated metals such as arsenic and cadmium as concentrations in the surrounding water increased, the same did not occur with metals such as zinc and nickel. In contrast, the miliolids *Quinqueloculina sabulosa* and *Triloculina oblonga* incorporated larger amounts of zinc and nickel as water concentration increased, while remaining steady as concentrations of arsenic and cadmium increased. This may reflect a fundamental difference in the biomineralization process between rotalid and miliolid foraminifera and warrants further investigation.

On the species level, incorporation rates were consistent in foraminifera of the same clade, with the exception of *A. tepida* incorporating more arsenic than *H. germanica*. While foraminiferal incorporation did vary in some isolated cases within individuals, there was no overall consistent distinguishable chamber-to-chamber variability.

While some foraminifera show a clear relationship between incorporation of heavy metals and metal content in the surrounding water, others do not. It is important to identify which taxa have the greatest potential for biomonitoring in certain environments and targeting specific pollutants. For example, when studying cadmium contaminations, taxa such as *A. tepida* and *H. germanica* could be useful because of their distinctive incorporation of cadmium. Other taxa such as *Q. sabulosa* and *T. oblonga*, are poor proxies for cadmium. This study shows that while foraminiferal incorporation can prove a

useful tool in heavy-metal pollution research, results may vary with the species examined and the metal tested.

Tables

Table 3.1. Metal concentration in water, mean incorporated metal, and standard deviation among chambers in samples of Sapelo Island foraminifera used in propagule experiments. Each foraminifer was analyzed at least three times on three separate chambers. In some cases when the metal concentration measured by ICP-MS is particularly close to 0, the instrument can produce a negative number. These values have been marked as BDL (below detection limit) and are denoted by an asterisk.

Sapelo Island				
Sample Number	**Species**	**Metal Concentration in Water (mg/L)**	**Mean Incorporated Me/Ca(mmol/mol)**	**Standard Deviation of Me/Ca Between Chambers (mmol/mol)**
Arsenic				
SapeloAs0*069-2_2	*A. tepida*	BDL*	1.57	1.74
SapeloAs0*069-2_3	*H. germanica*	BDL*	1.92	1.46
SapeloAs0*069-2_4	*H. germanica*	BDL*	0.19	0.85
SapeloAs0*69-1_1	*H. germanica*	0.32235	0.37	0.39
SapeloAs0*69-1_2	*H. germanica*	0.32235	7.71	3.44
SapeloAs0*69-1_3	*H. germanica*	0.32235	0.31	2.94
SapeloAs0*69-1_4	*H. germanica*	0.32235	2.88	0.08
SapeloAs0*69-1_4B	*H. germanica*	0.32235	2.77	0.29
SapeloAs0*69-1_5	*A. tepida*	0.32235	5.43	2.89
SapeloAs0*69-1_6	*H. germanica*	0.32235	5.43	5.23
SapeloAs0*69-2_1	*H. germanica*	BDL*	0.86	0.71
SapeloAs0*69-2_2	*H. germanica*	BDL*	0.12	1.24
SapeloAs0*69-2_3	*H. germanica*	BDL*	0.28	1.38
SapeloAs0*69-2_4	*H. germanica*	BDL*	0.47	0.73
SapeloAs0*69-2_5	*H. germanica*	BDL*	1.55	2.29
SapeloAs6*9-2_1	*A. tepida*	0.9265	12.23	14.11
SapeloAs6*9-2_3	*H. germanica*	0.9265	2.63	2.71
SapeloAs69-1_1	*H. germanica*	29.875	2.41	0.78
SapeloIslandControl1_1	*A. tepida*	0.00191	1.91	0
SapeloIslandControl1_1B	*A. tepida*	0.00495	4.95	0.0034
SapeloIslandControl1_1C	*H. germanica*	0.00065	0.65	0
SapeloIslandControl2_1	*H. germanica*	0.00065	0.65	0
SapeloIslandControl2_1B	*H. germanica*	BDL*	0.69	0.00012
SapeloIslandControl2_2	*H. germanica*	BDL*	1.75	0.0025

SapeloIslandControl2_3	*H. germanica*	BDL*	1.79	0
SapeloIslandControl2_3B	*H. germanica*	BDL*	4.8	0
SapeloIslandControl2_4	*H. germanica*	BDL*	0.18	0.0025
SapeloIslandControl2_5	*H. germanica*	BDL*	0.040	0.0025
Cadmium				
SapeloCd0*04-1_1	*A. tepida*	0.0714	14.76	1.74
SapeloCd0*04-1_2	*A. tepida*	0.0714	10.82	1.11
SapeloCd0*04-1_4	*H. germanica*	0.0714	9.19	0.71
SapeloCd0*04-1_5	*H. germanica*	0.0714	13.51	3.45
SapeloCd0*04-1_6	*H. germanica*	0.0714	19.78	3.62
SapeloCd0*04-1_7	*H. germanica*	0.0714	11.17	1.31
SapeloCd0*04-1_8	*H. germanica*	0.0714	10.97	0.89
SapeloCd0*04-1_9	*H. germanica*	0.0714	54.19	3.24
SapeloCd0*04-1_10	*H. germanica*	0.0714	22.31	4.79
SapeloCd0*04-1_11	*H. germanica*	0.0714	54.42	4.46
SapeloCd0*04-2_1	*A. tepida*	0.04658	41.15	14.22
SapeloCd0*4-1_1	*A. tepida*	0.0167	9.24	3.36
SapeloCd0*4-1_2	*H. germanica*	0.0167	12.55	0.28
SapeloCd0*4-1_3	*H. germanica*	0.0167	13.74	3.16
SapeloCd0*4-1_4	*H. germanica*	0.0167	15.49	6.60
SapeloCd0*4-1_5	*H. germanica*	0.0167	11.32	2.06
SapeloCd0*4-1_6	*H. germanica*	0.0167	20.76	5.68
SapeloCd0*4-1_7	*H. germanica*	0.0167	28.93	5.75
SapeloCd0*4-1_8	*H. germanica*	0.0167	15.69	6.01
SapeloCd0*4-1_9	*H. germanica*	0.0167	21.21	4.53
SapeloCd0*4-1_10	*H. germanica*	0.0167	9.71	0.74
SapeloCd0*4-2_2	*H. germanica*	0.02596	35.14	16.09
SapeloCd4-1_2	*H. germanica*	1.5175	956.87	99.89
SapeloCd4-1_3	*H. germanica*	1.5175	895.20	349.47
SapeloCd4-1_4	*H. germanica*	1.5175	811.25	74.10
SapeloCd4-1_6	*H. germanica*	1.5175	175.41	20.02
SapeloCd4-1_7	*H. germanica*	1.5175	199.97	27.79
SapeloCd4-1_8	*H. germanica*	1.5175	199.70	35.39
SapeloCd4-1_9	*H. germanica*	1.5175	745.97	169.76
SapeloCd4-2_1	*H. germanica*	1.344	735.11	71.04
SapeloCd4-2_2	*H. germanica*	1.344	753.77	32.21
SapeloCd4-2_3	*H. germanica*	1.344	946.61	55.52
SapeloCd4-2_4	*H. germanica*	1.344	908.05	62.73
SapeloIslandControl1_1	*A. tepida*	0.00001	0.014	0
SapeloIslandControl1_1B	*A. tepida*	0.00015	0.15	0.00057

SapeloIslandControl1_1C	*H. germanica*	BDL*	0.16	0
SapeloIslandControl2_1	*H. germanica*	BDL*	0.16	0
SapeloIslandControl2_1B	*H. germanica*	BDL*	0.023	0.00002
SapeloIslandControl2_2	*H. germanica*	BDL*	0.085	0.00007
SapeloIslandControl2_3	*H. germanica*	BDL*	0.064	0
SapeloIslandControl2_3B	*H. germanica*	BDL*	0.57	0
SapeloIslandControl2_4	*H. germanica*	BDL*	0.17	0.00008
SapeloIslandControl2_5	*H. germanica*	BDL*	0.11	0.00013
Nickel				
SapeloNi0*074-2_1	*H. germanica*	0.02257	22.17	1.77
SapeloNi0*074-2_2	*H. germanica*	0.02257	17.85	3.97
SapeloNi0*074-2_3	*H. germanica*	0.02257	15.59	1.93
SapeloNi0*074-2_4	*H. germanica*	0.02257	19.47	2.30
SapeloNi0*074-2_5	*H. germanica*	0.02257	14.54	4.23
SapeloNi0*074-2_7	*H. germanica*	0.02257	22.15	4.37
SapeloNi0*74-1_1	*H. germanica*	0.01634	3.56	1.97
SapeloNi0*74-1_2	*H. germanica*	0.01634	7.98	5.85
SapeloNi0*74-1_3	*A. tepida*	0.01634	5.68	1.37
SapeloNi0*74-1_4	*H. germanica*	0.01634	16.33	6.19
SapeloNi0*74-1_5	*H. germanica*	0.01634	7.49	6.48
SapeloNi0*74-1_6	*H. germanica*	0.01634	12.17	5.49
SapeloNi0*74-1_7	*H. germanica*	0.01634	9.19	3.63
SapeloNi0*74-1_8	*H. germanica*	0.01634	4.53	2.73
SapeloNi0*74-1_9	*H. germanica*	0.01634	4.35	1.57
SapeloNi0*74-1_10	*H. germanica*	0.01634	0.75	1.93
SapeloNi0*74-2_1	*A. tepida*	0.0285	0.055	1.48
SapeloNi0*74-2_2	*H. germanica*	0.0285	1.02	2.07
SapeloNi0*74-2_3	*H. germanica*	0.0285	0.88	1.96
SapeloNi0*74-2_4	*A. tepida*	0.0285	0.036	1.32
SapeloNi0*74-2_5	*H. germanica*	0.0285	1.94	0.39
SapeloNi0*74-2_6	*H. germanica*	0.0285	3.36	4.49
SapeloNi0*74-2_7	*H. germanica*	0.0285	1.55	1.84
SapeloNi0*74-2_8	*A. tepida*	0.0285	0.091	3.25
SapeloNi0*74-2_9	*A. tepida*	0.0285	0.96	2.44
SapeloNi0*74-2_10	*A. tepida*	0.0285	0.12	1.61
SapeloNi0*74-2_11	*H. germanica*	0.0285	0.44	0.61
SapeloNi7*4-2_1	*A. tepida*	0.32265	14.07	6.02
SapeloNi7*4-2_2	*A. tepida*	0.32265	23.97	11.83
SapeloNi74-1_1	*H. germanica*	6.24	5.86	3.94
SapeloIslandControl1_1	*A. tepida*	BDL*	15.37	0

SapeloIslandControl1_1B	*A. tepida*	BDL*	43.83	0.035
SapeloIslandControl1_1C	*H. germanica*	BDL*	26.13	0
SapeloIslandControl2_1	*H. germanica*	BDL*	26.13	0
SapeloIslandControl2_1B	*H. germanica*	BDL*	16.78	0.0075
SapeloIslandControl2_2	*H. germanica*	BDL*	18.70	0.020
SapeloIslandControl2_3	*H. germanica*	BDL*	21.47	0
SapeloIslandControl2_3B	*H. germanica*	BDL*	17.73	0
SapeloIslandControl2_4	*H. germanica*	BDL*	7.61	0.0059
SapeloIslandControl2_5	*H. germanica*	BDL*	5.54	0.0045
Zinc				
SapeloZn0*09-2_1	*A. tepida*	0.16815	52.02	48.33
SapeloZn0*09-2_2	*H. germanica*	0.16815	20.97	1.88
SapeloZn0*09-2_5	*A. tepida*	0.16815	11.55	4.23
SapeloZn0*9-1_1	*H. germanica*	0.02026	44.41	13.28
SapeloZn0*9-1_2	*H. germanica*	0.02026	28.29	2.87
SapeloZn0*9-1_3	*A. tepida*	0.02026	1.94	11.77
SapeloZn0*9-1_5	*A. tepida*	0.02026	32.07	3.79
SapeloZn0*9-1_6	*H. germanica*	0.02026	36.32	2.48
SapeloZn0*9-1_7	*H. germanica*	0.02026	39.72	3.09
SapeloZn0*9-1_9	*H. germanica*	0.02026	47.01	2.97
SapeloZn0*9-1_10	*H. germanica*	0.02026	39.16	3.93
SapeloZn0*9-1_11	*H. germanica*	0.02026	32.02	2.03
SapeloZn0*9-1_12	*H. germanica*	0.02026	33.37	9.65
SapeloZn0*9-1_13	*H. germanica*	0.02026	24.58	15.13
SapeloZn9-1_1	*H. germanica*	0.825	58.09	3.33
SapeloZn9-1_2	*H. germanica*	0.825	57.49	11.47
SapeloZn9-1_3	*H. germanica*	0.825	41.49	5.41
SapeloZn9-1_4	*H. germanica*	0.825	447.41	250.17
SapeloZn9-2_1	*H. germanica*	0.05495	716.05	33.07
SapeloZn9-2_2	*A. tepida*	0.05495	149.53	61.85
SapeloZn9-2_3	*A. tepida*	0.05495	84.24	26.83
SapeloZn9-2_4	*A. tepida*	0.05495	101.73	7.64
SapeloZn9-2_5	*H. germanica*	0.05495	922.38	208.19
SapeloZn9-2_6	*H. germanica* (deformed)	0.05495	927.75	169.67
SapeloZn9-2_7	*A. tepida* (deformed)	0.05495	161.39	65.74
SapeloZn9-2_8	*H. germanica*	0.05495	55.32	3.29
SapeloZn9-2_9	*H. germanica*	0.05495	950.79	177.09
SapeloZn9-2_10	*A. tepida* (deformed)	0.05495	102.08	34.17

SapeloZn9-2_11	*A. tepida* (deformed)	0.05495	123.35	20.09
SapeloZn9-2_12	*A. tepida* (deformed)	0.05495	139.56	36.49
SapeloZn9-2_13	*A. tepida* (deformed)	0.05495	172.35	27.10
SapeloZn90-2_1	*A. tepida* (deformed)	20.455	131.45	18.29
SapeloZn900-1_1	*H. germanica* (deformed)	518.5	4948.91	1,339.86
SapeloIslandControl1_1	*A. tepida*	0.00280	2.80	0
SapeloIslandControl1_1B	*A. tepida*	0.01441	14.41	0.0047
SapeloIslandControl1_1C	*H. germanica*	0.01380	13.80	0
SapeloIslandControl2_1	*H. germanica*	0.01380	13.80	0
SapeloIslandControl2_1B	*H. germanica*	0.01343	13.43	0.00045
SapeloIslandControl2_2	*H. germanica*	0.01542	15.42	0.0044
SapeloIslandControl2_3	*H. germanica*	0.00816	8.16	0
SapeloIslandControl2_3B	*H. germanica*	0.00577	5.77	0
SapeloIslandControl2_4	*H. germanica*	0.01356	13.56	0.0026
SapeloIslandControl2_5	*H. germanica*	0.02059	20.59	0.0037

Table 3.2. Metal concentration in water, mean incorporated metal, and standard deviation among chambers in samples of Little Duck Key foraminifera used in propagule experiments. Each foraminifer was analyzed at least three times on three separate chambers. In some cases when the metal concentration measured by ICP-MS is particularly close to 0, the instrument can produce a negative number. These values have been corrected to 0 and are denoted by an asterisk.

Little Duck Key				
Sample Number	**Species**	**Metal Concentration in Water (mg/L)**	**Mean Incorporated Me/Ca (mmol/mol)**	**Standard Deviation of Me/Ca Between Chambers (mmol/mol)**
Arsenic				
LDKAs0*069-1_1	*T. oblonga*	1.111	373.15	30.22
LDKAs0*069-2_1	*T. oblonga*	1.571	3.41	4.47
LDKControl-2_1	*Q. sabulosa*	BDL*	1.18	0.0032
LDKControl-2_1B	*Q. sabulosa*	BDL*	3.45	0.0029
LDKControl-2_2	*T. oblonga*	BDL*	0.34	0.0023
LDKControl-2_2B	*T. oblonga*	BDL*	0.29	0.0022
Cadmium				
LDKCd0*04-1_1	*Q. sabulosa*	0.1206	24.59	28.92
LDKCd0*04-1_2	*T. oblonga*	0.1206	343.93	35.55
LDKCd0*04-1_3	*E. mexicanum*	0.1206	103.88	10.13
LDKCd0*04-2_2	*Q. sabulosa*	0.09448	2.99	3.06
LDKCd0*04-2_3	*Q. sabulosa*	0.09448	1.51	1.53
LDKCd0*04-2_5	*Q. sabulosa*	0.09448	4.25	1.59
LDKCd0*04-2_6	*Q. sabulosa*	0.09448	10.41	18.14
LDKCd0*4-2_1	*Q. sabulosa*	0.3866	6.53	5.98
LDKControl-2_1	*Q. sabulosa*	BDL*	2.14	0.0007
LDKControl-2_1B	*Q. sabulosa*	BDL*	4.62	0.0023
LDKControl-2_2	*T. oblonga*	BDL*	3.62	0.0017
LDKControl-2_2B	*T. oblonga*	BDL*	4.47	0.0039
Nickel				
LDKNi0*074-1_1	*T. oblonga*	0.1229	25.22	5.87
LDKNi0*074-1_2	*T. oblonga*	0.1229	22.62	3.72
LDKNi0*074-1_3	*T. oblonga*	0.1229	16.46	2.91
LDKNi0*074-1_4	*T. oblonga*	0.1229	14.91	4.02
LDKNi0*074-1_5	*T. oblonga*	0.1229	24.27	6.82
LDKNi0*074-1_6	*T. oblonga*	0.1229	15.68	6.13
LDKNi0*074-1_7	*T. oblonga*	0.1229	20.98	9.31

LDKNi0*074-2_1	*Q. sabulosa*	0.08327	9.033	1.82
LDKNi0*074-2_3	*Q. sabulosa*	0.08327	5.91	4.56
LDKNi0*074-2_4	*Q. sabulosa*	0.08327	1.56	10.38
LDKNi0*074-2_6	*T. oblonga*	0.08327	5.97	2.18
LDKNi0*074-2_7	*Q. sabulosa*	0.08327	6.82	5.72
LDKNi0*74-1_2	*T. oblonga*	0.2325	47.69	8.25
LDKNi0*74-1_3	*T. oblonga*	0.2325	11.82	3.49
LDKNi0*74-2_1	*Q. sabulosa*	0.2988	110.38	40.99
LDKNi74-1_1	*E. mexicanum*	25.62	170.42	54.30
LDKControl-2_1	*Q. sabulosa*	0.00758	7.58	0.0079
LDKControl-2_1B	*Q. sabulosa*	0.00174	1.74	0.0024
LDKControl-2_2	*T. oblonga*	0.00578	5.78	0.0046
LDKControl-2_2B	*T. oblonga*	0.00501	5.01	0.0012
Zinc				
LDKZn0*09-1_3	*Q. sabulosa*	0.04465	53.15	31.04
LDKZn0*09-2_1	*Q. sabulosa*	0.04717	26.63	7.07
LDKZn0*09-2_2	*Q. sabulosa*	0.04717	38.01	10.48
LDKZn0*09-2_4	*T. oblonga*	0.04717	431.89	131.12
LDKZn0*09-2_5	*Q. sabulosa*	0.04717	22.49	6.43
LDKZn0*9-1_1	*E. mexicanum*	0.2505	298.76	32.90
LDKZn9-1_1	*Q. sabulosa*	2.415	366.54	16.16
LDKZn9-2_1	*T. oblonga*	1.839	179.25	20.96
LDKZn90-2_1	*T. oblonga*	5.605	700.44	101.64
LDKControl-2_1	*Q. sabulosa*	0.00512	5.12	0.0025
LDKControl-2_1B	*Q. sabulosa*	0.00836	8.36	0.0007
LDKControl-2_2	*T. oblonga*	0.02671	26.71	0.0030
LDKControl-2_2B	*T. oblonga*	0.03037	30.37	0.0021

Table 3.3. Two-way ANCOVA data comparing the amount of heavy-metal incorporation variance, for each metal, caused by water chemistry and foraminiferal clade. This analysis is for all of the foraminifera from both sites.

Arsenic	**Degrees of Freedom**	**Sum of Squares**	**Mean Squares**	**F Ratio**	**P Value**
Water Chemistry	1	1	1	0	0.99
Clade	1	18622	18622	5.016	0.032
Residuals	31	115097	3713		
Cadmium					
Water Chemistry	1	3523814	3523814	147.929	2.0E-16
Clade	1	177	177	0.007	0.93
Residuals	52	1238693	23821		
Nickel					
Water Chemistry	1	22737	22737	79.958	1.9E-12
Clade	1	1018	1018	3.579	0.064
Residuals	57	16209	284		
Zinc					
Water Chemistry	1	22671080	22671080	371.802	2.0E-16
Clade	1	6588	6588	0.108	0.74
Residuals	53	3231743	60976		

Table 3.4. Two-way ANCOVA data comparing the amount of heavy-metal incorporation variance, for each metal, caused by water chemistry and foraminiferal species. This analysis was conducted for the Sapelo Island and Little Duck Key foraminifera separately.

Sapelo Island					
Arsenic	**Degrees of Freedom**	**Sum of Squares**	**Mean Squares**	**F Ratio**	**P Value**
Water Chemistry	1	0.2	0.2	0.031	0.86
Species	1	49.95	49.95	7.953	0.0093
Residuals	25	157.01	6.28		
Cadmium					
Water Chemistry	1	3357327	3357327	120.172	1.3E-13
Species	1	372	372	0.013	0.91
Residuals	40	1117506	27938		
Nickel					
Water Chemistry	1	23	22.52	0.215	0.65
Species	1	5	4.82	0.046	0.83
Residuals	37	3872	104.65		
Zinc					
Water Chemistry	1	22544920	22544920	342.988	2.0E-16
Species	1	92564	92564	1.408	0.24
Residuals	40	2629238	65731		
Little Duck Key					
Arsenic	**Degrees of Freedom**	**Sum of Squares**	**Mean Squares**	**F Ratio**	**P Value**
Water Chemistry	1	24818	24818	0.836	0.43
Species	1	1116	1116	0.038	0.86
Residuals	3	89036	29679		
Cadmium					
Water Chemistry	1	1407	1407	0.160	0.69
Species	2	36363	18182	2.071	0.19
Residuals	8	70228	8778		
Nickel					
Water Chemistry	1	22130	22130	88.2	6.5E-08
Species	2	6694	3347	13.34	0.00039
Residuals	16	4015	251		
Zinc					
Water Chemistry	1	376734	376734	24.53	0.00079
Species	2	56974	28487	1.855	0.21
Residuals	9	138226	15358		

Table 3.5. R_2 values representing the strength of the relationship between metal content in the water and the incorporation of that metal by a foraminiferal species. These values have been ranked from strongest to weakest.

Species	Metal	R_2 Value
Haynesina germanica	cadmium	0.930
Quinqueloculina sabulosa	zinc	0.890
Ammonia tepida	cadmium	0.884
Triloculina oblonga	zinc	0.692
Ammonia tepida	arsenic	0.588
Triloculina oblonga	nickel	0.588
Triloculina oblonga	cadmium	0.520
Triloculina oblonga	arsenic	0.408
Quinqueloculina sabulosa	nickel	0.406
Haynesina germanica	zinc	0.278
Haynesina germanica	arsenic	0.151
Haynesina germanica	nickel	0.139
Ammonia tepida	zinc	0.136
Quinqueloculina sabulosa	cadmium	0.119
Ammonia tepida	nickel	0.070
Quinqueloculina sabulosa	arsenic	N/A

Figures

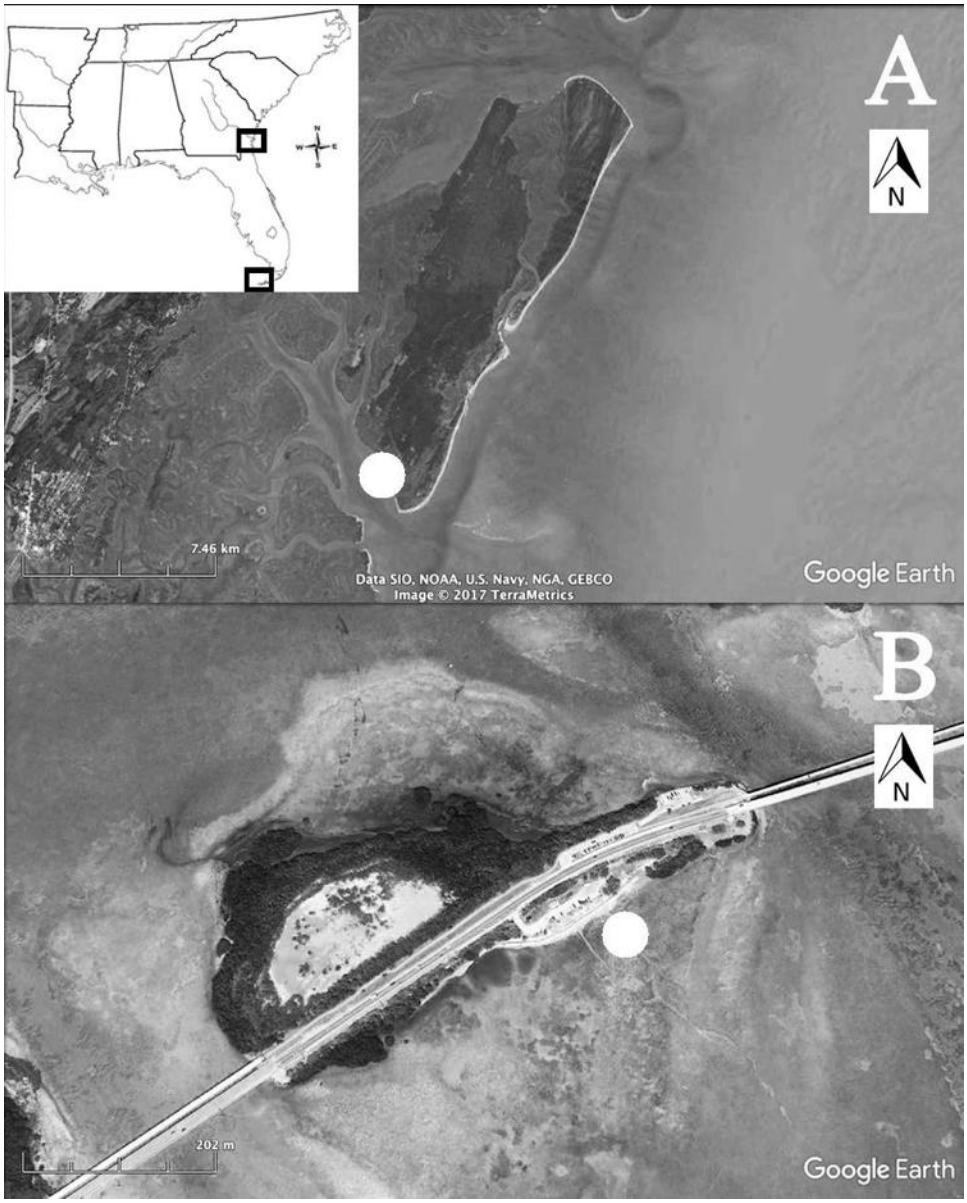

Fig. 3.1. Aerial views of the sampling sites: A Sapelo Island, Georgia, and B Little Duck Key, Florida (Google Earth).

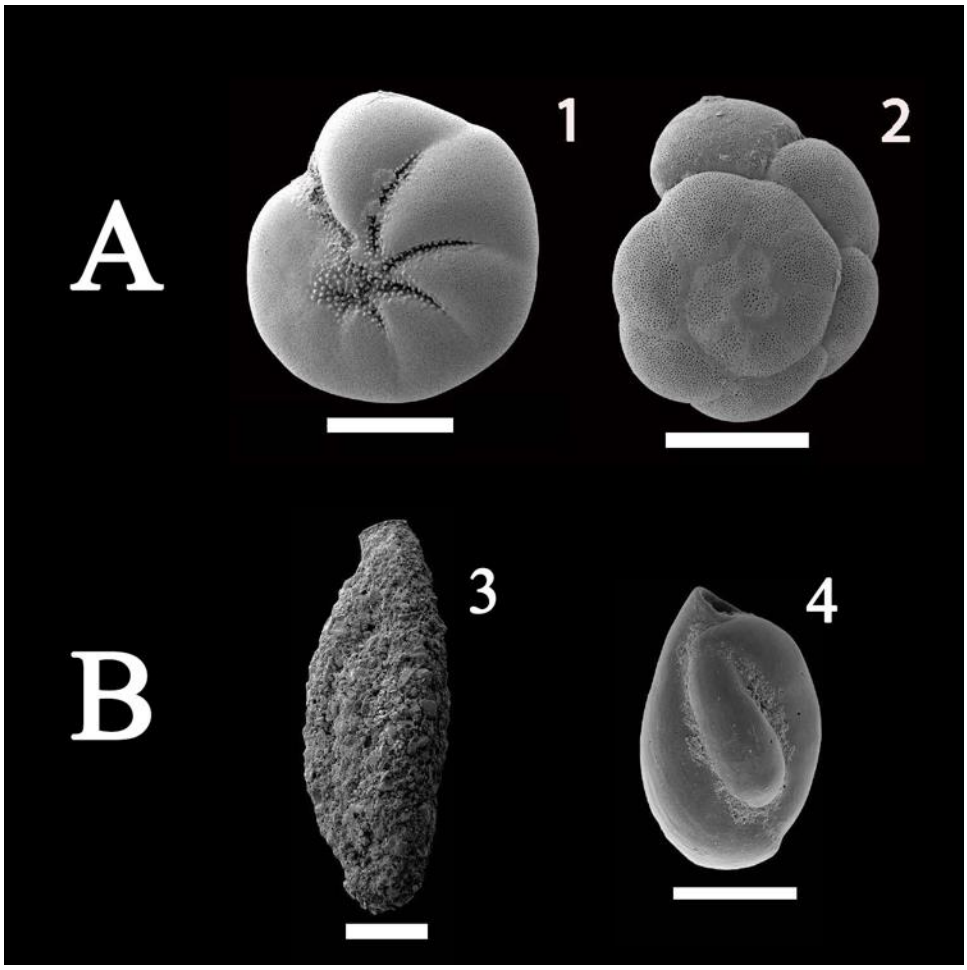

Fig. 3.2. SEM micrographs of the common foraminifera species that underwent LA-ICP-MS, Row A- Sapelo Island: **1** *Haynesina germanica* (Ehrenberg), **2** *Ammonia tepida* (Cushman) and Row B- Little Duck Key: **3** *Quinqueloculina sabulosa* (Cushman), **4** *Triloculina oblonga* (Montagu). All scale bars = 100 μm.

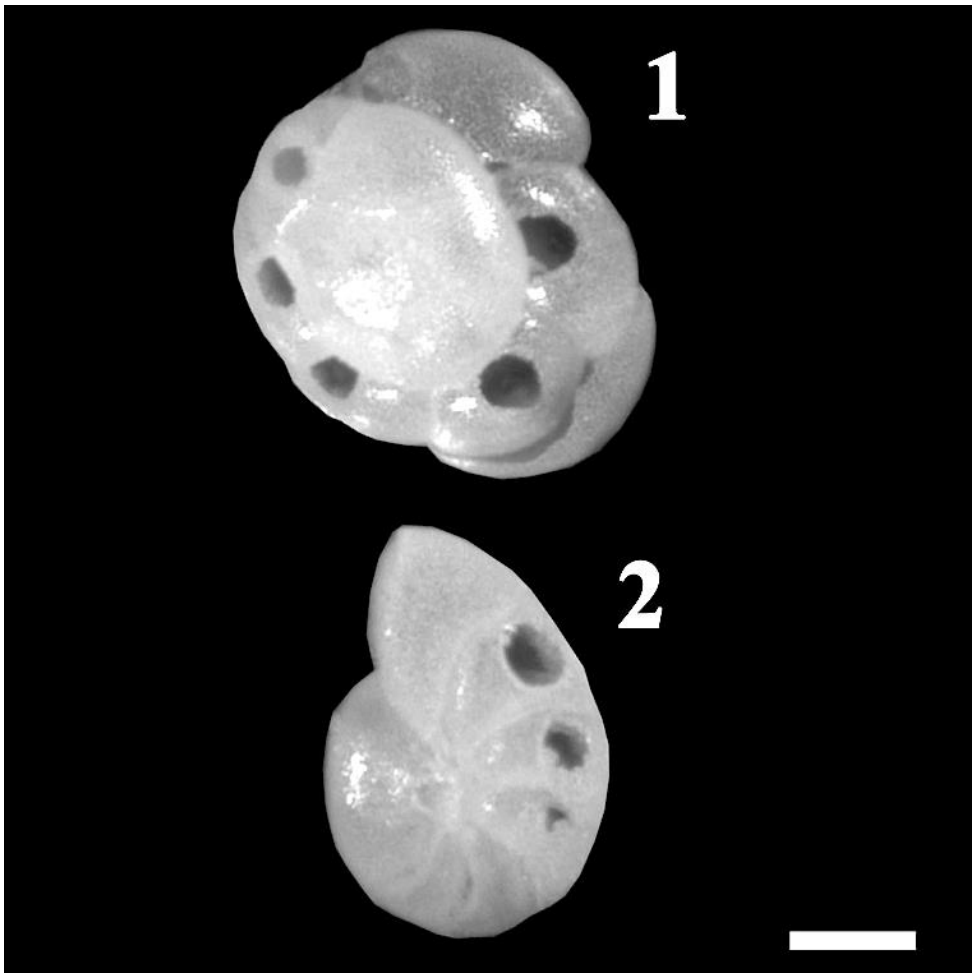

Fig. 3.3. Photographs of foraminifera species after LA-ICP-MS, **1** *Ammonia tepida* (Cushman), **2** *Haynesina germanica* (Ehrenberg). Scale bar = 75 μm.

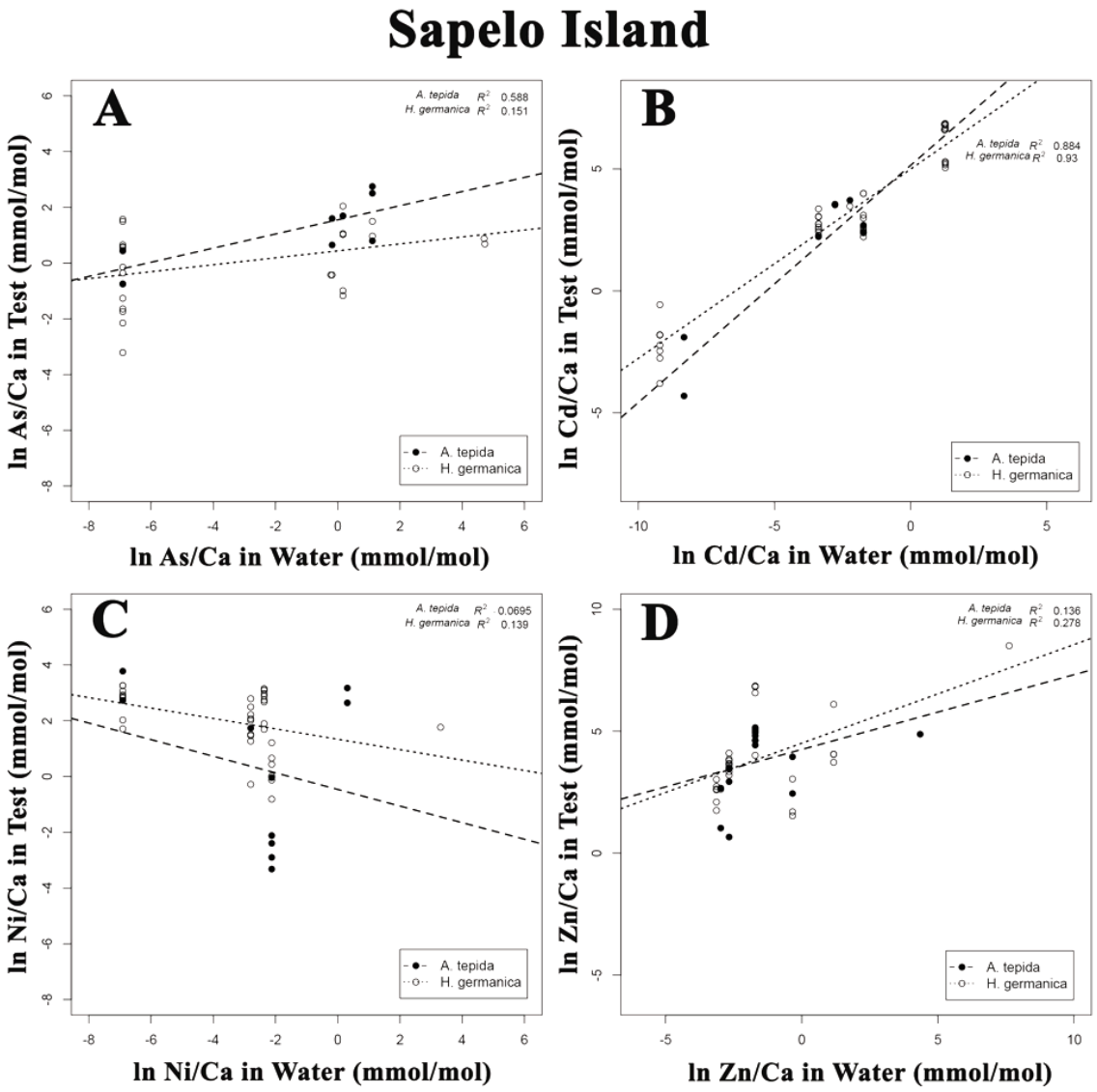

Fig. 3.4. Variation of incorporated trace metals in *A. tepida* and *H. germanica* compared to trace metal content in the experimental seawater for arsenic (A), cadmium (B), nickel (C), and zinc (D).

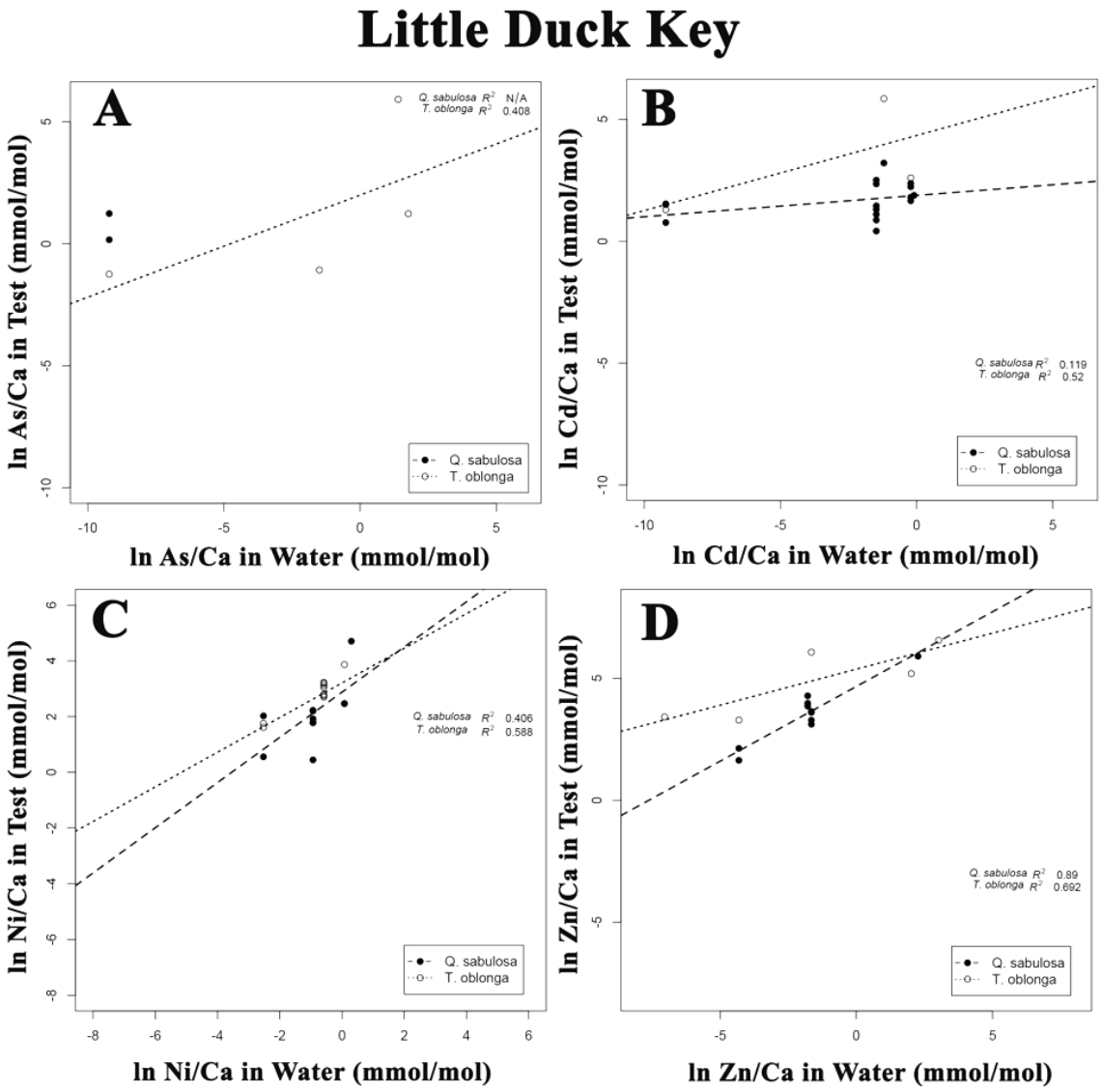

Fig. 3.5. Variation of incorporated trace metals in *Q. sabulosa* and *T. oblonga* compared to trace metal content in the experimental seawater for arsenic (A), cadmium (B), nickel (C), and zinc (D).

CHAPTER 4

EFFECTS OF VARIED TEMPERATURE AND SALINITY ON ASSEMBLAGES OF FORAMINIFERA GROWN WITH EXPOSURE TO HEAVY-METAL POLLUTANTS (NICKEL AND ZINC)[3]

[3] Smith, C.W., Goldstein, S.T. To be submitted to the Journal of Foraminiferal Research

Abstract

Benthic foraminifera are important environmental indicators of heavy-metal contaminants in marine environments because of their unique sensitivity to environmental change. However, this sensitivity can make parsing the effect of contaminants from other factors such as salinity and temperature difficult. To address this problem, this study compares individually the effects of heavy metals nickel and zinc on temperate rotalids and subtropical miliolids under different temperature and salinity regimes, including intermediate (22°C, 32 psu), elevated temperature (30°C, 32 psu), reduced temperature (18°C, 32 psu), elevated salinity (22°C, 40 psu), and reduced salinity (22°C, 12 psu). Assemblages of foraminifera were grown experimentally from propagules (small juveniles) collected from two shallow marine sites: Sapelo Island, Georgia, and Little Duck Key, Florida. Surface sediment was collected from both locations and sieved immediately after collection. Using the propagule method, assemblages of foraminifera were grown in a controlled setting from propagules in these sediment samples. Either nickel or zinc was added to each assemblage. Experimental conditions were held constant with only metal concentration, salinity, and temperature varying.

Increasing concentrations of nickel and zinc led to decreases in foraminiferal abundance under all temperatures and salinity conditions examined. In addition, high concentrations of nickel and especially zinc resulted in an increase of deformed tests of Sapelo Island foraminifera under intermediate (22°C, 32 psu) and high salinity (22°C, 40 psu) conditions. Far fewer deformities occurred in Sapelo Island assemblages in higher or lower salinities and temperatures. These results support the usefulness of foraminiferal

abundance and species abundance as tools for environmental analysis. Consistent with previous work, results also identify the problems associated with using test deformities alone as a bioindicator tool.

Introduction

Benthic foraminifera are known as important environmental indicators of contaminants in marine settings, specifically heavy metals (e.g., Alve, 1991; Alve, 1995; Yanko et al., 1998; Nigam et al., 2006; Frontalini & Coccioni, 2008; Martinez-Colon et al., 2009; Foster et al., 2012; Linshy et al., 2013; Martins et al., 2013; Brouillette Price et al., 2019; Smith & Goldstein, 2019). Their value as indicators stems from their sensitivity to changes in their environment (Boltovskoy et al., 1991; Alve, 1995; Yanko et al., 1994; Nigam et al., 2006; Martinez-Colon et al., 2009; Martins et al., 2013).

However, foraminiferal sensitivity to their environment can make distinguishing the effects of contaminants from other environmental factors difficult (e.g., Geslin et al., 2000; 2002; Lee et al., 2015). For example, foraminiferal assemblages change based on temperature, salinity, solubility of $CaCO_3$, water depth, wave action, light intensity, nutrition, substrate, and dissolved oxygen (e.g., Boltovskoy et al., 1991). In previous studies, the propagule method has provided a useful approach to this problem by allowing experimental control of the foraminiferal environment (Alve & Goldstein, 2002; 2003; 2010; 2014; Goldstein & Alve, 2011; Duffield et al., 2014; 2015; Weinmann & Goldstein, 2016; Weinmann et al., 2019; Brouillette Price et al., 2019; Smith & Goldstein, 2019; Smith et al., submitted). This allows for a more constrained analysis of contaminants and their effects on foraminiferal assemblages while limiting confounding factors. As shown in previous research, an ideal bioindicator foraminiferal species will be an easily

identifiable one that is clearly affected by heavy-metal contamination, in abundance, diversity, or test structure (e.g., Alve, 1991; Carnahan et al., 2008; Carnahan et al., 2009; Frontalini et al., 2009). However, if foraminifera are to be used effectively as bioindicators in natural marine settings, we must better understand how environmental factors can alter the effect of contaminants. For example, foraminifera in relatively extreme environments (higher or lower salinity, temperature, etc.) might be more resistant to the impacts of contaminants. It is also possible that foraminifera exposed to these conditions might be weaker and more susceptible to those impacts.

This study examines the effects of nickel and zinc at different temperatures and salinities, on abundance, diversity, and the occurrence of test deformities in experimentally grown assemblages (EGAs) of foraminifera. These EGAs were grown from propagules collected from two shallow-water sites: Sapelo island, Georgia, and Little Duck Key, Florida. The objectives are to (1) identify the impacts of nickel and zinc on foraminiferal assemblages experimentally grown under five different temperature and salinity regimes: intermediate (22°C, 32 psu), high temperature (30°C, 32 psu), low temperature (18°C, 32 psu), high salinity (22°C, 40 psu), and low salinity (22°C, 12 psu); (2) compare the potentially different effects that these contaminants have under these respective conditions; so that (3) the best bioindicator species irrespective of salinity and temperature for either location might be identified.

Materials and Methods

Sediment samples were taken from Sapelo Island (31.39021 N 81.28472 W) and Little Duck Key (24.68111 N 81.23194 W) during the summer of 2018 (Fig. 4.1). The upper few millimeters of surface sediment were collected within a ~1 square meter area

at each location. The sediment was sieved using 53- and 850-micron stainless steel sieves. The < 53-micron fraction was transported to the University of Georgia to be used as the source of propagules (e.g., Smith & Goldstein, 2019).

Using the propagule method (Goldstein & Alve, 2011; Alve & Goldstein, 2014), foraminiferal assemblages were grown in incubators from propagules present in the fine sediment (Alve & Goldstein, 2002; 2003; 2010). During growth, these EGAs were each exposed to either nickel or zinc. Nickel and zinc were chosen both because they are common heavy-metal contaminants in coastal marine settings (Alve, 1995), and also because both had produced morphological abnormalities in foraminifera in previous experiments (Smith & Goldstein, 2019; Smith et al., submitted).

The EGAs were grown in polypropylene containers (118 mL). Each container was filled with 20 mL of the < 53-micron sediment fraction from one of the two sites, and 40 mL of Instant Ocean artificial seawater. Following prior experiments, a set concentration of one heavy metal was added to the mixture in each container (Brouillette Price et al., 2019; Smith & Goldstein, 2019; Smith et al, submitted). Both nickel and zinc were added as dissolved chlorides. The concentrations added were based upon the United States Environmental Protection Agency's National Recommended Water Quality Criteria for Saltwater Criteria Maximum Concentration, which were 0.074 mg/L and 0.090 mg/L for nickel and zinc respectively. The Criteria Maximum Concentration (CMC) is the amount of heavy metal that can occur in an aquatic setting briefly before "resulting in an unacceptable effect" (U.S. EPA, 2006). Using these values as a starting place, the added concentrations increased by an order of magnitude for four additional levels for a total of five treatments. For each location, two EGAs were grown as controls without heavy

metals added. Overall, five groups of samples were created: intermediate, high temperature, low temperature, high salinity, and low salinity. Each group contained 44 EGAs total, 10 for each metal at each location, along with two control EGAs at each location, totaling 220 EGAs in all.

Beginning on June 1, 2018, containers were kept at a constant temperature and illuminated on a 12-hour cycle. The containers were rotated twice a week in the incubator to provide equal access to the light source. EGAs in the intermediate group were incubated at 22°C and 32 psu. The high temperature EGAs were incubated at 30°C and 32 psu, while the low temperature EGAs were incubated at 18°C and 32 psu. The high salinity EGAs were incubated at 22°C and 40 psu, while the low salinity EGAs were incubated at 22°C and 12 psu. The intermediate temperature and salinity were chosen to best represent the environment in which the sediment samples were collected. The higher and lower temperature and salinity values were chosen both to illustrate a range of possible effects on the foraminifera-heavy metal interaction, and to maintain realistic environmental values. The pH of the water in all the EGAs (8.1) remained the same as pre-experiment. After one month, the containers were harvested by sieving over a 63-micron sieve, and the contents fixed using a 10% formalin mixture, buffered with sodium carbonate to a pH of ~8.0–9.0, containing 1 g/L rose Bengal added as a vital stain (Walton, 1952; Murray & Bowser, 2000).

After one week, the fixative and stain mixture were removed, and the samples were rinsed with tap water and preserved in 50% ethanol. The contents were picked wet for foraminifera, which were identified, and counted. In each EGA, assemblage abundance and species abundance for every species were recorded, along with stained

and non-stained foraminifera. Diversity was calculated as species richness (S) and as Fisher's α. The Berger-Parker index was calculated as a measure of dominance (Berger & Parker, 1970; Hayek et al., 2010; Hayek & Buzas, 2013). Any shell deformities that occurred were recorded and standardized as the percentage deformed of the total assemblage. The dissolved heavy-metal concentration in the water of each EGA was measured using ICP-MS at the end of the experiment (e.g. Smith & Goldstein, 2019; Smith et al., submitted).

Using R software, assemblage total abundance and species abundance were plotted logarithmically against the heavy-metal content of each treatment. In the case of species abundance, only the two most common calcareous species at each location were plotted: *Ammonia tepida* (Cushman) and *Haynesina germanica* (Ehrenberg) at Sapelo Island, *Quinqueloculina sabulosa* Cushman and *Triloculina oblonga* (Montagu) at Little Duck Key (Fig. 4.2); R Core Team, 2019). The percentage of deformed tests was also plotted against heavy-metal content where applicable.

Results

Nickel and zinc caused an exponential decline in foraminiferal abundance as concentration increased over the CMC in EGAs from Sapelo Island and Little Duck Key (Figs. 4.3–4.6). This decline occurred in EGAs of all salinities (12, 32, and 40 psu) and temperatures (18, 22, and 30°C). In almost all cases, discrepancies occurred between the amount of metal added and the amount measured in solution after the experiment, which is consistent with previous research (Brouillette Price at al. 2019; Smith & Goldstein, 2019). Because of this, the post-experiment measurements were used throughout.

Abundances of the four most common species, *Ammonia tepida*, *Haynesina germanica*, *Quinqueloculina sabulosa*, and *Triloculina oblonga* declined in response to increased concentrations of nickel and zinc (Figs. 4.7–4.10). This decline occurred in each group of EGAs regardless of salinity or temperature, with three exceptions. In the high temperature EGAs exposed to nickel, *H. germanica* was never abundant and thus did not show a decline (Fig. 4.7), in the low salinity EGAs exposed to zinc, *Q. sabulosa* was never abundant and did not show a decline (Fig. 4.10), and in the low temperature EGAs exposed to zinc, *T. oblonga* was never abundant and also did not show a decline (Fig. 10).

Test deformities occurred in Sapelo Island EGAs exposed to nickel and zinc (Table 4.1), but only occurred in consistently high percentages (with a large sample size) in those exposed to zinc. Specifically, these high percentages occurred mostly in EGAs grown under intermediate conditions (22°C, 32 psu) exposed to zinc (Fig. 4.8). The percentage of deformed tests in these EGAs spikes at zinc concentrations of 0.055 mg/L (33.77 % deformed) and 0.825 mg/L (17.86 % deformed) respectively. The only other EGA with substantial deformities is in the high salinity group exposed to 0.88 mg/L of zinc (19.05 %; Table 4.1). Test deformities were virtually non-existent in EGAs from Little Duck Key exposed to both metals (Table 4.2). In all three assemblages with significant deformities, only rotalid species had deformed tests, with deformed *Ammonia tepida* present in all three, and deformed *Haynesina germanica* present in only one (0.055 mg/L; Table 4.3).

Diversity of the EGAs, measured as species richness, tended to decrease as nickel and zinc concentrations increased at Sapelo Island and Little Duck Key (Table 4.1 and

4.2). This is consistent with previous research (Smith & Goldstein, 2019). In the Sapelo Island EGAs, species richness decreased at nickel concentrations above 0.029 mg/L (22°C, 32 psu), 0.454 mg/L (22°C, 12 psu), 0.355 mg/L (22°C, 40 psu), 1.376 mg/L (18°C, 32 psu), and 0.84 mg/L (22°C, 40 psu). In those exposed to zinc, species richness decreased at concentrations above 0.825 mg/L (22°C, 32 psu), 0.172 mg/L (22°C, 12 psu), 0.88 mg/L (22°C, 40 psu), 0.286 mg/L (18°C, 32 psu), and 0.273 mg/L (30°C, 32 psu). In the Little Duck Key EGAs, species richness decreased at nickel concentrations above 0.299 mg/L (22°C, 32 psu), 0.106 mg/L (22°C, 12 psu), 0.199 mg/L (22°C, 40 psu), 0.02 mg/L (18°C, 32 psu), and 0.175 mg/L (30°C, 32 psu). In those exposed to zinc, species richness decreased at concentrations above 0.274 mg/L (22°C, 32 psu), 1.3 mg/L (22°C, 12 psu), 0.934 mg/L (22°C, 40 psu), 1.174 mg/L (18°C, 32 psu), and 0.723 mg/L (22°C, 32 psu).

Fisher's α shows no consistent pattern in response to larger concentrations of nickel or zinc in Sapelo Island and Little Duck Key EGAs (Tables 4.1 and 4.2). In some cases, in contrast to species richness, it even increases in response to greater concentrations of heavy metal.

In contrast, dominance as measured by Berger-Parker, generally increases in response to nickel or zinc (Tables 4.1 and 4.2). In intermediate (22°C, 32 psu) and high salinity (22°C, 40 psu), Sapelo Island EGAs exposed to both metals, dominance tends to increase as concentration increases. In low salinity (22°C, 12 psu) and low temperature (18°C, 32 psu) Little Duck Key EGAs exposed to nickel, dominance starts high, decreases, and then increases as concentration increases. In low temperature (18°C, 32

psu) Little Duck Key EGAs exposed to zinc and high temperature (30°C, 32 psu) Little Duck Key EGAs exposed to both metals, dominance increases as concentration increases.

Discussion

Previous studies have shown that foraminiferal population density tends to decline in response to heavy-metal contamination (e.g., Alve, 1995; Yanko et al., 1998; Linshy et al., 2013; Brouillette Price et al., 2019; Smith & Goldstein, 2019). The results of this study are consistent with these findings; increased nickel and zinc concentrations result in the exponential decline of overall abundance and individual species abundances in both the Sapelo Island and Little Duck Key EGAs (Smith & Goldstein, 2019). This pattern occurs in EGAs exposed to each set of environmental conditions. The only noticeable difference is a depressed initial abundance in EGAs with low concentrations of metal in high and low salinity and temperature settings (Figs. 4.3–4.6).

Temperature and salinity had the most dramatic effect on the number of test deformities in the assemblages. Deformities primarily occurred in assemblages exposed to zinc, not nickel, which aligns with previous work (Smith & Goldstein, 2019). However, substantial deformities only occurred in assemblages incubated at 22°C and 32 or 40 psu. Assemblages at low salinities, high temperatures, and low temperatures contained a few deformities, but not substantial percentages.

Abundance and Diversity

The most prevalent foraminifera in this study (*Ammonia tepida* and *Haynesina germanica* from Sapelo Island, *Quinqueloculina sabulosa* and *Triloculina oblonga* from Little Duck Key) were all common in assemblages with salinity at 32 psu. However, in assemblages with salinity at 12 psu or 40 psu, these species proved much less common.

Foraminiferal response to salinity depends heavily on the species involved and their specific salinity preferences (Boltovskoy et al., 1991). Both elevated and lowered salinities can act as a stressor on foraminiferal populations (Murray, 1973; Brasier, 1975; Scott & Medioli, 1980a; Boltovskoy et al., 1991). The combination of elevated or lowered salinities and heavy-metal contamination could amplify the negative effects on foraminifera. However, in this study, foraminiferal response to increased heavy-metal concentrations remained fairly consistent across all salinities tested with total abundance declining, in most cases exponentially. The coefficients for each plot are relatively similar to one another and show similar declines (Figs. 4.3–4.6). Because the abundance of foraminifera in the uncontaminated high and low salinity assemblages were comparatively low, the decrease in abundance as nickel and zinc concentration increases is less dramatic in most cases.

Both locations in this study are warm-water locations, with Sapelo Island varying more seasonally (7–31°C) than Little Duck Key (17–31°C; Goldstein & Alve, 2011; Weinmann & Goldstein, 2016). The most prevalent foraminifera in this study were all common in assemblages with temperature at 22°C. However, in assemblages with temperature at 18°C or 30°C, these species proved much less abundant. As with salinity, similar coefficients indicate foraminiferal response to increased heavy-metal concentrations remained relatively consistent across all temperatures tested with total abundance declining exponentially in most cases (Figs. 4.3–4.6). Because the abundance of foraminifera in the high and low temperature control assemblages were comparatively low (Tables 4.1 and 4.2), the decrease in abundance as nickel and zinc concentration increases is less severe in most cases.

The decline of species richness and more inconsistent response of Fisher's α are both consistent with previous findings (Smith & Goldstein, 2019). Species richness is the number of species present, while Fisher's α is equivalent to the number of singletons present. The decline in number of species makes sense as less species are able to tolerate the contamination as heavy metal concentration increases. The number of singletons is less likely to decrease, because as concentration increases, often there are more singletons of species that had been more prevalent at lower concentrations. Because of this, species richness is probably a better indicator of diversity in this specific case. Regardless, diversity responds in similar ways to greater nickel and zinc concentrations regardless of salinity or temperature (Tables 4.1 and 4.2), which supports the use of diversity in heavy-metal contamination monitoring.

Test Deformities

Salinity may be related to morphologic test changes in foraminifera (Boltovskoy et al., 1991). In salinities lower than a species' preference, tests are reportedly smaller, more thin-walled, and have decreased ornamentation (Tappan, 1951; Morishima, 1955; Kurc, 1961; Wright, 1968; Murray, 1991; Murray, 2006). Other types of morphologic change have been reported in response to hypersaline environments (Brasier, 1975; Scott & Medioli, 1980). However, no test deformities were present in the hypersaline or hyposaline assemblages grown without exposure to a metal. The only significant deformities occurred in the two assemblages grown at normal salinity (32 psu), and in one assemblage at high salinity (40 psu), both exposed to elevated concentrations of zinc.

No major differences in the composition of species assemblages exist in the three EGAs with significant test deformities, (Table 4.3). In all three, the primary species

effected are *Ammonia tepida*, with deformed *Haynesina germanica* present only in one of the intermediate EGAs (0.055 mg/L). The relative lack of deformities in the high and low salinity assemblages exposed to zinc is puzzling. Studies have reported extensive deformities, specifically in *A. tepida*, in environments that are consistently hypersaline (Stouff, 1999a; 1999b; Debenay et al., 2001; Geslin et al., 2002). However, other research has shown that foraminifera can occur in hypersaline environments with virtually no test deformities (Scott et al., 1976; Malmgren, 1984; Boltovskoy et al., 1991). Another possible explanation is the lack of salinity fluctuation during the experiment. In all of the EGAs, the salinity, whether elevated, intermediate, or reduced, was constant throughout. The root cause of test deformities in hypersaline and hyposaline environments could be caused by the fluctuation of salinity and not the high or low salinity alone (Arnal, 1955; Tufescu, 1968; Closs & Madeira, 1968; Boltovskoy et al., 1991; Murray, 2006; Lee et al., 2015).

Temperature is also suspected to play a significant role in foraminiferal test structure (Carpenter, 1856; Schnitker, 1974; Walton and Sloan, 1990; Boltovskoy et al., 1991; Murray, 2006). Specifically, decreases in temperature are thought to cause size increases of tests (Bandy, 1963; Arnold, 1967; Boltovskoy et al., 1991), however, some contradictory evidence shows the opposite to be true (Phleger and Hamilton, 1946; Theyer, 1971). Regarding other morphological changes, results seem to vary depending on the species involved (Schnitker, 1974; Miller et al., 1982; Walton & Sloan, 1990; Boltovskoy et al., 1991; Murray, 2006). For example, temperature variation reportedly causes multiple test shapes in *Ammonia beccarii* (Linnaeus; Schnitker, 1974; Walton and Sloan, 1990) and *Elphidium excavatum* (Terquem; Miller et al., 1982). In this study,

similar to salinity, temperature alone caused no noticeable deformities in the foraminifera. This is unusual as previous propagule experiments from Sapelo Island have shown numerous deformities in foraminifera grown with exposure to zinc at 18°C (Brouillette Price et al., 2019). The depressed foraminiferal abundance in high and low temperature assemblages possibly resulted in fewer deformed tests. Temperature variation could also cause less significant test deformities comparable to other factors such as pollution and salinity.

Conclusions

Nickel and zinc have a negative effect on foraminiferal population abundance at concentrations above the U.S. EPA's Criteria Maximum Concentration. This negative effect was present under all salinity and temperature conditions tested. Diversity in richness showed decline in response to higher metal concentrations in some, but not all cases, while diversity in Fisher's α is more inconsistent in response.

The most common calcareous species from each location (*Haynesina germanica* and *Ammonia tepida* at Sapelo Island and *Quinqueloculina sabulosa* and *Triloculina oblonga* at Little Duck Key) declined as nickel and zinc concentrations increased under all environmental conditions. However, these species persisted at greater concentrations across the range of salinities and temperatures tested, making them viable bioindicators in multiple types of environments.

Confirming, previous studies, zinc was more likely to cause major test deformities than nickel, and rotalid species such as *Ammonia tepida* and *Haynesina germanica* were much more susceptible to deformation than miliolid species. However, these deformities only occurred in assemblages at temperatures of 22°C and salinities of 32 psu and 40 psu.

In EGAs exposed to higher or lower salinities and temperatures, very few deformities occurred.

Tables

Table 4.1. Diversity data, including number of specimens (N), number of species (S), Fisher's α, Berger-Parker Index, and the percentage of deformed tests for the assemblages grown from Sapelo Island propagules. The symbol N/A denotes an undetectable value.

Sapelo Island (22º 32 PSU)							
Expected (mg/L)		**Actual (mg/L)**	***N***	***S***	**Deformed Tests (%)**	**Fisher's α**	**Berger-Parker**
Nickel							
0.074 (A)		0.011	36	4	0	1.15	0.44
0.074 (B)		0.023	37	4	5.41	1.14	0.59
0.74 (A)		0.016	260	7	0.77	1.32	0.37
0.74 (B)		0.029	225	8	1.33	1.62	0.33
7.4 (A)		0.438	40	3	0	0.75	0.40
7.4 (B)		0.323	35	2	2.86	0.46	0.46
74 (A)		6.24	8	2	0	0.85	0.50
74 (B)		26.73	3	2	33.33	2.62	0.67
740 (A)		151.1	17	3	0	1.06	0.88
740 (B)		264.4	14	2	0	0.64	0.71
Zinc							
0.09 (A)		0.015	109	6	0	1.37	0.34
0.09 (B)		0.168	104	9	0	2.36	0.38
0.9 (A)		0.02	132	4	1.52	0.78	0.65
0.9 (B)		0.024	110	7	0.91	1.66	0.28
9.0 (A)		0.825	28	5	17.86	1.77	0.54
9.0 (B)		0.055	77	4	33.77	0.89	0.53
90 (A)		17.05	0	0	0	0	0
90 (B)		20.46	8	1	37.50	0.30	1
900 (A)		518.5	1	1	0	N/A	1
900 (B)		634.5	0	0	0	0	0
Controls							
	Nickel (mg/L)	**Zinc (mg/L)**					
1	0.0406	0.0123	124	3	0	0.55	0.55
2	0.0424	0.0115	111	2	1.80	0.34	0.74
Sapelo Island (22º 12 PSU)							
Expected (mg/L)		**Actual (mg/L)**	***N***	***S***	**Deformed Tests (%)**	**Fisher's α**	**Berger-Parker**
Nickel							
0.074 (A)		0.007	56	5	0	1.33	0.50
0.074 (B)		0.008	128	5	0	1.04	0.55

0.74 (A)	0.019	142	5	0	1.01	0.73
0.74 (B)	0.019	136	5	0	1.02	0.75
7.4 (A)	0.454	30	5	0	1.71	0.33
7.4 (B)	0.509	41	5	0	1.49	0.54
74 (A)	6.58	21	4	4.76	1.46	0.48
74 (B)	5.88	10	3	10	1.45	0.80
740 (A)	154.4	22	3	0	0.94	0.68
740 (B)	316.4	15	2	0	0.62	0.60
Zinc						
0.09 (A)	0	203	6	0	1.16	0.66
0.09 (B)	0.059	166	6	0	1.22	0.61
0.9 (A)	0.172	60	4	0	0.96	0.77
0.9 (B)	0.01	60	6	0	1.66	0.38
9.0 (A)	0.817	62	2	0	0.39	0.95
9.0 (B)	0.634	45	1	0	0.18	1
90 (A)	9.78	13	2	0	0.66	0.62
90 (B)	24.09	18	2	0	0.57	0.61
900 (A)	615.8	4	1	0	0.43	1
900 (B)	865.7	5	2	0	1.24	0.80
Controls						
	Nickel (mg/L)	**Zinc (mg/L)**				
1	0.0255	0.00501	105	5	0	1.09	0.43
2	0.0205	0.00688	132	6	0	1.29	0.42
Sapelo Island (22º 40 PSU)						
Expected (mg/L)	**Actual (mg/L)**	***N***	***S***	**Deformed Tests (%)**	**Fisher's α**	**Berger-Parker**
Nickel						
0.074 (A)	0.015	97	4	0	0.84	0.56
0.074 (B)	0.015	108	3	0	0.57	0.47
0.74 (A)	0.027	60	3	1.67	0.66	0.67
0.74 (B)	0.027	94	6	0	1.43	0.45
7.4 (A)	0.203	93	7	0	1.75	0.38
7.4 (B)	0.355	131	5	0	1.03	0.56
74 (A)	15.1	11	1	0	0.27	1
74 (B)	9.49	9	1	0	0.29	1
740 (A)	145.5	17	2	0	0.59	0.65
740 (B)	238.9	15	3	0	1.12	0.40
Zinc						
0.09 (A)	0	160	6	0	1.23	0.60
0.09 (B)	0	152	6	0	1.25	0.49

0.9 (A)	0.005	108	7	3.70	1.67	0.53
0.9 (B)	0	117	7	1.71	1.63	0.62
9.0 (A)	0.88	21	2	19.05	0.54	0.52
9.0 (B)	0.113	8	2	0	0.85	0.63
90 (A)	11.15	0	0	0	0.00	0
90 (B)	11.07	0	0	0	0.00	0
900 (A)	581.9	16	2	0	0.60	0.81
900 (B)	636.5	24	3	0	0.90	0.71

Controls

	Nickel (mg/L)	Zinc (mg/L)					
1	0.0202	0.00403	118	4	0	0.80	0.55
2	0.0203	0.00614	128	5	0	1.04	0.40

Sapelo Island (18º 32 PSU)

Expected (mg/L)	Actual (mg/L)	*N*	*S*	Deformed Tests (%)	Fisher's α	Berger-Parker
Nickel						
0.074 (A)	0.02	65	5	0	1.26	0.48
0.074 (B)	0.012	64	6	0	1.62	0.34
0.74 (A)	0.019	31	6	0	2.21	0.29
0.74 (B)	0.015	69	6	0	1.58	0.26
7.4 (A)	0.909	55	6	0	1.71	0.40
7.4 (B)	1.376	78	5	6.41	1.19	0.72
74 (A)	9.64	10	3	0	1.45	0.50
74 (B)	9.64	4	2	0	1.59	0.50
740 (A)	242.4	15	2	0	0.62	0.60
740 (B)	301.5	7	1	0	0.32	1
Zinc						
0.09 (A)	0.007	52	5	0	1.36	0.35
0.09 (B)	0.008	48	4	2.08	1.04	0.58
0.9 (A)	0.024	85	3	2.35	0.61	0.78
0.9 (B)	0.024	115	3	0.87	0.56	0.75
9.0 (A)	0.286	21	2	0	0.54	0.81
9.0 (B)	0.179	85	4	8.24	0.87	0.65
90 (A)	12.12	15	2	0	0.62	0.73
90 (B)	9.96	10	2	0	0.75	0.80
900 (A)	683.5	5	1	0	0.38	1
900 (B)	698.3	15	2	0	0.62	0.73

Controls

	Nickel (mg/L)	Zinc (mg/L)					
1	0.0390	0.00574	98	5	0	1.11	0.46

2	0.0380	0.517	124	6	0	1.32	0.43

Sapelo Island (30º 32 PSU)

Expected (mg/L)	Actual (mg/L)	*N*	*S*	Deformed Tests (%)	Fisher's α	Berger-Parker
Nickel						
0.074 (A)	0.0124	41	3	0	0.75	0.85
0.074 (B)	0.0152	212	7	0	1.39	0.47
0.74 (A)	0.0263	220	4	0	0.69	0.48
0.74 (B)	0.0287	141	6	0	1.27	0.55
7.4 (A)	0.192	100	6	0	1.40	0.54
7.4 (B)	0.1744	39	5	0	1.52	0.33
74 (A)	1.3	21	2	0	0.54	0.62
74 (B)	0.84	35	4	8.57	1.16	0.37
740 (A)	111.3	10	2	0	0.75	0.70
740 (B)	116.9	9	2	0	0.80	0.56
Zinc						
0.09 (A)	0	104	7	0	1.69	0.43
0.09 (B)	0	80	6	0	1.50	0.55
0.9 (A)	0	104	4	0	0.83	0.76
0.9 (B)	0	60	4	0	0.96	0.55
9.0 (A)	0.103	143	5	9.79	1.01	0.52
9.0 (B)	0.273	57	3	7.02	0.67	0.49
90 (A)	1.64	12	2	0	0.69	0.58
90 (B)	3.42	15	3	0	1.12	0.53
900 (A)	595.7	0	0	0	0.00	0
900 (B)	291	3	2	0	2.62	0.67
Controls						
	Nickel (mg/L)	**Zinc (mg/L)**				
1	0.0351	1.068	104	4	0	0.83	0.61
2	0.0336	0.00956	98	4	0	0.84	0.35

Table 4.2. Diversity data, including number of specimens (N), number of species (S), Fisher's α, Berger-Parker Index, and the percentage of deformed tests for the assemblages grown from Little Duck Key propagules. The symbol N/A denotes an undetectable value.

Little Duck Key (22º 32 PSU)							
Expected (mg/L)	**Actual (mg/L)**	***N***	***S***	**Deformed Tests (%)**	**Fisher's α**	**Berger-Parker**
Nickel							
0.074 (A)	0.123	100	11	0	3.15	0.32
0.074 (B)	0.083	102	7	0	1.70	0.29
0.74 (A)	0.233	73	10	0	3.13	0.22
0.74 (B)	0.299	35	7	0	2.63	0.31
7.4 (A)	1.341	12	9	0	16.34	0.25
7.4 (B)	1.748	27	6	0	2.39	0.81
74 (A)	25.62	6	5	0	14.11	0.33
74 (B)	17.86	2	2	0	N/A	0.50
740 (A)	290.1	7	2	0	0.93	0.71
740 (B)	336.7	8	2	0	0.85	0.75
Zinc							
0.09 (A)	0.045	46	6	0	1.84	0.35
0.09 (B)	0.047	72	7	0	1.92	0.25
0.9 (A)	0.251	22	8	0	4.52	0.36
0.9 (B)	0.274	21	5	0	2.07	0.38
9.0 (A)	2.415	1	1	0	N/A	1
9.0 (B)	1.839	3	3	0	N/A	0.33
90 (A)	5.4	3	3	0	N/A	0.33
90 (B)	5.61	3	3	0	N/A	0.33
900 (A)	9.1	0	0	0	0	0
900 (B)	10.8	0	0	0	0	0
Controls							
	Nickel (mg/L)	**Zinc (mg/L)**					
1	0.0188	0.00369	88	7	0	1.79	0.33
2	0.0169	0.00316	84	9	0	2.55	0.25
Little Duck Key (22º 12 PSU)							
Expected (mg/L)	**Actual (mg/L)**	***N***	***S***	**Deformed Tests (%)**	**Fisher's α**	**Berger-Parker**
Nickel							
0.074 (A)	0.11	38	3	0	0.76	0.71
0.074 (B)	0.091	57	3	0	0.67	0.61
0.74 (A)	0.098	0	0	0	0	0

0.74 (B)	0.097	30	7	0	2.87	0.33
7.4 (A)	0.106	24	5	0	1.92	0.42
7.4 (B)	0.083	33	5	0	1.64	0.33
74 (A)	0.21	4	2	0	1.59	0.75
74 (B)	0.22	10	2	0	0.75	0.70
740 (A)	1.8	11	2	0	0.72	0.91
740 (B)	1.4	6	2	0	1.05	0.67
Zinc						
0.09 (A)	0	45	2	0	0.43	0.76
0.09 (B)	0	51	3	0	0.70	0.76
0.9 (A)	0	0	0	0	0	0
0.9 (B)	0	5	4	0	9.24	0.40
9.0 (A)	0	11	4	0	2.26	0.64
9.0 (B)	0	12	2	0	0.69	0.75
90 (A)	0	0	0	0	0	0
90 (B)	0	0	0	0	0	0
900 (A)	1.3	2	1	0	0.80	1
900 (B)	1.4	2	1	0	0.80	1
Controls						
	Nickel (mg/L)	**Zinc (mg/L)**				
1	0.00901	0.00349	61	4	0	0.96	0.67
2	0.00685	0.00668	57	4	0	0.98	0.51

Little Duck Key (22º 40 PSU)

Expected (mg/L)	**Actual (mg/L)**	***N***	***S***	**Deformed Tests (%)**	**Fisher's α**	**Berger-Parker**
Nickel						
0.074 (A)	0.093	148	7	0	1.53	0.26
0.074 (B)	0.076	159	5	0	0.98	0.33
0.74 (A)	0.194	108	6	0	1.37	0.23
0.74 (B)	0.199	122	6	0	1.32	0.29
7.4 (A)	2.113	82	4	0	0.88	0.71
7.4 (B)	1.376	92	5	0	1.13	0.61
74 (A)	8.52	3	3	0	N/A	0.33
74 (B)	8.88	2	1	0	0.80	1
740 (A)	337.5	0	0	0	0	0
740 (B)	337.9	1	1	0	N/A	1
Zinc						
0.09 (A)	0	141	6	0	1.27	0.26
0.09 (B)	0	135	6	0	1.29	0.28
0.9 (A)	0	98	7	0	1.73	0.29

0.9 (B)		0	101	8	0	2.04	0.32
9.0 (A)		2.929	42	8	0	2.93	0.31
9.0 (B)		0.934	53	7	0	2.16	0.43
90 (A)		4.96	0	0	0	0	0
90 (B)		5.59	0	0	0	0	0
900 (A)		8.6	0	0	0	0	0
900 (B)		11	7	2	0	0.93	0.57
Controls							
	Nickel (mg/L)	**Zinc (mg/L)**					
1	0.0166	0.00124	154	6	0	1.24	0.27
2	0.0151	0.00628	139	7	0	1.55	0.28
Little Duck Key (18º 32 PSU)							
Expected (mg/L)		**Actual (mg/L)**	***N***	***S***	**Deformed Tests (%)**	**Fisher's α**	**Berger-Parker**
Nickel							
0.074 (A)		0.029	89	9	0	2.50	0.51
0.074 (B)		0.034	97	10	0	2.80	0.53
0.74 (A)		0.225	38	11	0	5.19	0.26
0.74 (B)		0.306	54	10	0	3.61	0.30
7.4 (A)		0.018	28	8	0	3.74	0.29
7.4 (B)		0.02	45	7	0	2.32	0.29
74 (A)		39.04	8	5	0	5.70	0.38
74 (B)		41.09	5	2	0	1.24	0.60
740 (A)		377.3	2	1	0	0.80	1
740 (B)		447.6	0	0	0	0	0
Zinc							
0.09 (A)		0	44	7	0	2.34	0.30
0.09 (B)		0	57	7	0	2.09	0.23
0.9 (A)		0	16	9	0	8.50	0.25
0.9 (B)		0	20	6	0	2.91	0.30
9.0 (A)		1.271	1	1	0	N/A	1
9.0 (B)		1.174	0	0	0	0	0
90 (A)		8.42	4	2	0	1.59	0.50
90 (B)		8.39	6	2	0	1.05	0.83
900 (A)		13.4	4	1	0	0.43	1
900 (B)		11.8	1	1	0	N/A	1
Controls							
	Nickel (mg/L)	**Zinc (mg/L)**					
1	0.0170	0.00206	122	8	0	1.92	0.50
2	0.0152	0.00618	122	10	0	2.58	0.39

Little Duck Key (30º 32 PSU)							
Expected (mg/L)	**Actual (mg/L)**	***N***	***S***	**Deformed Tests (%)**	**Fisher's α**	**Berger-Parker**
Nickel						
0.074 (A)	0.07	180	11	0	2.58	0.21
0.074 (B)	0.07	157	10	0	2.38	0.25
0.74 (A)	0.192	110	6	0	1.36	0.27
0.74 (B)	0.175	100	6	0	1.40	0.25
7.4 (A)	1.307	85	12	0	3.81	0.20
7.4 (B)	1.239	95	14	0	4.53	0.25
74 (A)	1.86	4	4	0	N/A	0.25
74 (B)	2.79	10	4	0	2.47	0.40
740 (A)	377.4	2	1	0	0.80	1
740 (B)	306.2	3	1	0	0.53	1
Zinc						
0.09 (A)	0	168	7	0	1.48	0.33
0.09 (B)	0	177	7	0	1.46	0.34
0.9 (A)	0	30	7	0.03	2.87	0.37
0.9 (B)	0	56	6	0	1.70	0.34
9.0 (A)	1.091	10	6	0	6.33	0.20
9.0 (B)	0.723	15	7	0	5.10	0.53
90 (A)	2.26	1	1	0	N/A	1
90 (B)	3.11	2	2	0	N/A	1
900 (A)	4.8	2	2	0	N/A	0.50
900 (B)	3.8	5	2	0	1.24	0.60
Controls						
	Nickel (mg/L)	**Zinc (mg/L)**				
1	0.0163	0.0729	197	9	0	1.94	0.24
2	0.0145	0.00472	145	8	0	1.82	0.22

Table 4.3. A breakdown of species with deformed tests in three assemblages with significant number of deformities.

Conditions	**22º 32 psu**				**22º 40 psu**	
Concentration	**0.825 mg/L Zinc**		**0.055 mg/L Zinc**		**0.88 mg/L Zinc**	
Species	***N***	**Deformed**	***N***	**Deformed**	***N***	**Deformed**
Ammonia tepida	9	5	41	19	11	4
Haynesina germanica	15	0	17	7	0	0

Figures

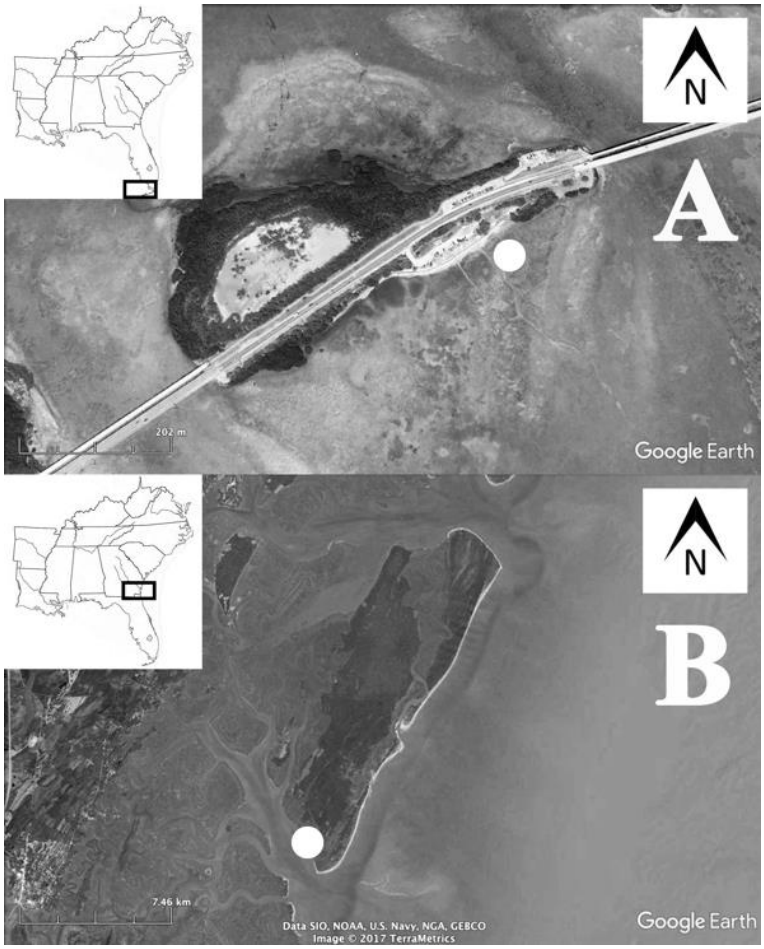

Fig. 4.1. Aerial views of the sampling sites in both study areas: **A** Little Duck Key, Florida (24.68111 N 81.23194 W), and **B** Sapelo Island, Georgia (31.39021 N 81.28472 W) (Google Earth).

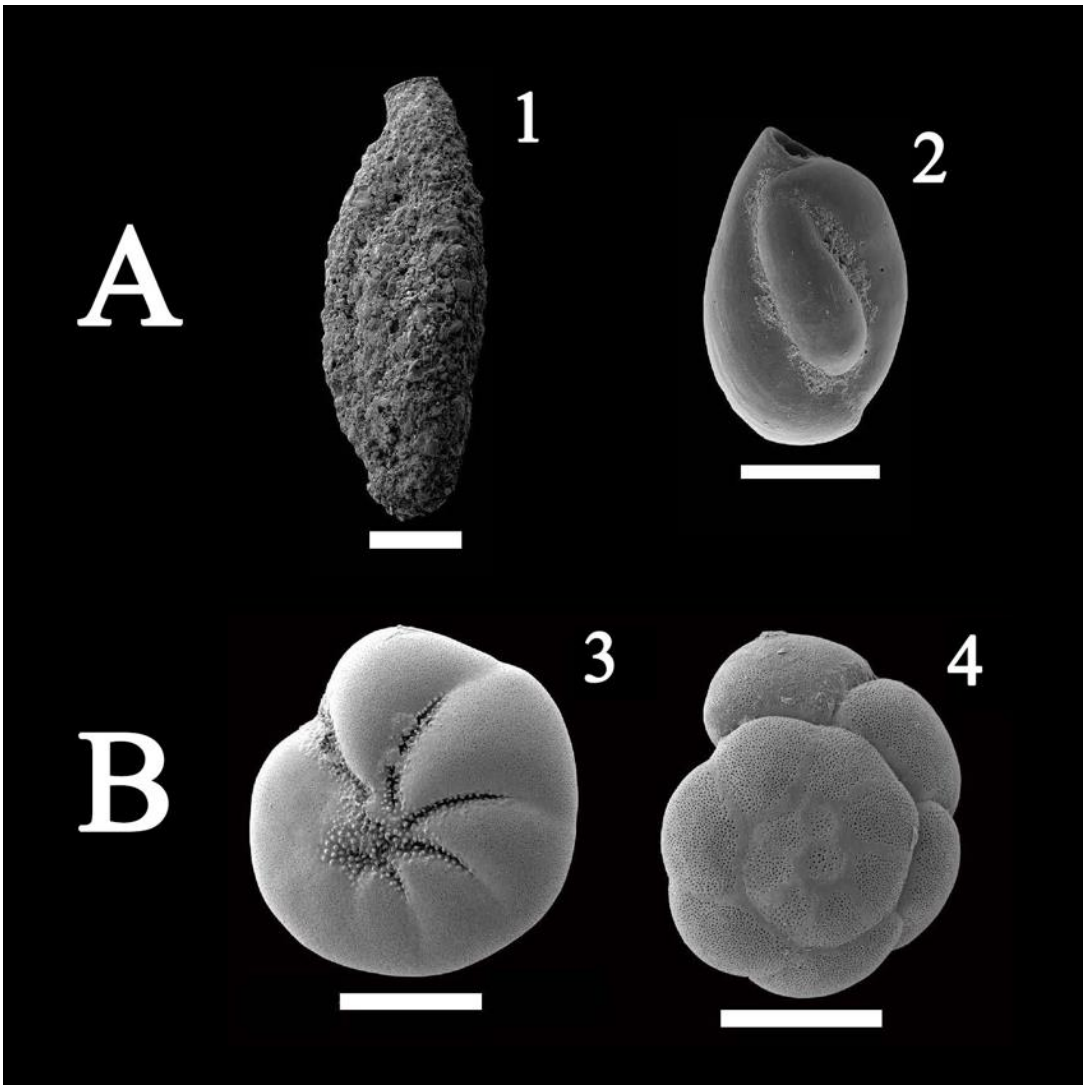

Fig. 4.2. SEM micrographs of the most common foraminifera species, Row A- Little Duck Key: 1 *Quinqueloculina sabulosa* (Cushman), 2 *Triloculina oblonga* (Montagu) and Row B- Little Duck Key: 3 *Haynesina germanica* (Ehrenberg), 4 *Ammonia tepida* (Cushman). All scale bars = 100 μm.

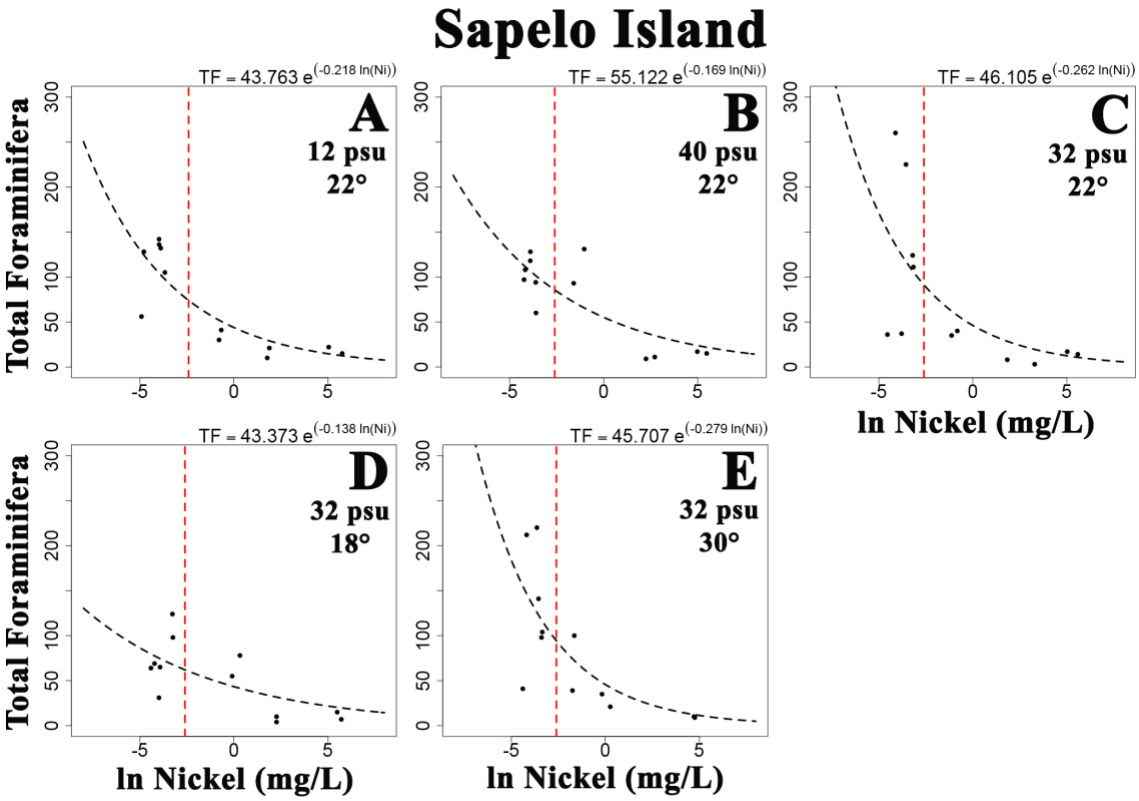

Fig. 4.3. Entire foraminiferal abundance in response to the natural log of the concentration of nickel in Sapelo Island assemblages: **A** low salinity (18 psu, 22°), **B** high salinity (40 psu, 22°), **C** intermediate (32 psu, 22°), **D** low temperature (32 psu, 18°), and **E** high temperature (32 psu, 30°). The vertical dashed lines indicate the U.S. EPA's CMC (Criteria Maximum Concentration) of nickel. The curved and diagonal dashed lines represent the exponential regression line.

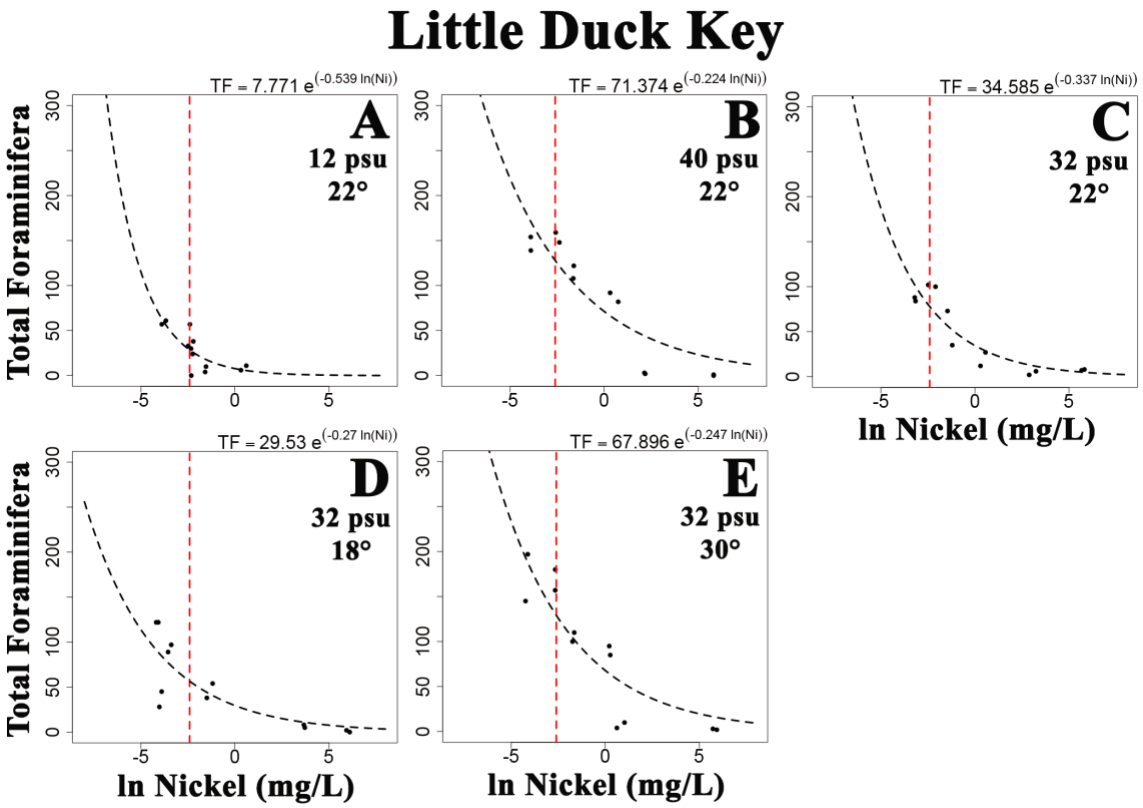

Fig. 4.4. Entire foraminiferal abundance in response to the natural log of the concentration of nickel in Little Duck Key assemblages: **A** low salinity (18 psu, 22°), **B** high salinity (40 psu, 22°), **C** intermediate (32 psu, 22°), **D** low temperature (32 psu, 18°), and **E** high temperature (32 psu, 30°). The vertical dashed lines indicate the U.S. EPA's CMC (Criteria Maximum Concentration) of nickel. The curved and diagonal dashed lines represent the exponential regression line.

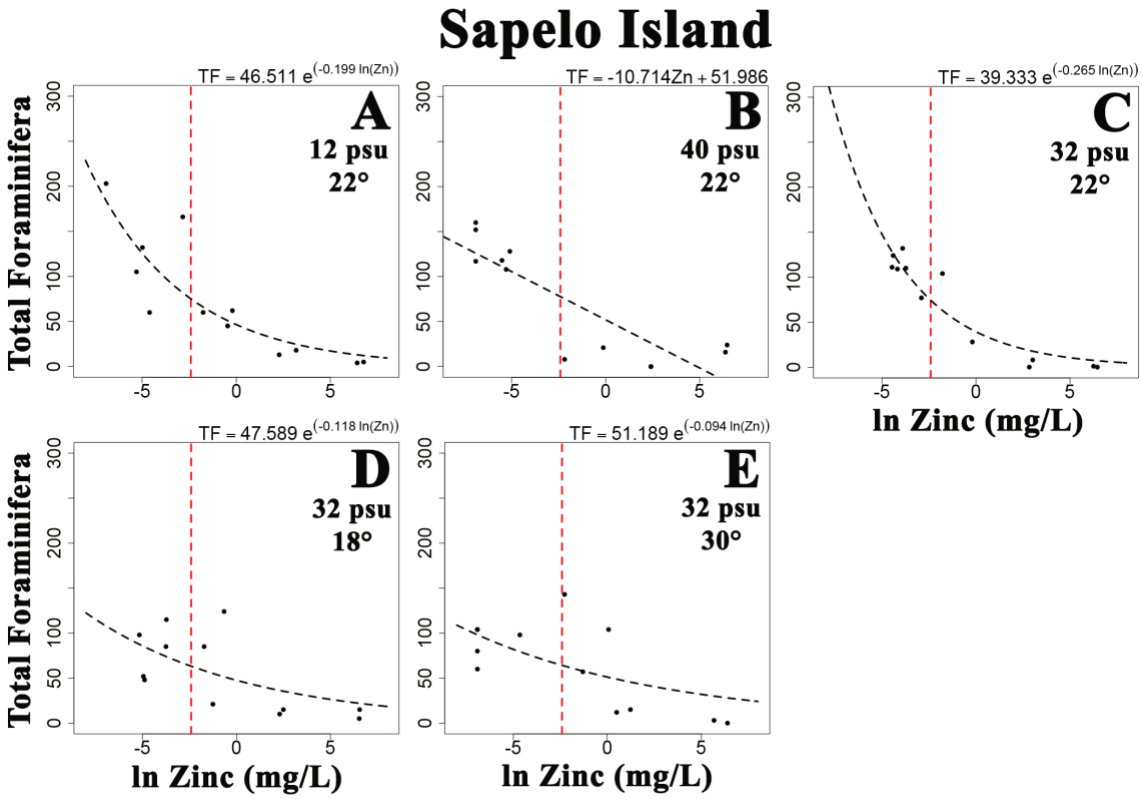

Fig. 4.5. Entire foraminiferal abundance in response to the natural log of the concentration of zinc in Sapelo Island assemblages: **A** low salinity (18 psu, 22°), **B** high salinity (40 psu, 22°), **C** intermediate (32 psu, 22°), **D** low temperature (32 psu, 18°), and **E** high temperature (32 psu, 30°). The vertical dashed lines indicate the U.S. EPA's CMC (Criteria Maximum Concentration) of nickel. The curved and diagonal dashed lines represent the exponential regression line.

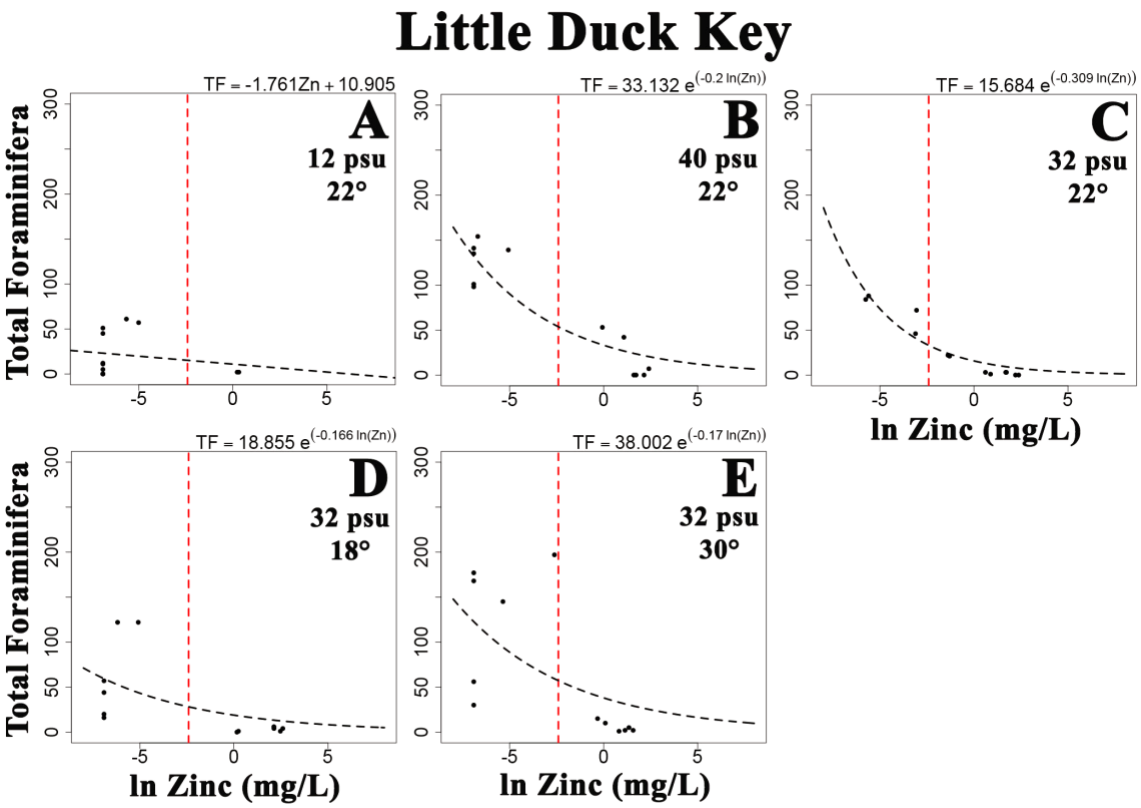

Fig. 4.6. Entire foraminiferal abundance in response to the natural log of the concentration of zinc in Little Duck Key assemblages: **A** low salinity (18 psu, 22°), **B** high salinity (40 psu, 22°), **C** intermediate (32 psu, 22°), **D** low temperature (32 psu, 18°), and **E** high temperature (32 psu, 30°). The vertical dashed lines indicate the U.S. EPA's CMC (Criteria Maximum Concentration) of nickel. The curved and diagonal dashed lines represent the exponential regression line.

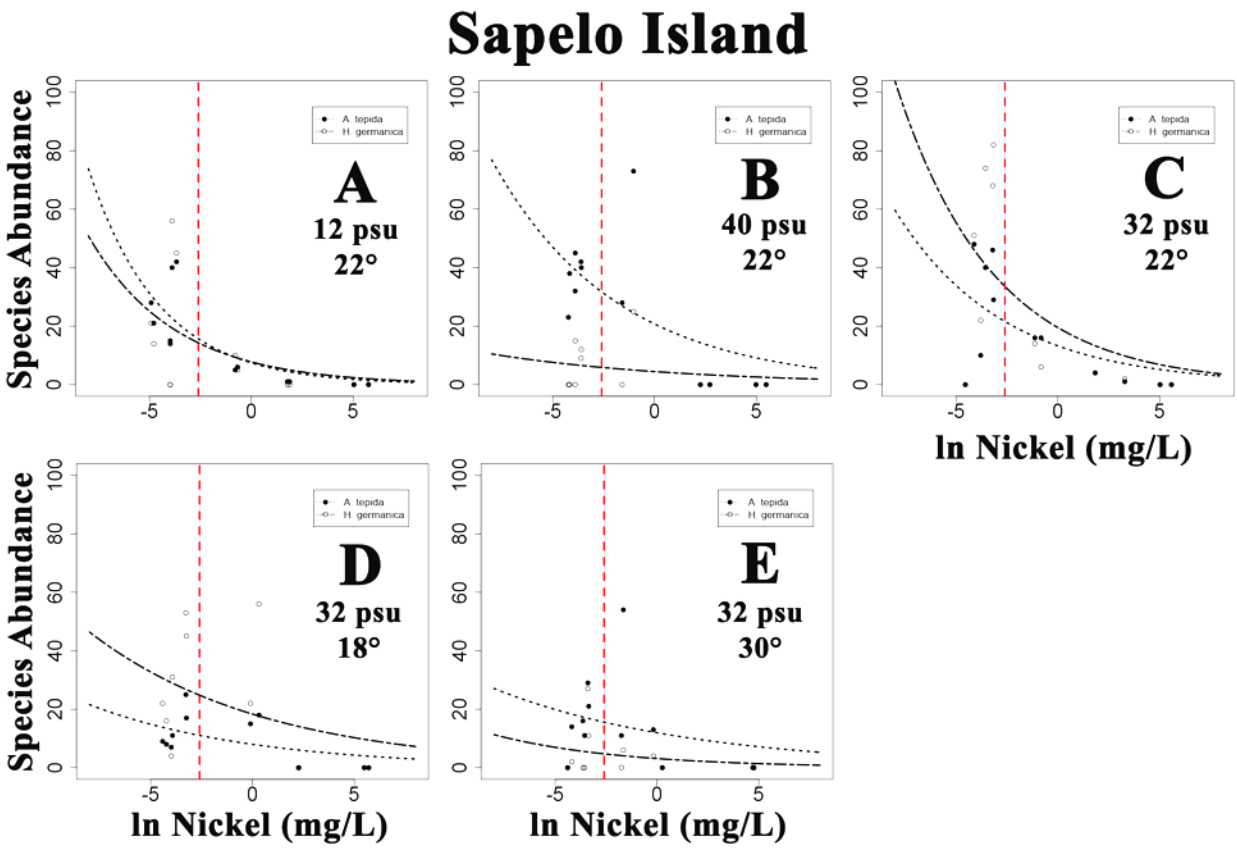

Fig. 4.7. Abundance of *Ammonia tepida* and *Haynesina germanica* in response to the natural log of the concentration of nickel: **A** low salinity (18 psu, 22°), **B** high salinity (40 psu, 22°), **C** intermediate (32 psu, 22°), **D** low temperature (32 psu, 18°), and **E** high temperature (32 psu, 30°). These were grown from propagules collected at Sapelo Island. The vertical dashed lines indicate the U.S. EPA's CMC (Criteria Maximum Concentration) of nickel. The curved and diagonal dashed lines represent the exponential regression line for each species.

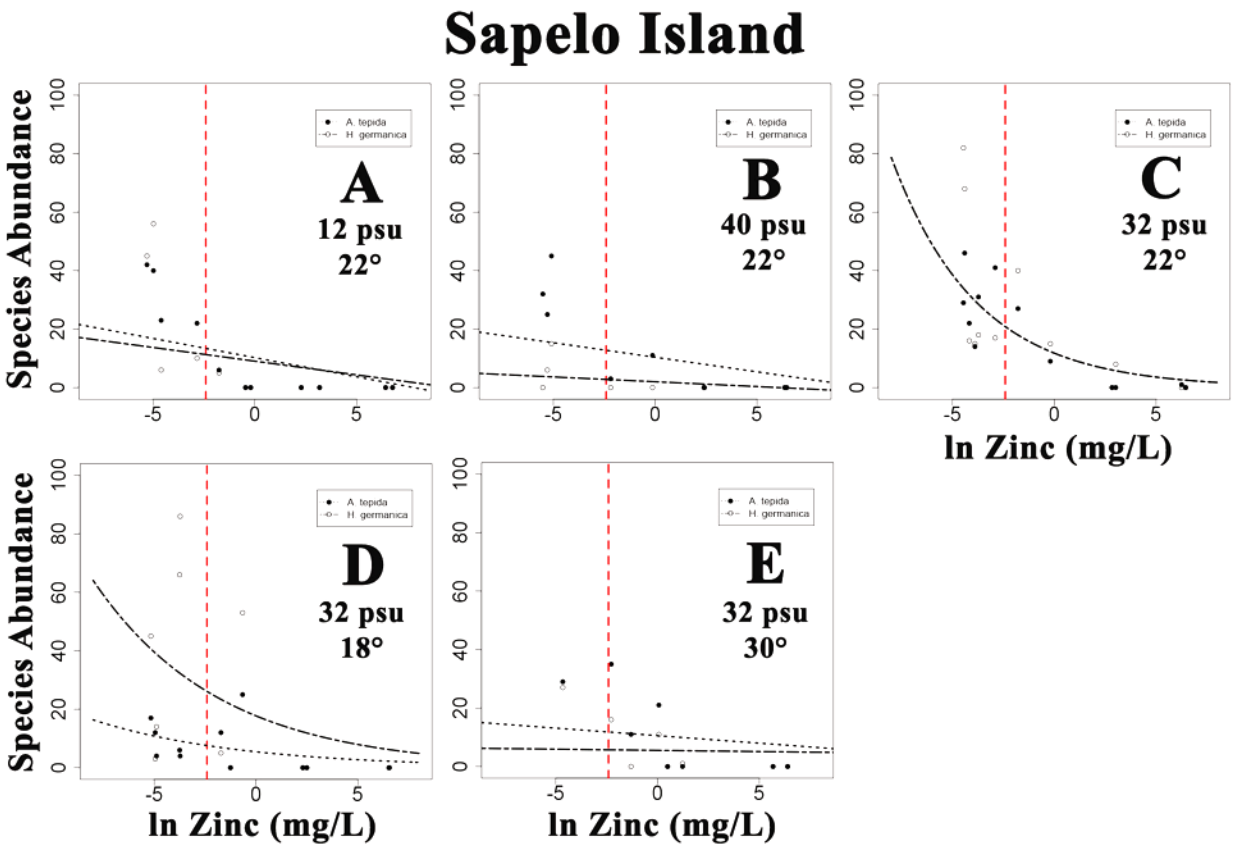

Fig. 4.8. Abundance of *Ammonia tepida* and *Haynesina germanica* in response to the natural log of the concentration of zinc: **A** low salinity (18 psu, 22°), **B** high salinity (40 psu, 22°), **C** intermediate (32 psu, 22°), **D** low temperature (32 psu, 18°), and **E** high temperature (32 psu, 30°). These were grown from propagules collected at Sapelo Island. The vertical dashed lines indicate the U.S. EPA's CMC (Criteria Maximum Concentration) of zinc. The curved and diagonal dashed lines represent the exponential regression line for each species.

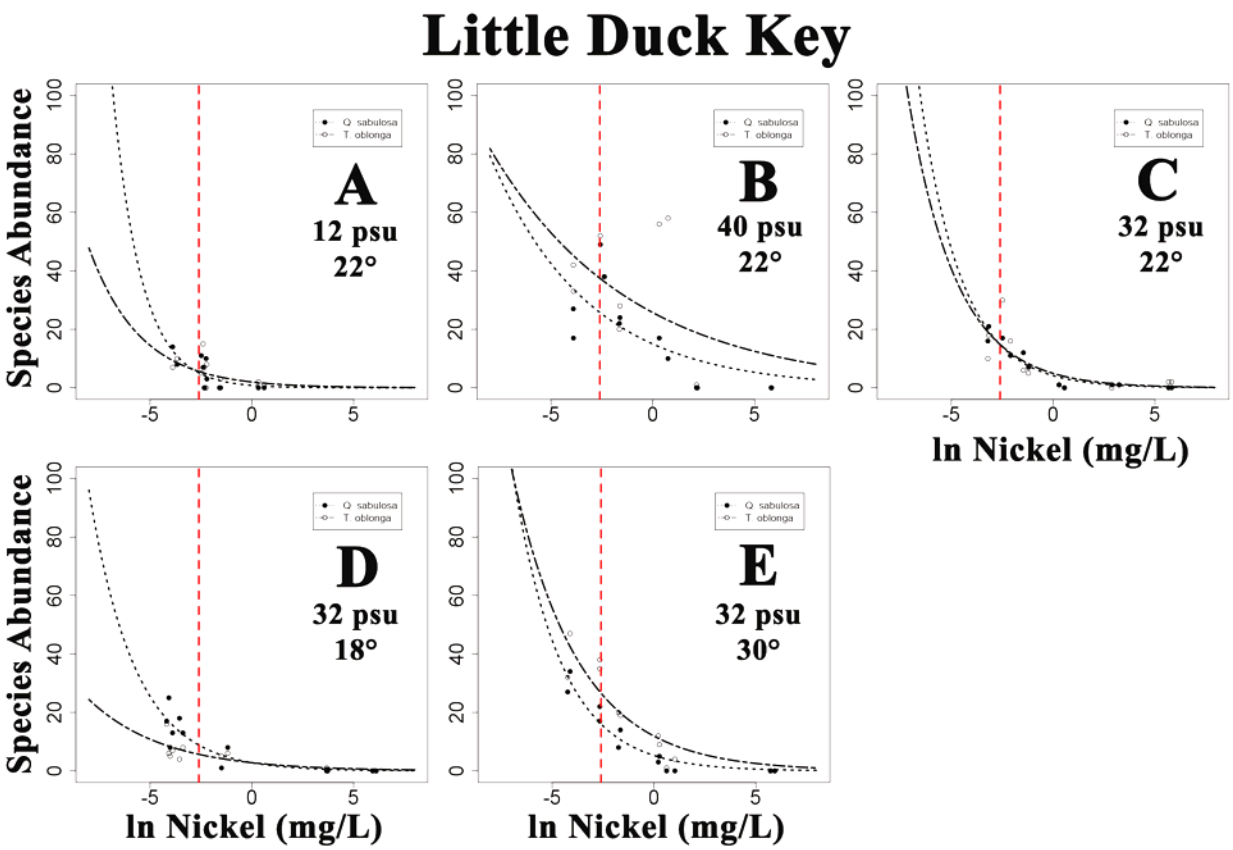

Fig. 4.9. Abundance of *Quinqueloculina sabulosa* and *Triloculina oblonga* in response to the natural log of the concentration of nickel: **A** low salinity (18 psu, 22°), **B** high salinity (40 psu, 22°), **C** intermediate (32 psu, 22°), **D** low temperature (32 psu, 18°), and **E** high temperature (32 psu, 30°). These were grown from propagules collected at Sapelo Island. The vertical dashed lines indicate the U.S. EPA's CMC (Criteria Maximum Concentration) of nickel. The curved and diagonal dashed lines represent the exponential regression line for each species.

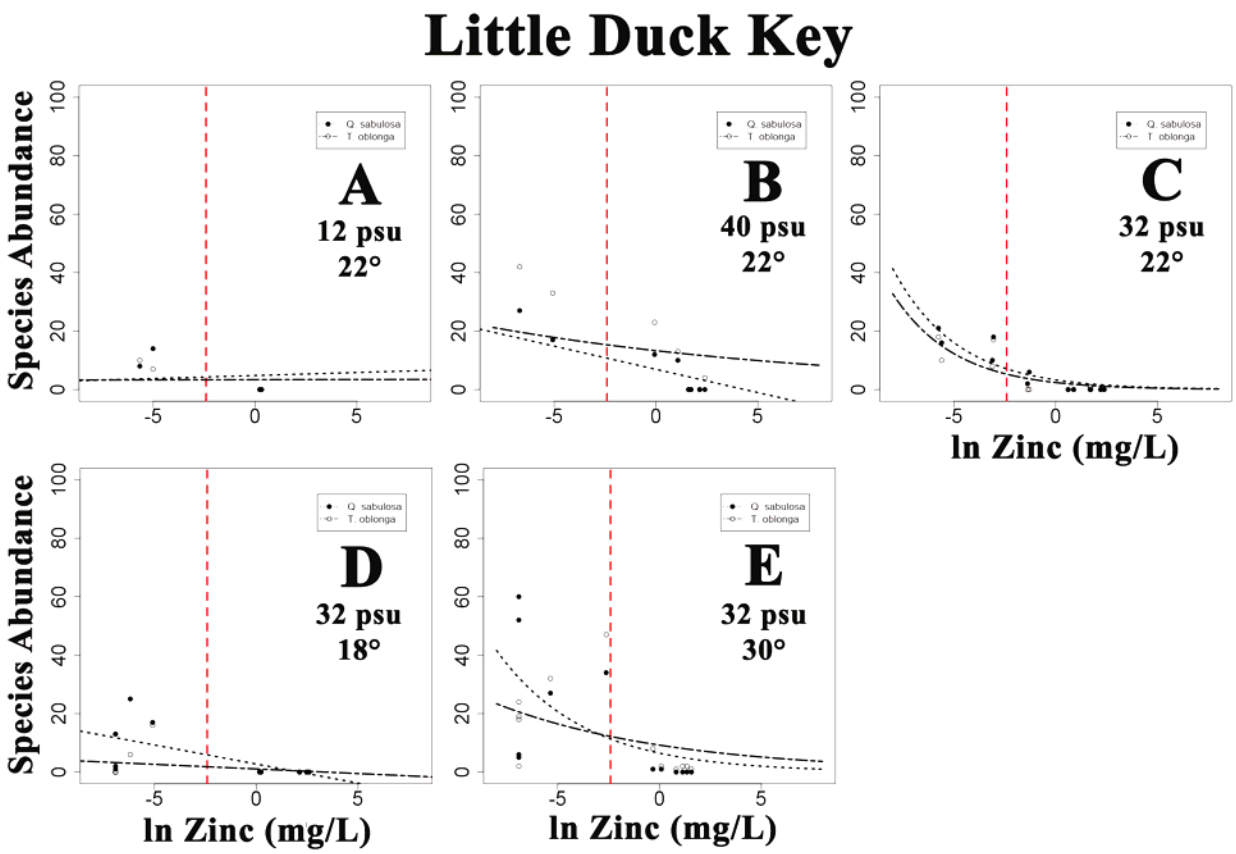

Fig. 4.10. Abundance of *Quinqueloculina sabulosa* and *Triloculina oblonga* in response to the natural log of the concentration of zinc: **A** low salinity (18 psu, 22°), **B** high salinity (40 psu, 22°), **C** intermediate (32 psu, 22°), **D** low temperature (32 psu, 18°), and **E** high temperature (32 psu, 30°). These were grown from propagules collected at Sapelo Island. The vertical dashed lines indicate the U.S. EPA's CMC (Criteria Maximum Concentration) of zinc. The curved and diagonal dashed lines represent the exponential regression line for each species.

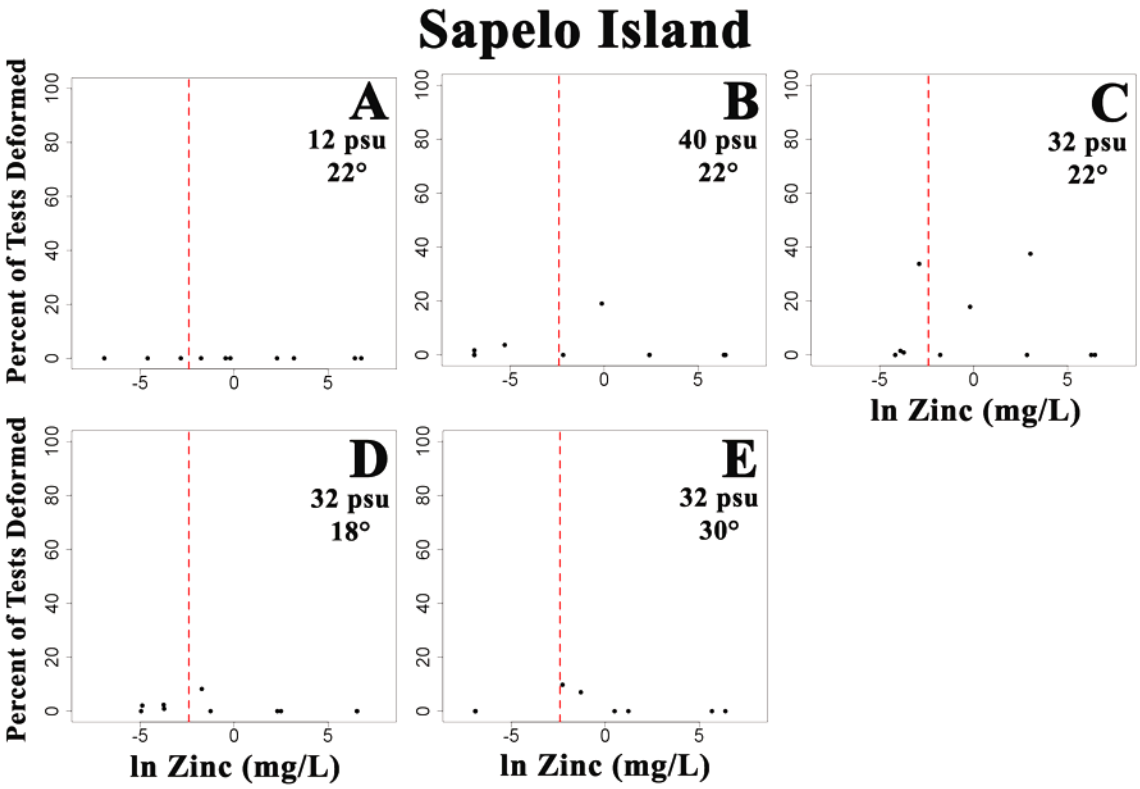

Fig. 4.11. Proportion of test deformities in response to the natural log of zinc concentration in assemblages grown from Sapelo Island propagules: **A** low salinity (18 psu, 22°), **B** high salinity (40 psu, 22°), **C** intermediate (32 psu, 22°), **D** low temperature (32 psu, 18°), and **E** high temperature (32 psu, 30°).

CHAPTER 5

CONCLUSIONS

In chapter 2, arsenic, cadmium, nickel, and zinc all had a negative impact on foraminiferal abundance and diversity where the concentration increased over the CMC. There appeared to be little difference between the effects of the elements based on their respective metabolic utility. *Haynesina germanica* and *Ammonia tepida* at Sapelo Island and *Quinqueloculina sabulosa* and *Quinqueloculina bosciana* at Little Duck Key were identified as bioindicators for each location. All of these species declined as arsenic, cadmium, nickel, and zinc concentrations increased, but were still present even at the greater concentrations. In the Sapelo Island assemblages, *Psammophaga sapela* also showed great potential as a bioindicator, because it tended to be the last species present at the highest metal concentrations. Zinc was more likely to cause major test deformities than arsenic, cadmium, and nickel. There were also major differences between rotalids and miliolids. While the rotalid species *A. tepida* and *H. germanica* were more vulnerable to test deformities when exposed to zinc than the other foraminifera, the comparative lack of deformities seen in the miliolid species such as *Q. sabulosa* and *Triloculina oblonga* suggests major differences in calcification between the two clades.

In chapter 3, LA-ICP-MS indicated incorporation of arsenic, cadmium, nickel and zinc in all species analyzed. Analysis revealed a clear difference between the rotalids and miliolids in their tendency to incorporate heavy metals. *Haynesina germanica* and *Ammonia tepida* readily incorporated metals such as arsenic and cadmium as

concentrations in the surrounding water increased but did not do the same with zinc and nickel. Conversely, *Quinqueloculina sabulosa* and *Triloculina oblonga* incorporated larger amounts of zinc and nickel as water concentration increased but did not do the same with arsenic and cadmium. This could further highlight fundamental differences in the biomineralization process between rotalid and miliolid foraminifera. With the exception of *A. tepida* incorporating more arsenic than *H. germanica*, incorporation rates were consistent in foraminifera of the same clade. There was no consistent chamber-to-chamber variability apparent, although variation was apparent in some isolated cases within individuals. *A. tepida* and *H. germanica* showed a clear relationship between incorporation of cadmium and cadmium content in the surrounding water, implying that these species and perhaps other rotalids as well, might be especially useful in studies involving cadmium, even at high contamination levels. In contrast, *Q. sabulosa* and *T. oblonga* show a clear relationship between incorporation of zinc and zinc content in the surrounding water.

In chapter 4, the negative effect of nickel and zinc was present at all salinities and temperatures tested. As in chapter 2, the most prevalent calcareous species (in this case, *Haynesina germanica* and *Ammonia tepida* at Sapelo Island and Quinqueloculina sabulosa and *Triloculina oblonga* at Little Duck Key) declined as nickel and zinc concentrations increased. However, these species persisted at greater concentrations across the range of salinities and temperatures tested. This implies that these species are viable bioindicators in multiple types of environments. Just as in chapter 2, zinc was the most likely heavy metal to cause major test deformities with rotalids *Ammonia tepida* and *Haynesina germanica* proving more susceptible to deformation than the miliolids. But,

these deformities only occurred in assemblages at temperatures of 22°C and salinities of 32 psu and 40 psu. In assemblages exposed to other salinities and temperatures, very few deformities occurred.

Future research should focus on better understanding of the calcification process in miliolids and rotalids, with particular focus on pathway of elements from the surrounding seawater. In addition, the relationship between zinc and foraminiferal test deformities has been demonstrated by multiple studies and warrants further investigation. More work must also be done on the different environmental factors that affect foraminiferal assemblages, especially pH and sediment type, as both may play key roles in foraminiferal response to heavy metals.

Benthic foraminiferal usage in environmental monitoring research has increased greatly in recent years. While the sensitivity of these organisms justifies their importance as biomonitoring tools, it is vital to properly identify the best species to use in specific situations with specific contaminants. Further knowledge of the varying factors that can impact the relationship between foraminifera and heavy metals, including salinity, temperature, differing test construction, substrate, and bioavailability, is also important in fully realizing the potential of benthic foraminifera as environmental indicators.

REFERENCES

Abu-Zied, R. H., Talha, Al-Dubai, T. A. M., Bantan, R. A., 2016, Environmental conditions of shallow waters alongside the southern Corniche of Jeddah based on benthic foraminifera, physio-chemical parameters and heavy metals: Journal of Foraminiferal Research, v. 46, p. 149–170.

Adriano, D. C., 2001, Trace Elements in Terrestrial Environments: Biogeochemistry, Bioavailability, and Risks of Metals: Springer-Verlag, New York, 186 p.

Alloway, B. J., 2013, Sources of Heavy Metals and Metalloids in Soils: Alloway, B.J. (ed) Heavy Metals in Soils: Springer, Dordrecht, Environmental Pollution, v. 22, p. 11–50.

Altin-Ballero, D. Z., Habura, A., and Goldstein, S. T., 2013, *Psammophaga sapela* n. sp., a new monothalamous foraminiferan from Coastal Georgia, USA: Fine structure, gametogenesis, and phylogenetic placement: Journal of Foraminiferal Research, v. 43, p. 113–126.

Alve, E., 1991, Benthic foraminifera reflecting heavy metal pollution in Sorljord, Western Norway: Journal of Foraminiferal Research, v. 34, p. 1641–1652.

Alve, E., 1995, Benthic foraminiferal responses to estuarine pollution: A review: Journal of Foraminiferal Research, v. 25, p. 190–203.

Alve, E., and Goldstein, S. T., 2002, Resting stage in benthic foraminiferal propagules: a key feature for dispersal? Evidence from two shallow-water species: Journal of Micropaleontology, v. 21, p. 95–96.

Alve, E., and Goldstein, S. T., 2003, Propagule transport as a key method of dispersal in benthic foraminifera (Protista): Limnology and Oceanography, v. 48, p. 2163–2170.

Alve, E., and Goldstein, S. T., 2010, Dispersal, survival and delayed growth of benthic foraminiferal propagules: Journal of Sea Research, v. 63, p. 36–51.

Alve, E., and Goldstein, S. T., 2014, The propagule method as an experimental tool in foraminiferal ecology, in Kitazato, H., and Bernhard, J. M. (eds.), Approaches to Study Living Foraminifera, Environmental Science and Engineering, Springer, Tokyo, p. 1–12.

Anderson, O. R., 1988, Comparative Protozoology: Ecology, Physiology, Life History, Springer-Verlag, Heidelberg, 482 p.

Angell, R. W., 1979, Calcification during chamber development in *Rosalina floridana*: Journal of Foraminiferal Research, v. 9, p. 341–353.

Angell, R. W., 1980, Test morphogenesis (chamber formation) in the foraminifer *Spiroloculina hyalina* Schulze: Journal of Foraminiferal Research, v. 10, p. 89–101.

Anke, M., Groppel, B., Kronemann, H., Grün, M., 1984, Nickel—an essential element: IARC Scientific Publications: v. 53, p. 339–365.

Arnal, R. E., 1955, Significance of abnormal foraminifera: Geological Society of America Bulletin, v. 66, p. 1641.

Arnold, Z. M., 1967, Biological observations on the foraminifer *Calcituba polymorpha* Roboz: Archiv fur Protistenkunde, v. 110, p. 28–304.

Bandy, O. L., 1963, Larger living foraminifera of the continental borderland of southern California: Cushman Foundation for Foraminiferal Research, v. 14, p. 121–126.

Bandy, O. L., Ingle, J. C., and Resig, J. M., 1964, Foraminiferal trends, Laguna Beach outfall area, California: Limnology and Oceanography, v. 9, p. 112–123.

Bergamin, L., Di Bella, L., Ferraro, L., Frezza, V., Pierfranceschi, G., Romano, E., 2019, Benthic foraminifera in a coastal marine area of the eastern Ligurian Sea (Italy): Response to environmental stress: Ecological Indicators, v. 96, p. 16–31.

Berger, W. H., and Parker, F. L., 1970, Diversity of planktonic foraminifera in deep-sea sediments: Science, v. 168, p. 1345–1347.

Boltovskoy, E., and Wright, R., 1976, Recent foraminifera. Dr. W. Junk Publishers, The Hague.

Boltovskoy, E., Scott, D. B., and Medioli, F. S., 1991, Morphological variations of benthic foraminiferal tests in response to changes in ecological parameters: a review: Journal of Paleontology, v. 65, p. 175–185.

Boyle, E. A., 1981, Cadmium, zinc, copper, and barium in foraminifera tests: Earth and Planetary Science Letters, v. 53, p. 11–35.

Boyle, E. A., 1988, Cadmium: Chemical tracer of deepwater paleoceanography: Paleoceanography, v. 3, p. 471–489.

Branson, O., 2019, LAtools Python Toolbox Version 0.3.8.

Brasier, M. D., 1975, Morphology and habitat of living benthonic Foraminiferids from Caribbean carbonate environment: Revista Española de Micropaleontologia, v. 7, p. 567–569.

Brouillette, E., 2009, An experimental approach to understand the responses of benthic foraminifera to Cd, Pb, Hg, and Zn. Unpublished Master's thesis, Department of Geology, University of Georgia, 80 p.

Brouillette, E. R., and Goldstein, S. T., 2008, An experimental approach to understanding the response of benthic foraminifera to Cd, Hg, Pb, and Zn: Gulf Coast Association of Geological Societies Transactions, v. 58, p. 143–146.

Brouillette Price, E., Kabengi, N., and Goldstein, S. T., 2019, Effects of heavy-metal contaminants (Cd, Pb, Zn) on benthic foraminiferal assemblages grown from propagules, Sapelo Island, Georgia (USA): Marine Micropaleontology, v. 147, p. 1–11.

Carnahan, E., Hoare, A. M., Hallock, P., Lidz, B. H., and Reich, C. D., 2008, Distribution of heavy metals and foraminiferal assemblages in sediments of Biscayne Bay, Florida, USA: Journal of Coastal Research, v. 24, p. 159–169.

Carnahan, E., Hoare, A. M., Hallock, P., Lidz, B. H., and Reich, C. D., 2009, Foraminiferal assemblages in Biscayne Bay, Florida, USA: Responses to urban and agricultural influence in a subtropical estuary: Marine Pollution Bulletin, v. 59, p. 8–12.

Carpenter, W. B., 1856, Researches in the foraminifera: Royal Society of London, Philosophical Transactions, v. 146, p. 547–569.

Closs, D., and Madeira, M. L., 1968, Seasonal variations of brackish foraminifera in the Patos Lagoon, southern Brazil: Universidade do Rio Grande do Sul, Escola de Geologia, Publicacao especial, v. 15, p. 1–51.

Debenay, J. P., Geslin., E., Eichler, B. B., Duleba, W., Sylvestre, F., and Eichler, P., 2001, Foraminiferal assemblages in a hypersaline lagoon, Araruama (R.J.) Brazil: Journal of Foraminiferal Research, v. 31, p. 133–151.

de Noojier, L. J., Reichart, G. J., Duenas Bohorquez, A. D. B., Wolthers, M., Ernst, S. R., Mason, P. R. D., Van der Zwaan, G. J., 2007, Copper incorporation in foraminiferal calcite: results from culturing experiments: Biogeosciences Discussions, v. 4, p. 961–991.

de Nooijer, L. J., Langer, G., Bijma, J., 2009, Physiological controls on seawater uptake and calcification in the benthic foraminifer *Ammonia tepida*: Biogeosciences, v. 6, p. 2669–2675.

de Nooijer, L. J., Toyofuku, T., Kitazato, H., 2009, Foraminifera promote calcification by elevating their intracellular pH: Proceedings of the National Academy of Sciences of the United States of America, v. 106, p. 15374–15378.

de Noojier, L. J., Spero, H. J., Erez, J., Bijma, J., and Reichart, G. J., 2014, Biomineralization in perforate foraminifera: Earth-Science Reviews, v. 135, p. 48–58.

de Rijk, S., 1995, Salinity control on the distribution of salt marsh Foraminifera (Great Marshes, Massachusetts): Journal of Foraminiferal Research, v. 25, p. 156–166.

Desideri, D., Cantaluppi, C., Ceccotto, Meli, M. A., Roselli, C., and Feduzi, L., 2016, Essential and toxic elements in seaweeds for human consumption: Journal of Toxicology an Environmental Health, v. 79, p. 112–122.

Dissard, D., Nehrke, G., Reichart, G. J., Bijma, J., 2010a, The impact of salinity on the Mg/Ca and Sr/Ca ratio in the benthic foraminifera *Ammonia tepida*: Results from culture experiments: Geochimica et Cosmochimica Acta, v. 74, p. 928–940.

Dissard, D., Nehrke, G., Reichart, G. J., Bijma, J., 2010b, Impact of seawater pCO_2 on calcification and Mg/Ca and Sr/Ca ratios in benthic foraminifera calcite: Results from culturing experiments with *Ammonia tepida*: Biogeosciences, v. 7, p. 81–93.

Duffield, C. J., Edvardsen, B., Eikrem, W., and Alve, E., 2014, Effects of different potential food sources on upper-bathyal benthic foraminifera: An experiment with propagules: Journal of Foraminiferal Research, v. 44, 416–433.

Duffield, C. J., Hess, S., Norling, K., and Alve, E., 2015, The response of *Nonionella iridea* and other benthic foraminifera to "fresh" organic matter enrichment and physical disturbance" Marine Micropaleontology, v. 120, p. 20–30.

Elderfield, H., Bertram, C. J., Erez, J., 1996, A biomineralization model for the incorporation of trace elements into foraminiferal calcium carbonate: Earth and Planetary Science Letters, v. 142, p. 409–423.

Emiliani, C., 1955, Pleistocene temperatures: Journal of Geology, v. 63, p. 538–578.

Erez, J., 2003, The source of ions for biomineralization in foraminifera and their implications for paleoceanographic proxies: Reviews in mineralogy and geochemistry, v. 54, p. 115–149.

Erez, J., Luz, B., 1983, Experimental paleotemperature equation for planktonic foraminifera: Geochimica Cosmochimica Acta, v. 47, p. 1025–1031.

Fehrenbacher, J. S., Spero, H. J., Russell, A. D., Vetter, L., Eggins, S., 2015, Optimizing LA-ICP-MS analytical procedures for elemental depth profiling of foraminifera shells: Chemical Geology, v. 407, p. 2–9.

Foster, W. J., Armynot du Chatelet, E., Rogerson, M., 2012, Testing benthic foraminiferal distributions as a contemporary quantitative approach to biomonitoring estuarine heavy metal pollution: Marine Pollution Bulletin, v. 64, p. 1039–1048.

Frontalini, F., and Coccioni, R., 2008, Benthic foraminifera for heavy metal pollution monitoring: A case study from the central Adriatic Sea coast of Italy: Estuarine, Coastal and Shelf Science, v. 76, p. 404–417.

Frontalini, F., Buosi, C., Da Pelo, S., Coccioni, R., Cherchi, A., and Bucci, C., 2009, Benthic foraminifera as bio-indicators of trace element pollution in the heavily contaminated Santa Gilla lagoon (Cagliari, Italy): Marine Pollution Bulletin, v. 58, p. 858–877.

Frontalini, F., Nardelli, M. P., Curzi, D., Martin-Gonzelez, A., Sabbatini, A., Negri, A., Losada, M. T., Gobbi, P., Coccioni, R., Bernhard, J. M., 2018, Benthic foraminiferal ultrastructural alteration induced by heavy metals: Marine Micropaleontology, v. 138, p. 83–89.

Frontalini, F., Semprucci, S., Di Bella, L., Caruso, A., Cosentino, C., Maccotta, A., Scopelliti, G., Sbrocca, C., Bucci, C., Balsamo, M., Martins, M. V., Armynot du Chatelet, E., and Coccioni, R., 2018, The response of cultured meiofaunal and benthic foraminiferal communities to lead exposure: Results from mesocosm experiments: Environmental Toxicology and Chemistry, v. 37, p. 2439–2447.

Geerken, E., de Noojier, L. J., van Dijk, I., Reichart, G. J., 2018, Impact of salinity on element incorporation in two benthic foraminiferal species with contrasting magnesium contents: Biogeosciences, v. 15, p. 2205–2218.

Gerhardt, A., 2002, Bioindicator species and their use in biomonitoring: Environmental Monitoring, v. 1, p. 77–123.

Geslin, E., Debenay, J., Duleba, W., and Bonetti, C., 2002, Morphological abnormalities of foraminiferal tests in Brazilian environments: comparison between polluted and non-polluted areas: Marine Micropaleontology, v. 45, p. 151–168.

Geslin, E., Stouff, V., Debenay, J., and Lesourd, M., 2000, Environmental variation and foraminiferal test abnormalities: from Environmental Micropaleontology, Topics in Geobiology, v. 15, ed. Martin, R., Kluwer Academic/Plenum Publishers, New York, p. 191–215.

Goldstein, S. T., 1999, Foraminifera: A biological overview. In: Gupta, B.K.S. (Ed.) Modern foraminifera: Kluwer Academic Publishers, Dordrecht, p. 37–55.

Goldstein, S. T., and Alve, E., 2011, Experimental assembly of foraminiferal communities from coastal propagule banks: Marine Ecology Progress Series, v. 437, p. 1–11.

Goldstein, S. T., Corliss, B. H., 1994, Deposit feeding in selected deep-sea and shallow-water benthic foraminifera: Deep Sea Research Part I: Oceanographic Research Papers, v. 41, p. 229–241.

Goldstein, S. T., and Frey, R. W., 1986, Salt marsh foraminifera, Sapelo Island, Georgia: Senckenbergiana maritima, v. 18, p. 97–121.

Hallock, P., Glenn, E. C., 1986, Larger foraminifera: A tool for paleoenvironemtal analysis of Cenozoic carbonate deposition facies: PALAIOS, v. 1, p. 55–64.

Hansen, H. J., 1999, Shell construction in modern calcareous Foraminifera. In: Gupta B.K.S. (Ed.) Modern foraminifera: Kluwer Academic Publishers, Dordrecht, p. 57–70.

Hart, M. B., Stubbles, S. J., Smart, C. W., Fisher, J. K., Hoddinot, C., Marshall-Penn, I., and Yeo, A., 2014, Foraminifera from the Fowey Estuary, Cornwall: Geoscience in South-West England, v. 13, p. 304–315.

Hayek, L. A. C., and Buzas, M. A., 2010, Surveying natural populations: quantitative tools for assessing biodiversity, Columbia University Press, 596 p.

Hayek, L. A. C., and Buzas, M. A., 2013, On the proper and efficient use of diversity measures with individual field samples: Journal of Foraminiferal Research, v. 43, p. 305–313.

Haynes, J., 1981, Foraminifera, John Wiley, New York, 348 p.

Hemleben, C., Anderson, O. R., Berthold, W., Spindler, M., 1986, Calcification and chamber formation in Foraminifera — a brief overview: Leadbetter, B.S.C. and Riding, R. (Eds.) Biomineralization in Lower Plants and Animals, Systematics Association, Special Volume 30, p. 237–249.

James, A., and Evison, L. (eds.), 1979, Biological Indicators of Water Quality, John Wiley and Sons, New York, 650 p.

Julian II, P., 2015, South Florida Coastal Sediment Ecological Risk Assessment: Bulletin of Environmental Contamination and Toxicology, v. 95, p. 188–193.

Katz, M. E., Cramer, B. S., Franzese, A., Honisch, B., Miller, K. G., Rosenthal, Y., Wright, J. D., 2010, Traditional and emerging geochemical proxies in foraminifera: Journal of Foraminiferal Research, v. 40, p. 165–192.

Khalifa, G. M., Kirchenbuechler, D., Koifman, N., Klienerman, O., Talmon, Y., Elbaum, M., Addadi, L., Weiner, S., Erez, J., 2016, Biomineralization pathways in a foraminifer revealed using a novel correlative cryo-fluorescence-SEM-EDS technique: Journal of Structural Biology, v. 196, p. 155–163.

Kramar, U., Munsel, D., Berner, Z., Bijma, J., Nehrke, G., 2010, Determination of trace element incorporation into tests of in vitro grown foraminifera by micro-SYXRF-A basis for the development of paleoproxies: AIP Conference Proceedings, v. 1221, p. 154–159.

Kurc, G., 1961, Foraminiferes et ostracodes de l'étang de Thau: Revue des Travaux: Institut des Péches Maritimes, v. 25, p. 134–248.

Ladeira, A. C. Q., and Ciminelli, V. S. T., 2004, Adsorption and description of arsenic on an oxisol and its constituents: Water Research, v. 38, p. 2087–2094.

Lee, Y. G., Kim, S., Kim, Y. W., Jeong, D. U., Lee, J. S., Woo, H. J., and Shin, H. C., 2015, Benthic foraminifera as bioindicators of salinity variation in Lake Shinwa, South Korea: Journal of Foraminiferal Research, v. 45, p. 235–249.

Linshy, R. S., Kurtarkar, S. R., and Nigam, R., 2013, Experiment to decipher the effect of heavy metal cadmium on coastal benthic foraminifer *Pararotalia nipponica* (Asano): Journal of the Paleontological Society of India, v. 58, p. 205–211.

Locklin, J. A., and Maddocks, R. F., 1982, Recent foraminifera around petroleum production platforms on the southwest Louisiana shelf, Trans Gulf Assoc. Geol. Soc., v. 32, p. 377–397.

Lopez, E., 1979, Algal chloroplasts in the protoplasm of three species of benthic foraminifera: taxonomic affinity, viability and persistence: Marine Biology, v. 53, p. 201–211.

Malmgren, B. A., 1984, Analysis of the environmental influence on the morphology of *Ammonia beccarii* (Linné) in southern European Salinas: Geobios, v. 17, p. 737–746.

Maret, W., 2016, The metals in the biological periodic system of the elements: Concepts and conjectures: International Journal of Molecular Sciences, v. 17, p. 66–72.

Martin, R. E., (Ed.) 2000, Environmental micropaleontology: the application of microfossils to environmental geology, Springer Science & Business Media, New York, 459 p.

Martinez-Colon, M., Hallock, P., and Green-Ruiz, C., 2009, Strategies for using shallow-water benthic foraminifera as bioindicators of potentially toxic elements: A review, Journal of Foraminiferal Research, v. 39, p. 278–299.

Martins, V. A., Frontalini, F., Tramonte, K. M., Figueira, R. C. L., Miranda, P., Sequeira, C., Fernandez-Fernandez, S., Dias, J. A., Yamashita, C., Reno, R., Laut, L. L. M., Silva, F. S., Rodrigues, M. A. C., Bernardes C., Nagai, R., Sousa, S. H. M., Mahiques, M., Rubio, B., Bernabeu, A., Rey, D., Rocha, F., 2013, Assessment of the health quality of Ria de Aviero (Portugal): Heavy metals and benthic foraminifera: Marine Pollution Bulletin, v. 70, p. 18–33.

Martins, M. V. A., Hohenegger, J., Frontalini, F., Laut, L., Miranda, P., Rodrigues, M. A., Duleba, W., Geraldes, M. C., and Rocha, F., 2018, Heterogeneity of environments in a coastal lagoon mouth by the comparison between living and dead benthic foraminiferal assemblages (Ria de Aveiro Portugal): Estuarine, Coastal, and Shelf Science, v. 213, p. 199–216.

Mertz, W., 1981, The essential trace elements: Science, v. 213, p. 1332–1338.

Miller, A. A. L., Scott, D. B., and Medioli, F. S., 1982, *Elphidium excavatum* (Terquem): Ecophenotypic versus subspecific variation: Journal of Foraminiferal Research, v. 12, p. 116–144.

Morishima, M., 1955, Deposits of foraminiferal tests in the Tokyo Bay, Japan: University of Kyoto, College of Science, Memoires, v. 22, p. 213–222.

Munsel, D., Kramar, U., Dissard, D., Nehrke, G., Berner, Z., Bijma, J., Reichart, G. J., Neumann, T., 2010, Heavy metal uptake in foraminiferal calcite: results of multi-element culture experiments: Biogeosciences Discussions, v. 7, p. 953–977.

Murray, J. W., 1973, Distribution and Ecology of Living Benthic Foraminiferids, Crane, Russak and Co., New York, 274 p.

Murray, J. W., 1991, Ecology and Palaeocology of Benthic Foraminifera, Longman, London, 397 p.

Murray, J. W., and Bowser, S. S., 2000, Mortality, protoplasm decay rate, and reliability of staining techniques to recognize ‘living’ foraminifera: A review: Journal of Foraminiferal Research, v. 30, p. 66–70.

Murray, J. W., 2006, Ecology and applications of benthic foraminifera, Cambridge University Press, New York, 426 p.

Nardelli, M. P., 2013, Experimental chronic exposure of the foraminifer *Pseudotriloculina rotunda* to Zinc: Acta Protozoologica, v. 52, p. 193–202.

Nardelli, M. P., Malferrari, D., Ferretti, A., Bartolini, A., Sabbatini, A., Negri, A., 2016, Zinc incorporation in the miliolid foraminifer *Pseudotriloculina rotunda* under laboratory conditions: Marine Micropaleontology, v. 126, p. 42–49.

Natland, M. L., 1935, The temperature and depth-distribution of some Recent and fossil foraminifera in the southern California region: Scripps Institute of Oceanography Technical Report, v. 3, 255 p.

Neff, J. M., 1997, Ecotoxicology of arsenic in the marine environment: Environmental Toxicology and Chemistry, v. 16, p. 917–927.

Nehrke, G., Keul, N., Langer, G., de Noojier, L. J., Bijma, J., 2013, A new model for biomineralization and trace element signatures of foraminifera tests: Biogeosciences, v. 10, p. 6759–6767.

Nielsen, F. H., 1998, Ultratrace elements in nutrition: Current knowledge and speculation: The Journal of Trace Elements in Experimental Medicine, v. 11, p. 251–274.

Nigam, R., Saraswat, R., and Panchang, R., 2006, Application of foraminifers in ecotoxicology: Retrospect, perspect and prospect: Environmental International, v. 32, p. 273–283.

Nurnberg, D., Bijma, J., Hemleben, C., 1996, Assessing the reliability of magnesium in foraminiferal calcite as a proxy for water mass temperatures: Geochimica et Cosmochimica, v. 60, p. 803–814.

Olugbode, O. I., Hart, M. B., and Stubbles, S. J., 2005, Foraminifera from Restronguet Creek: Monitoring recovery from the Wheal Jane pollution incident: Geoscience in South-West England, v. 11, p. 92–92.

Phleger, F. B., and Hamilton, W. A., 1946, Foraminifera of two submarine cores from the North Atlantic Basin: Geological Society of America Bulletin, v. 57, p. 951–966.

Poonkothai, M. V. B. S., Vijayavathi, B. S., 2012, Nickel as an essential element and a toxicant: International Journal of Environmental Sciences, v. 1, p. 285–288.

R Core Team (2018). R: A language and environment for statistical computing. R Foundation for Statistical Computing, Vienna, Austria. URL http://www.R-project.org/.

R Core Team (2019). R: A language and environment for statistical computing. R Foundation for Statistical Computing, Vienna, Austria. URL http://www.R-project.org/.

Rainbow, P. S., 2007, Trace metal bioaccumulation: Models, metabolic availability and toxicity: Environmental International, v. 33, p. 576–582.

Resig, J., 1960, Foraminiferal ecology around ocean outfalls off southern California. In: Person, E. (Ed.) Disposal in the Marine Environment, Pergamon Press, London, p. 104–121.

Rosenthal, Y., Boyle, E. A., Slowey, N., 1997, Temperature control on the incorporation of magnesium, strontium, fluorine, and cadmium into benthic foraminiferal shells from Little Bahama Bank: Prospects for thermocline paleoceanography: Geochimica et Cosmochimica Acta, v. 61, p. 3633–3643.

Roychoudhury, A. N., 2007, Spatial and seasonal variations in depth profile of trace metals in saltmarsh sediments from Sapelo Island, Georgia, USA: Estuarine, Coastal and Shelf Science, v. 72, p. 675–689.

Schafer, C. T., 1970, Studies of benthic foraminifera in Restigouche Estuary: Faunal distribution patterns near pollution sources: Maritime Sediments, v. 6, p. 121–134.

Schiebel, R., Smart, S. M., Jentzen, A., Jonkers, L., Morard, R., Meilland, J., Michel, E., Coxall, H. K., Hull, P. M., de Garidel-Thoron, T., Aze, T., 2018, Advances in planktonic foraminifer research: New perspectives for paleoceanography: Revue de Micropaleontologie, v. 61, p. 113–138.

Schnitker, D., 1974, Ecophenotypic variation in *Ammonia beccarii* (Linné): Journal of Foraminiferal Research, v. 4, p. 216–223.

Scott, D. B., and Medioli, F. S., 1980a, Quantitative studies of marsh foraminiferal distributions in Nova Scotia: Implications for sea level studies: Cushman Foundation for Foraminiferal Research, Special Publication, v. 17, 58 p.

Scott, D. B., Medioli, F. S., and Schafer, C. T., 2001, Monitoring in coastal marine environments using foraminifera and thecamoebians as indicators, Cambridge University Press, 1–177.

Scott, D. B., Mudie, P. J., and Bradshaw, J. S., 1976, Benthic foraminifera of the three southern California lagoons: Ecology and Recent stratigraphy: Journal of Foraminiferal Research, v. 6, p. 59–75.

Smith, C.W., and Goldstein, S.T., 2019, The effects of selected heavy metal elements on experimentally grown foraminiferal assemblages from Sapelo Island, Georgia and

Little Duck Key, Florida, USA: Journal of Foraminiferal Research v. 49 (3), p. 303–318.

Smith, C.W., Fehrenbacher, J., and Goldstein, S.T., submitted, Incorporation of heavy metals in experimentally grown foraminifera from Sapelo Island, Georgia and Little Duck Key, Florida, USA, Marine Micropaleontology.

Stouff, V., 1998, Interet des elevages de foraminiferes en laboratoroire: Etudes biologiques et ultrastructurales, These de Doctorat, Universite d'Angers et EPHE, France, p. 405.

Stouff, V., Debenay, J. P., and Lesourd, M., 1999a, Origin of double and multiple tests in benthic foraminifera: Observations in laboratory cultures: Marine Micropaleontology, v. 36, p. 189–204.

Stouff, V., Geslin, E., Debenay, J. P., and Lesourd, M., 1999a, Origin of morphological abnormalities in *Ammonia* (foraminifera): Studies in laboratory and natural environments: Journal of Foraminiferal Research, v. 29, p. 152–170.

Stubbles, S. J., 1999, Responses of recent benthic foraminifera to metal pollution in South West England estuaries: A study of impact and change: Unpublished Ph.D. thesis, Plymouth University.

Stubbles, S. J., Green, J. C., Hart, M. B., and Williams, C. L., 1996, Response of foraminifera to the presence of heavy metal contamination and acidic mine drainage: Minerals, Metals and the Environment II, Prague. Institute of Mining and Mineralogy, London, Special Publication, p. 217–235.

Tansel, B., Rafiuddin, S., 2016, Heavy metal content in relation to particle size and organic content of surficial sediments in Miami River and transport potential: International Journal of Sediment Research, v. 31, p. 324–329.

Tappan, H., 1951, Foraminifera from the Arctic Slope of Alaska: U.S. Geological Survey Professional Paper, v. 236A, p. 1–20.

Tawfik, D. S., and Viola, R. E., 2011, Arsenate replacing phosphate: alternative life chemistries and ion promiscuity: Biochemistry, v. 50, p. 1128–1134.

Tchounwou, P. B., Yedjou, C. G., Patlolla, A. K., Sutton, D. J., 2012, Heavy Metal Toxicity and the Environment: Luch, A. (Ed.) Molecular, Clinical and Environmental Toxicology, Experientia Supplementum, v. 101, p. 133–164.

Ter Kuile, B., Erez, J., Padan, E., 1989, Mechanisms for the uptake of inorganic carbon by two species of symbiont-bearing foraminifera: Marine Biology, v. 103, p. 241–251.

Theyer, F., 1966, Size-depth variation in *Cyclammina cancellata* Brady, Peru-Chile Trench Area: Antarctic Research, v. 15, p. 309–318.

Titelboim, D., Sadekov, A., Hyams-Kaphzan, O., Almogi-Labin, A., Herut, B., Kucera, M., Abramovich, S., 2018, Foraminiferal single chamber analyses of heavy metals as a tool for monitoring permanent and short term anthropogenic footprints: Marine Pollution Bulletin, v. 128, p. 65–71.

Traina, S. J., and Laperche, V., 1999, Contaminant bioavailability in soils, sediments, and aquatic environments: Proceedings of the National Academy of Science USA, v. 96, p. 3365–3371.

Tufescu, M., 1968, *Ammonia tepida* (Cushman) (ord. Foraminifera). Some features of its variability in the Black Sea Basin: Revue Roumaine de Biologie et Zoologie, v. 13, p. 169–177.

Uthus, E. O., 2003, Arsenic essentiality: A role affecting methionine metabolism: Journal of Trace Elements in Experimental Medicine: The Official Publication of the International Society for Trace Element Research in Humans, v. 16, p. 345–355.

van Dijk, I., de Noojier, L. J., and Reichart, G. J., 2017, Trends in element incorporation in hyaline and porcelaneous foraminifera as a function of pCO 2: Biogeosciences, v. 14, p. 497–510.

Walton, W., 1952, Techniques for recognition of living foraminifera: Contributions to the Cushman Foundation for Foraminiferal Research, v. 3, p. 56–60.

Walton, W. R., and Sloan, B. J., 1990, The genus *Ammonia* Brünnich, 1772: Its geographic distribution and morphologic variability: Journal of Foraminiferal Research, v. 20, p. 128–156.

Watkins, J. G., 1961, Foraminiferal ecology around the Orange County, California ocean sewer outfall: Micropaleontology, v. 7, p. 199–206.

Weber, M., and Casazza, L. R., 2006, The effects of heavy metal contamination on the foraminifera of a San Francisco Bay salt marsh: FORAMS 2006- International Symposium on Foraminifera, Natal, Brazil, Anuario do Instituto de Geociencias, v. 29, p. 443–444

Weinmann, A. E., and Goldstein, S. T., 2016, Changing structure of benthic foraminiferal communities: Implications from experimentally grown assemblages from coastal Georgia and Florida, U.S.A.: Marine Ecology, v. 37, p. 891–906.

Weinmann, A. E., Goldstein, S. T., Triantaphyllou, M. V., and Langer, M. R., 2019, Effects of sampling site, season, and substrate on foraminiferal assemblages grown from propagule banks from lagoon sediments of Corfu Island (Greece, Ionian Sea): PLoS one, v. 14, e0219015.

Wright, R. C., 1968, Miliolidae (foraminiferos) recientes del estuario del Rio Quequen Grande (Prov. De Buenos Aires): Museo Argentino de Ciencias Naturales, Revista de Hidrobiologia, v. 2, p. 225–256.

Yanko, V., Kronfeld, J., and Flexer, A., 1994, Response of benthic foraminifera to various pollution sources: implication for pollution monitoring: Journal of Foraminiferal Research, v. 28, p. 177–200.

Yanko, V., Ahmad, A. and Bresler, V., 1998, Morphological deformities of benthic foraminiferal tests in response to pollution by heavy metals: implications for pollution monitoring: Journal of Foraminiferal Research, v. 28, p. 177–200.

Yanko, V., Arnold, A. J., and Parker, W. C., 1999, Effects of marine pollution on benthic foraminifera, in Sen Gupta, B. K. (ed.), Modern Foraminifera: Kluwer Academic Publishers, Dordrecht, p. 217–235.

Zeng, H., Uthus, E. O., Combs, G. F., 2005, Mechanistic aspects of the interaction between selenium and arsenic: Journal of Inorganic Biochemistry, v. 99, p. 1269–1274.

APPENDIX A

R CODE AND SUPPLEMENTARY DATA FOR CHAPTER 2

Part 1: R Code

R code for all plotting and statistical analysis conducted, including functions and scripts that run the commands.

R Function for plotting population density or species abundance against metal concentration.

```
y <- c()
x <- c()
logx <- log(x)
plot (logx, y, xlab="Metal (ppm)", ylab="", pch=19,
xlim=c(-8, 8), ylim=c(0, 300)
, cex.lab=2, cex.axis=2, cex.main=2, cex.sub=2)
abline(v=c((log(CMC_Concentration)), (log(0.000001))),
col=c('red','blue'), lty=c(2,1), lwd =c(3,3))
#Exponential Trendline
f <- function(logx,a,b) {a * exp(b * logx)}
fit <- nls(y ~ f(logx,a,b), start = c(a=1, b=1))
co <- coef(fit)
curve(f(x, a=co[1], b=co[2]), add = TRUE,,lty=2, lwd=3)

#Exponential Coefficients
lm_coef <- coef(fit) # extract coefficients
lm_coefA <- round(lm_coef[1],3)
lm_coefB <- round(lm_coef[2],3)
mtext((bquote("TF" == .(lm_coefA)~"e"
^(.(lm_coefB)~"ln(Ni)"))), adj=1, padj=0, cex=2) # display
equation

#Linear Trendline (if necessary)
fit<- lm(y~logx)
abline(fit,lty=2,lwd = 3)

#Linear Coefficients (if necessary)
lm_coef <- round(coef(fit), 3) # extract coefficients
mtext(bquote(y == .(lm_coef[2])*x + .(lm_coef[1])),
```

```
adj=1, padj=0,cex=2) # display equation
```

Part 2: Data

Foraminiferal count data for chapter 2.

Sapelo Island										
Arsenic	**0.069 ppm 1**	**0.069 ppm 2**	**0.69 1**	**0.69 2**	**6.9 ppm 1**	**6.9 ppm 2**	**69 ppm 1**	**69 ppm 2**	**690 ppm 1**	**690 ppm 2**
Actual Concentration	**0.0434 ppm**	**0.1282 ppm**	**0.0612 ppm**	**0.058 ppm**	**0.0512 ppm**	**0.0538 ppm**	**0.059 ppm**	**0.0576 ppm**	**0.0804 ppm**	**0.0992 ppm**
Ovammina opaca	2	2	8	14	8	4	13	1	3	1
Psammophaga sapela	5	5	6	3	16	2	16	12	3	9
Ammonia tepida	3	23	28	21	39	16	24	33	33	38
Haynesina germanica	12	15	37	44	37	52	37	20	29	38
Buliminella elegantissima	1	2	4	3	4	3	3	2	0	4
Miliammina fusca	2	13	148	1	21	10	10	39	50	4
Textularia candeiana	4	2	6	8	18	10	26	8	9	4
Textularia earlandi	4	3	10	14	4	2	3	3	5	0
Textularia palustris	1	2	10	1	5	12	2	9	0	0
Ammottium salsum	0	0	0	0	1	0	0	0	0	0
Quinqueloculina jugosa	1	0	0	0	0	0	0	0	0	2
Elphidium excavatum	9	8	27	15	24	30	26	21	17	21
Cadmium	**0.04 ppm 1**	**0.04 ppm 2**	**0.4 ppm 1**	**0.4 ppm 2**	**4 ppm 1**	**4 ppm 2**	**40 ppm 1**	**40 ppm 2**	**400 ppm 1**	**400 ppm 2**
Actual Concentration	**3.43 ppm**	**3.45 ppm**	**4.34 ppm**	**0.532 ppm**	**149 ppm**	**182 ppm**	**149 ppm**	**182 ppm**	**508 ppm**	**566 ppm**
Ovammina opaca	7	8	18	4	0	1	0	1	0	1
Psammophaga sapela	16	47	8	27	11	18	19	26	13	1
Ammonia tepida	31	40	8	46	0	0	5	0	0	0
Haynesina germanica	45	48	17	35	2	4	8	3	1	2
Buliminella elegantissima	9	8	22	12	0	0	0	0	0	0
Miliammina fusca	11	0	11	2	14	0	0	0	0	0
Textularia candeiana	4	1	3	25	0	0	0	0	0	0
Textularia earlandi	2	0	7	15	1	1	1	0	0	0
Textularia palustris	2	0	1	30	0	0	0	0	0	0
Ammottium salsum	0	0	0	0	0	0	0	0	0	0
Quinqueloculina jugosa	0	1	1	1	0	1	0	0	1	0

Elphidium excavatum	29	28	5	13	1	2	4	1	0	0
Nickel	**0.074 ppm 1**	**0.074 ppm 2**	**0.74 ppm 1**	**0.74 ppm 2**	**7.4 ppm 1**	**7.4 ppm 2**	**74 ppm 1**	**74 ppm 2**	**740 ppm 1**	**740 ppm 2**
Actual Concentration	**0.011 ppm**	**0.0097 ppm**	**0.009 ppm**	**0.0087 ppm**	**0.0106 ppm**	**0.00209 6 ppm**	**0.4094 ppm**	**0.03438 ppm**	**1.2794 ppm**	**1.819 ppm**
Ovammina opaca	4	3	2	1	0	0	0	19	1	0
Psammophaga sapela	14	13	7	3	3	1	1	21	9	6
Ammonia tepida	43	31	6	28	28	3	0	30	0	0
Haynesina germanica	61	63	27	60	37	13	3	27	3	2
Buliminella elegantissima	2	6	1	1	0	2	0	1	0	0
Miliammina fusca	18	29	15	16	8	14	2	0	3	0
Textularia candeiana	8	9	2	8	3	4	0	4	0	0
Textularia earlandi	6	5	0	6	1	1	0	2	0	0
Textularia palustris	1	4	0	1	2	4	1	1	0	0
Ammottium salsum	0	0	0	0	0	0	0	0	0	0
Quinqueloculina jugosa	18	2	2	1	1	0	0	1	0	0
Elphidium excavatum	40	22	9	0	19	4	0	11	0	0
Zinc	**0.09 ppm 1**	**0.09 ppm 2**	**0.9 ppm 1**	**0.9 ppm 2**	**9 ppm 1**	**9 ppm 2**	**90 ppm 1**	**90 ppm 2**	**900 ppm 1**	**900 ppm 2**
Actual Concentration	**0.0195 ppm**	**0.0354 ppm**	**0.0188 ppm**	**0.0165 ppm**	**0.0597 ppm**	**0.0545 ppm**	**11.4 ppm**	**4.14 ppm**	**328 ppm**	**246 ppm**
Ovammina opaca	1	2	1	6	2	12	0	1	0	0
Psammophaga sapela	1	1	0	8	21	9	1	4	2	4
Ammonia tepida	3	15	49	42	10	46	0	0	0	0
Haynesina germanica	18	27	42	53	19	18	0	1	2	2
Buliminella elegantissima	1	8	5	5	0	0	0	0	0	0
Miliammina fusca	25	14	5	17	0	6	0	0	0	0
Textularia candeiana	1	0	5	16	0	0	0	0	0	0
Textularia earlandi	1	0	1	10	0	0	0	0	0	0
Textularia palustris	6	1	8	11	0	0	0	0	0	0
Ammottium salsum	0	0	0	0	0	0	0	0	0	0
Quinqueloculina jugosa	0	0	1	20	0	0	0	0	0	0
Elphidium excavatum	3	9	18	20	5	10	0	0	0	0
Controls	**1**	**2**								
Ovammina opaca	5	8								
Psammophaga sapela	11	10								

Ammonia tepida	34	23
Haynesina germanica	39	29
Buliminella elegantissima	9	7
Miliammina fusca	59	47
Textularia candeiana	7	8
Textularia earlandi	11	8
Textularia palustris	19	14
Ammottium salsum	0	0
Quinqueloculina jugosa	0	0
Elphidium excavatum	24	19

Little Duck Key

Arsenic	**0.069 ppm 1**	**0.069 ppm 2**	**0.69 1**	**0.69 2**	**6.9 ppm 1**	**6.9 ppm 2**	**69 ppm 1**	**69 ppm 2**	**690 ppm 1**	**690 ppm 2**
Actual Concentration	**0.116 ppm**	**0.298 ppm**	**0.116 ppm**	**0.147 ppm**	**0.224 ppm**	**0.214 ppm**	**6.082 ppm**	**5.512 ppm**	**57.062 ppm**	**51.562 ppm**
Ammonia tepida	1	0	0	0	0	0	0	0	0	2
Archais angulatus	0	0	0	0	0	0	0	0	0	0
Bolivina lowmani	8	1	11	1	5	2	0	0	1	1
Bolivina pulchella	9	2	3	0	2	1	1	0	0	0
Bolivina striatula	0	0	0	0	0	0	0	0	0	0
Buliminella elegantissima	0	0	0	0	1	0	0	0	0	0
Cibicides spp.	1	0	0	0	0	0	0	0	0	0
Cornuspira planorbis	0	0	0	0	0	0	0	0	0	1
Discorbis mira	0	0	0	0	0	0	0	0	0	0
Elphidium discoidale	0	0	0	0	0	0	0	0	0	3
Elphidium mexicanum	1	7	0	0	11	1	0	1	0	1
Hauerina bradyi	0	0	0	0	0	0	0	0	0	0
Miliolinella circularis	2	0	2	0	4	3	0	0	0	1
Miliolinella subrotunda	0	0	0	0	0	0	0	0	0	3
Nonionoides grateloupi	0	0	0	0	1	0	0	0	0	0
Ovammina opaca	38	65	41	16	7	48	0	0	0	0
Peneroplis pertusus	0	0	0	0	0	0	0	0	0	0
Quinqueloculina agglutinans	2	0	0	0	0	0	0	0	0	0
Quinqueloculina bosciana	9	6	2	3	8	8	0	2	0	8
Quinqueloculina laevigata	0	0	1	0	0	0	0	0	0	0

Quinqueloculina lamarckiana	0	0	1	0	2	4	0	0	0	0
Quinqueloculina poeyana	0	0	2	0	0	4	0	0	0	0
Quinqueloculina polygona	0	0	0	0	0	0	0	0	0	0
Quinqueloculina sabulosa	6	8	11	1	14	21	0	0	0	5
Quinqueloculina seminula	5	3	0	3	8	3	0	2	0	4
Reophax gaussicus	11	13	8	2	6	3	1	8	0	0
Rosalina floridana	0	0	1	0	0	0	0	0	1	0
Rosalina globularis	1	0	0	0	0	0	0	0	0	0
Sorites marginalis	1	0	0	0	0	0	0	0	1	0
Textularia candeiana	11	11	12	30	28	4	0	9	0	0
Textularia earlandi	7	1	0	0	0	0	0	0	0	0
Triloculina oblonga	0	3	0	0	10	2	0	0	0	0
Triloculina rotunda	0	0	0	0	0	0	0	0	0	1
Triloculina tricarinata	0	1	0	0	0	0	0	0	0	1
Cadmium	**0.04 ppm 1**	**0.04 ppm 2**	**0.4 ppm 1**	**0.4 ppm 2**	**4 ppm 1**	**4 ppm 2**	**40 ppm 1**	**40 ppm 2**	**400 ppm 1**	**400 ppm 2**
Actual Concentration	**0.00108 ppm**	**0.00017 ppm**	**0.0119 ppm**	**0.0157 ppm**	**0.148 ppm**	**0.05 ppm**	**0.137 ppm**	**0.146 ppm**	**1.08 ppm**	**1.35 ppm**
Ammonia tepida	1	0	0	0	0	0	1	0	0	0
Archais angulatus	0	0	0	0	0	0	0	0	0	0
Bolivina lowmani	7	16	1	4	0	4	0	2	0	0
Bolivina pulchella	2	6	0	1	1	1	1	0	0	0
Bolivina striatula	0	0	0	0	0	0	0	0	0	0
Buliminella elegantissima	1	0	0	0	0	2	0	0	0	0
Cibicides spp.	0	0	0	0	0	0	0	0	0	0
Cornuspira planorbis	0	0	0	0	0	0	0	0	0	0
Discorbis mira	1	0	0	0	0	0	0	0	0	0
Elphidium discoidale	0	0	0	0	0	0	0	0	0	1
Elphidium mexicanum	6	8	7	4	0	0	11	0	2	0
Hauerina bradyi	0	0	0	0	0	0	0	0	0	0
Miliolinella circularis	0	1	0	4	0	0	7	1	0	0
Miliolinella subrotunda	0	0	0	0	0	0	0	0	0	0
Nonionoides grateloupi	0	0	0	0	0	0	0	0	0	0
Ovammina opaca	14	41	36	55	50	5	4	0	0	0

Peneroplis pertusus	0	0	0	0	0	0	1	0	0	0
Quinqueloculina agglutinans	0	0	0	0	0	0	0	0	0	0
Quinqueloculina bosciana	9	18	6	6	0	8	7	6	1	1
Quinqueloculina laevigata	0	0	0	0	0	0	1	1	0	0
Quinqueloculina lamarckiana	0	1	0	0	0	0	1	0	0	0
Quinqueloculina poeyana	8	4	0	2	0	0	2	1	0	2
Quinqueloculina polygona	0	0	0	0	0	0	2	2	0	0
Quinqueloculina sabulosa	3	15	7	13	2	13	1	2	0	0
Quinqueloculina seminula	9	10	5	2	0	7	4	1	2	0
Reophax gaussicus	8	7	6	6	2	7	2	2	0	0
Rosalina floridana	1	0	1	0	0	0	0	2	0	0
Rosalina globularis	1	0	0	0	0	0	0	0	0	0
Sorites marginalis	0	0	0	0	0	0	0	0	0	0
Textularia candeiana	3	13	5	11	0	10	0	0	0	0
Textularia earlandi	0	0	1	0	0	0	1	3	0	0
Triloculina oblonga	0	5	26	5	1	0	0	0	0	0
Triloculina rotunda	0	0	0	0	0	0	0	0	0	0
Triloculina tricarinata	0	0	0	0	0	0	0	0	0	0
Nickel	**0.74 ppm 1**	**0.074 ppm 2**	**0.74 ppm 1**	**0.74 ppm 2**	**7.4 ppm 1**	**7.4 ppm 2**	**74 ppm 1**	**74 ppm 2**	**740 ppm 1**	**740 ppm 2**
Actual Concentration	**0.0063 ppm**	**0.0096 ppm**	**0.0086 ppm**	**0.0093 ppm**	**0.0535 ppm**	**0.03559 ppm**	**0.5585 ppm**	**0.4075 ppm**	**3.2585 ppm**	**0.9765 ppm**
Ammonia tepida	2	0	0	1	0	0	0	0	0	1
Archais angulatus	0	0	0	0	0	0	0	0	0	0
Bolivina lowmani	10	4	4	8	1	4	0	0	0	0
Bolivina pulchella	3	1	3	0	2	0	1	0	0	0
Bolivina striatula	0	0	0	0	0	0	0	0	0	0
Buliminella elegantissima	0	0	0	0	1	0	0	1	0	0
Cibicides spp.	0	0	0	0	0	0	0	0	0	0
Cornuspira planorbis	0	0	0	0	0	0	0	1	0	0
Discorbis mira	0	0	0	0	0	0	0	0	0	0
Elphidium discoidale	0	0	0	0	0	0	0	0	0	0
Elphidium mexicanum	27	5	74	11	0	11	0	0	1	0
Hauerina bradyi	0	0	0	0	0	0	0	0	0	0

Miliolinella circularis	1	0	0	0	0	0	0	0	0	2
Miliolinella subrotunda	0	0	0	0	0	0	0	0	0	0
Nonionoides grateloupi	0	0	0	0	0	0	0	0	0	0
Ovammina opaca	16	31	14	0	8	13	0	0	0	1
Peneroplis pertusus	0	0	0	0	0	0	0	0	0	0
Quinqueloculina agglutinans	0	0	0	0	0	0	0	0	0	0
Quinqueloculina bosciana	25	6	9	13	3	9	1	6	2	2
Quinqueloculina laevigata	2	0	3	1	0	0	0	0	2	0
Quinqueloculina lamarckiana	0	0	0	0	0	0	0	0	0	0
Quinqueloculina poeyana	2	0	1	4	0	2	0	2	0	0
Quinqueloculina polygona	0	0	0	0	0	0	0	0	0	0
Quinqueloculina sabulosa	9	2	3	18	2	6	0	0	0	0
Quinqueloculina seminula	29	11	10	7	2	5	0	6	2	0
Reophax gaussicus	15	22	19	7	5	16	0	1	0	0
Rosalina floridana	0	0	0	0	0	0	0	0	0	0
Rosalina globularis	0	0	0	0	0	0	0	0	0	0
Sorites marginalis	0	0	0	0	0	0	0	0	0	0
Textularia candeiana	6	12	14	19	1	7	2	0	0	0
Textularia earlandi	0	0	0	0	0	0	0	0	0	0
Triloculina oblonga	21	8	12	13	0	0	0	0	0	0
Triloculina rotunda	0	0	0	0	0	0	0	0	0	0
Triloculina tricarinata	0	0	0	0	0	0	0	0	0	0
Zinc	**0.09 ppm 1**	**0.09 ppm 2**	**0.9 ppm 1**	**0.9 ppm 2**	**9 ppm 1**	**9 ppm 2**	**90 ppm 1**	**90 ppm 2**	**900 ppm 1**	**900 ppm 2**
Actual Concentration	**0.0219 ppm**	**0.0262 ppm**	**0.0244 ppm**	**0.0239 ppm**	**0.0321 ppm**	**0.0425 ppm**	**0.263 ppm**	**0.221 ppm**	**3.61 ppm**	**6.09 ppm**
Ammonia tepida	3	1	0	0	0	0	0	0	1	0
Archais angulatus	0	0	0	0	0	0	0	0	0	0
Bolivina lowmani	19	9	4	5	2	8	0	0	0	2
Bolivina pulchella	3	4	1	1	2	0	0	0	0	0
Bolivina striatula	3	0	0	0	0	0	0	0	0	0
Buliminella elegantissima	4	2	0	0	1	1	0	0	0	0
Cibicides spp.	0	0	0	0	0	0	0	0	0	0
Cornuspira planorbis	0	0	0	0	1	1	0	0	0	0

Discorbis mira	0	0	0	0	0	0	0	0	0	0
Elphidium discoidale	0	0	0	0	0	0	0	0	0	0
Elphidium mexicanum	8	4	6	4	3	6	1	2	1	4
Hauerina bradyi	0	0	0	0	0	0	0	0	0	0
Miliolinella circularis	4	0	0	1	0	0	1	1	0	0
Miliolinella subrotunda	0	0	4	0	0	0	0	0	0	0
Nonionoides grateloupi	0	0	0	0	0	0	0	0	0	0
Ovammina opaca	0	70	35	20	35	41	0	0	0	0
Peneroplis pertusus	0	0	0	0	0	0	0	0	0	0
Quinqueloculina agglutinans	0	0	0	0	0	0	0	0	0	0
Quinqueloculina bosciana	22	4	7	7	5	11	1	6	0	4
Quinqueloculina laevigata	0	0	1	0	0	0	0	2	0	0
Quinqueloculina lamarckiana	1	0	2	0	0	0	0	3	0	0
Quinqueloculina poeyana	32	1	2	3	0	0	0	2	0	1
Quinqueloculina polygona	0	0	0	0	0	0	0	1	0	0
Quinqueloculina sabulosa	0	6	29	38	25	8	0	0	0	0
Quinqueloculina seminula	25	4	7	3	5	8	0	8	1	3
Reophax gaussicus	0	8	10	18	8	14	1	2	0	0
Rosalina floridana	0	0	0	0	0	0	0	0	0	0
Rosalina globularis	1	0	0	0	0	0	0	0	0	0
Sorites marginalis	0	0	0	0	1	0	1	0	0	0
Textularia candeiana	0	11	5	6	17	11	0	1	0	0
Textularia earlandi	0	0	1	0	0	0	0	0	0	0
Triloculina oblonga	0	8	9	2	0	0	0	0	0	0
Triloculina rotunda	0	0	0	1	0	0	0	0	0	0
Triloculina tricarinata	1	0	0	0	0	0	0	0	3	0
Controls	**1**	**2**								
Ammonia tepida	0	0								
Archais angulatus	0	0								
Bolivina lowmani	7	10								
Bolivina pulchella	5	1								
Bolivina striatula	0	0								

Buliminella elegantissima	0	1
Cibicides spp.	0	0
Cornuspira planorbis	0	0
Discorbis mira	0	0
Elphidium discoidale	0	2
Elphidium mexicanum	4	16
Hauerina bradyi	4	0
Miliolinella circularis	2	4
Miliolinella subrotunda	0	0
Nonionoides grateloupi	0	0
Ovammina opaca	43	29
Peneroplis pertusus	0	0
Quinqueloculina agglutinans	0	0
Quinqueloculina bosciana	4	6
Quinqueloculina laevigata	1	0
Quinqueloculina lamarckiana	0	1
Quinqueloculina poeyana	0	1
Quinqueloculina polygona	0	0
Quinqueloculina sabulosa	2	19
Quinqueloculina seminula	14	6
Reophax gaussicus	13	11
Rosalina floridana	0	1
Rosalina globularis	0	0
Sorites marginalis	0	0
Textularia candeiana	8	10
Textularia earlandi	0	0
Triloculina oblonga	0	5
Triloculina rotunda	0	0
Triloculina tricarinata	0	0

APPENDIX B

R CODE FOR CHAPTER 3

R code for all plotting and statistical analysis conducted, including functions and scripts that run the commands.

R Function for plotting incorporation against metal concentration.

```
ATy <- c()
ATx <- c()
logATx <- log(ATx)
logATy <- log(ATy)
plot (logATx, logATy, xlab = "Metal in Water (Me/Ca)", ylab
= "Incorporated Metal (Me/Ca)", pch=19, xlim=c(-10, 4),
ylim=c(-10, 4)
, cex.lab=1, cex.axis=1, cex.main=1, cex.sub=1)
HGy <- c
HGx <- c
logHGy <- log(HGy)
logHGx <- log(HGx)
points(logHGx, logHGy, pch=1)

#Exponential Trendline
f <- function(logx,a,b) {a * exp(b * logx)}
fit <- nls(y ~ f(logx,a,b), start = c(a=2, b=2))
co <- coef(fit)
curve(f(x, a=co[1], b=co[2]), add = TRUE,,lty=2, lwd=3)
abline(v=c((log(0.090/0.400)), (log(0.000001))),
col=c('red','blue'), lty=c(2,1), lwd =c(3,3))

#Linear Trendline (if necessary)
ATfit<- lm(logATy~logATx)
abline(ATfit,lty=2,lwd = 2)
HGfit<- lm(logHGy~logHGx)
abline(HGfit,lty=3,lwd = 2)

#R-Squared Values
```

```
ATSummary <- summary(ATfit)
HGSummary <- summary(HGfit)
ATr2 = ATSummary$adj.r.squared
HGr2 = HGSummary$adj.r.squared
ATr2label = bquote(italic(R)^2 == .(format(ATr2, digits =
3)))
text(x = 3, y = 4.2, labels = ATr2label, cex=0.8)
text(x = 0.9, y = 4.2, "A. tepida", cex=0.8, font=3)
HGr2label = bquote(italic(R)^2 == .(format(HGr2, digits =
3)))
text(x = 3, y = 3.7, labels = HGr2label, cex=0.8)
text(x = 0.9, y = 3.7, "H. germanica",cex=0.8,font=3)

#Legend
legend(0, -8, legend=c("A. tepida", "H. germanica"), lty=
c(2,3), pch=c(19,1),cex=1)
```

APPENDIX C

R CODE AND SUPPLEMENTARY DATA FOR CHAPTER 4

Part 1: R Code

R code for all plotting and statistical analysis conducted, including functions and scripts that run the commands.

R Function for plotting population density or species abundance against metal concentration.

```
ATy <- c()
ATx <- c()
logATx <- log(ATx)
plot (logATx, ATy, xlab = "Metal (mg/L)", ylab = "",
pch=19, xlim=c(-8, 8), ylim=c(0, 100), cex.lab=2,
cex.axis=2, cex.main=2, cex.sub=2)
HGy <- c
HGx <- c
logHGx <- log(HGx)
points(logHGx, HGy, pch=1)
abline(v=c((log(CMC)), (log(0.000001))),
col=c('red','blue'), lty=c(2,1), lwd =c(3,3))

#Legend
legend(3, 95, legend=c("Species", "Species"), lty= c(3,6),
pch=c(19,1),cex=1)

#Exponential Trendline
f <- function(logATx,a,b) {a * exp(b * logATx)}
fit <- nls(ATy ~ f(logATx,a,b), start = c(a=1, b=1))
co <- coef(fit)
curve(f(x, a=co[1], b=co[2]), add = TRUE,,lty=3, lwd=3)
f <- function(logHGx,a,b) {a * exp(b * logHGx)}
fit <- nls(HGy ~ f(logHGx,a,b), start = c(a=1, b=1))
co <- coef(fit)
curve(f(x, a=co[1], b=co[2]), add = TRUE,,lty=6, lwd=3)

#Linear Trendline (If necessary)
```

```
fit<- lm(ATy~logATx)
abline(fit,lty=3,lwd = 3)

fit<- lm(HGy~logHGx)
abline(fit,lty=6,lwd = 3)
```

Part 2: Data

Foraminiferal count data for chapter 4.

Sapelo Island										
Nickel										
Metal Added (mg/L)	**0.074**	**0.074**	**0.74**	**0.74**	**7.4**	**7.4**	**74**	**74**	**740**	**740**
Actual Concentration (mg/L)	**0.01065**	**0.02257**	**0.01634**	**0.0285**	**0.43795**	**0.32265**	**6.24**	**26.725**	**151.05**	**264.4**
Temperature (Celsius)	**22º**	**22º**	**22º**	**22º**	**22º**	**22º**	**22º**	**22º**	**22º**	**22º**
Salinity (PSU)	**32**	**32**	**32**	**32**	**32**	**32**	**32**	**32**	**32**	**32**
Ovammina opaca	0	0	2	3	5	5	0	0	1	4
Psammophaga sapela	0	0	14	14	2	0	0	0	1	0
Ammonia tepida	0	10	48	40	16	16	4	1	0	0
Haynesina germanica	0	22	51	74	6	14	4	2	0	0
Buliminella elegantissima	0	0	0	0	0	0	0	0	0	0
Miliammina fusca	11	0	96	68	2	0	0	0	15	10
Textularia candeiana	16	2	47	16	6	0	0	0	0	0
Textularia earlandi	4	0	0	6	0	0	0	0	0	0
Textularia palustris	5	3	2	4	0	0	0	0	0	0
Triloculina oblonga	0	0	0	0	1	0	0	0	0	0
Ammottium salsum	0	0	0	0	0	0	0	0	0	0
Reophax cf. R. arcticus	0	0	0	0	2	0	0	0	0	0
Quinqueloculina jugosa	0	0	0	0	0	0	0	0	0	0
Elphidium excavatum	0	0	0	0	0	0	0	0	0	0
Metal Added (mg/L)	**0.074**	**0.074**	**0.74**	**0.74**	**7.4**	**7.4**	**74**	**74**	**740**	**740**
Actual Concentration (mg/L)	**0.00733**	**0.00834**	**0.01868**	**0.01872**	**0.4539**	**0.5094**	**6.582**	**5.879**	**154.4**	**316.4**
Temperature (Celsius)	**22º**	**22º**	**22º**	**22º**	**22º**	**22º**	**22º**	**22º**	**22º**	**22º**
Salinity (PSU)	**12**	**12**	**12**	**12**	**12**	**12**	**12**	**12**	**12**	**12**
Ovammina opaca	2	13	8	7	8	22	6	8	6	9
Psammophaga sapela	4	10	9	12	4	6	4	1	1	0

Ammonia tepida	28	21	15	14	5	6	1	1	0	0
Haynesina germanica	21	14	0	0	10	5	0	0	0	0
Buliminella elegantissima	0	0	0	0	0	0	0	0	0	0
Miliammina fusca	0	70	104	102	0	0	10	0	15	6
Textularia candeiana	1	0	6	1	3	2	0	0	0	0
Textularia earlandi	0	0	0	0	0	0	0	0	0	0
Textularia palustris	0	0	0	0	0	0	0	0	0	0
Triloculina oblonga	0	0	0	0	0	0	0	0	0	0
Ammottium salsum	0	0	0	0	0	0	0	0	0	0
Reophax cf. R. arcticus	0	0	0	0	0	0	0	0	0	0
Quinqueloculina jugosa	0	0	0	0	0	0	0	0	0	0
Elphidium excavatum	0	0	0	0	0	0	0	0	0	0
Metal Added (mg/L)	**0.074**	**0.074**	**0.74**	**0.74**	**7.4**	**7.4**	**74**	**74**	**740**	**740**
Actual Concentration (mg/L)	**0.01452**	**0.0154**	**0.02733**	**0.02697**	**0.2029**	**0.3554**	**15.1**	**9.486**	**145.5**	**238.9**
Temperature (Celsius)	**22º**	**22º**	**22º**	**22º**	**22º**	**22º**	**22º**	**22º**	**22º**	**22º**
Salinity (PSU)	**40**	**40**	**40**	**40**	**40**	**40**	**40**	**40**	**40**	**40**
Ovammina opaca	0	0	8	14	2	0	11	9	6	6
Psammophaga sapela	0	0	0	11	5	5	0	0	0	3
Ammonia tepida	23	38	40	42	28	73	0	0	0	0
Haynesina germanica	0	0	12	9	0	25	0	0	0	0
Buliminella elegantissima	0	0	0	0	0	0	0	0	0	0
Miliammina fusca	54	51	0	13	0	0	0	0	11	6
Textularia candeiana	18	19	0	5	9	25	0	0	0	0
Textularia earlandi	0	0	0	0	11	3	0	0	0	0
Textularia palustris	0	0	0	0	35	0	0	0	0	0
Triloculina oblonga	0	0	0	0	0	0	0	0	0	0
Ammottium salsum	0	0	0	0	0	0	0	0	0	0
Reophax cf. R. arcticus	2	0	0	0	0	0	0	0	0	0
Quinqueloculina jugosa	0	0	0	0	3	0	0	0	0	0
Elphidium excavatum	0	0	0	0	0	0	0	0	0	0

Metal Added (mg/L)	**0.074**	**0.074**	**0.74**	**0.74**	**7.4**	**7.4**	**74**	**74**	**740**	**740**
Actual Concentration (mg/L)	**0.0197**	**0.01213**	**0.01856**	**0.01465**	**0.9089**	**1.376**	**9.642**	**9.637**	**242.4**	**301.5**
Temperature (Celsius)	**18º**	**18º**	**18º**	**18º**	**18º**	**18º**	**18º**	**18º**	**18º**	**18º**
Salinity (PSU)	**32**	**32**	**32**	**32**	**32**	**32**	**32**	**32**	**32**	**32**
Ovammina opaca	14	12	8	18	11	1	3	0	9	7
Psammophaga sapela	5	12	9	16	2	2	5	2	6	0
Ammonia tepida	11	9	7	8	15	18	0	0	0	0
Haynesina germanica	31	22	4	16	22	56	0	0	0	0
Buliminella elegantissima	0	0	0	0	0	0	0	0	0	0
Miliammina fusca	0	0	2	8	4	1	2	2	0	0
Textularia candeiana	0	3	0	3	0	0	0	0	0	0
Textularia earlandi	4	6	0	0	1	0	0	0	0	0
Textularia palustris	0	0	0	0	0	0	0	0	0	0
Triloculina oblonga	0	0	1	0	0	0	0	0	0	0
Ammottium salsum	0	0	0	0	0	0	0	0	0	0
Reophax cf. R. arcticus	0	0	0	0	0	0	0	0	0	0
Quinqueloculina jugosa	0	0	0	0	0	0	0	0	0	0
Elphidium excavatum	0	0	0	0	0	0	0	0	0	0
Metal Added (mg/L)	**0.074**	**0.074**	**0.74**	**0.74**	**7.4**	**7.4**	**74**	**74**	**740**	**740**
Actual Concentration (mg/L)	**0.01243**	**0.01523**	**0.02634**	**0.0287**	**0.192**	**0.1744**	**1.301**	**0.8388**	**111.3**	**116.9**
Temperature (Celsius)	**30º**	**30º**	**30º**	**30º**	**30º**	**30º**	**30º**	**30º**	**30º**	**30º**
Salinity (PSU)	**32**	**32**	**32**	**32**	**32**	**32**	**32**	**32**	**32**	**32**
Ovammina opaca	3	17	5	7	11	4	8	0	3	5
Psammophaga sapela	0	12	0	5	8	2	13	11	0	0
Ammonia tepida	0	14	16	11	54	11	0	13	0	0
Haynesina germanica	0	2	0	0	6	0	0	4	0	0
Buliminella elegantissima	0	0	0	0	0	0	0	0	0	0
Miliammina fusca	35	56	105	77	0	0	0	0	7	4
Textularia candeiana	0	99	94	36	20	9	0	7	0	0

Textularia earlandi	0	0	0	0	0	0	0	0	0	0
Textularia palustris	0	0	0	0	0	0	0	0	0	0
Triloculina oblonga	0	0	0	0	0	0	0	0	0	0
Ammottium salsum	0	0	0	0	0	0	0	0	0	0
Reophax cf. R. arcticus	3	12	0	5	1	13	0	0	0	0
Quinqueloculina jugosa	0	0	0	0	0	0	0	0	0	0
Elphidium excavatum	0	0	0	0	0	0	0	0	0	0
Zinc										
Metal Added (mg/L)	**0.09**	**0.09**	**0.9**	**0.9**	**9**	**9**	**90**	**90**	**900**	**900**
Actual Concentration (mg/L)	**0.01538**	**0.16815**	**0.02026**	**0.02417**	**0.825**	**0.05495**	**17.045**	**20.455**	**518.5**	**634.5**
Temperature (Celsius)	**22º**	**22º**	**22º**	**22º**	**22º**	**22º**	**22º**	**22º**	**22º**	**22º**
Salinity (PSU)	**32**	**32**	**32**	**32**	**32**	**32**	**32**	**32**	**32**	**32**
Ovammina opaca	0	4	0	23	1	8	0	0	0	0
Psammophaga sapela	0	2	0	6	2	11	0	0	0	0
Ammonia tepida	22	27	14	31	9	41	0	0	1	0
Haynesina germanica	16	40	15	18	15	17	0	8	0	0
Buliminella elegantissima	0	0	0	0	0	0	0	0	0	0
Miliammina fusca	5	7	86	22	1	0	0	0	0	0
Textularia candeiana	12	13	17	7	0	0	0	0	0	0
Textularia earlandi	37	3	0	3	0	0	0	0	0	0
Textularia palustris	17	4	0	0	0	0	0	0	0	0
Triloculina oblonga	0	0	0	0	0	0	0	0	0	0
Ammottium salsum	0	0	0	0	0	0	0	0	0	0
Reophax cf. R. arcticus	0	0	0	0	0	0	0	0	0	0
Quinqueloculina jugosa	0	0	0	0	0	0	0	0	0	0
Elphidium excavatum	0	4	0	0	0	0	0	0	0	0
Metal Added (mg/L)	**0.09**	**0.09**	**0.9**	**0.9**	**9**	**9**	**90**	**90**	**900**	**900**
Actual Concentration (mg/L)	**0**	**0.05856**	**0.1723**	**0.01004**	**0.8171**	**0.6342**	**9.784**	**24.09**	**615.8**	**865.7**
Temperature (Celsius)	**22º**	**22º**	**22º**	**22º**	**22º**	**22º**	**22º**	**22º**	**22º**	**22º**
Salinity (PSU)	**12**	**12**	**12**	**12**	**12**	**12**	**12**	**12**	**12**	**12**

Ovammina opaca	17	14	46	8	59	45	8	11	4	1
Psammophaga sapela	14	11	3	5	3	0	5	7	0	0
Ammonia tepida	16	22	6	23	0	0	0	0	0	0
Haynesina germanica	5	10	5	6	0	0	0	0	0	0
Buliminella elegantissima	0	0	0	0	0	0	0	0	0	0
Miliammina fusca	133	101	0	15	0	0	0	0	0	4
Textularia candeiana	18	8	0	3	0	0	0	0	0	0
Textularia earlandi	0	0	0	0	0	0	0	0	0	0
Textularia palustris	0	0	0	0	0	0	0	0	0	0
Triloculina oblonga	0	0	0	0	0	0	0	0	0	0
Ammottium salsum	0	0	0	0	0	0	0	0	0	0
Reophax cf. R. arcticus	0	0	0	0	0	0	0	0	0	0
Quinqueloculina jugosa	0	0	0	0	0	0	0	0	0	0
Elphidium excavatum	0	0	0	0	0	0	0	0	0	0
Metal Added (mg/L)	**0.09**	**0.09**	**0.9**	**0.9**	**9**	**9**	**90**	**90**	**900**	**900**
Actual Concentration (mg/L)	**0**	**0**	**0.00503**	**0**	**0.8799**	**0.1127**	**11.15**	**11.07**	**581.9**	**636.5**
Temperature (Celsius)	**22º**	**22º**	**22º**	**22º**	**22º**	**22º**	**22º**	**22º**	**22º**	**22º**
Salinity (PSU)	**40**	**40**	**40**	**40**	**40**	**40**	**40**	**40**	**40**	**40**
Ovammina opaca	0	0	8	10	10	5	0	0	3	5
Psammophaga sapela	16	21	1	4	0	0	0	0	0	2
Ammonia tepida	12	21	25	24	11	3	0	0	0	0
Haynesina germanica	9	6	6	4	0	0	0	0	0	0
Buliminella elegantissima	0	0	0	0	0	0	0	0	0	0
Miliammina fusca	96	75	57	72	0	0	0	0	13	17
Textularia candeiana	12	17	5	2	0	0	0	0	0	0
Textularia earlandi	15	12	6	1	0	0	0	0	0	0
Textularia palustris	0	0	0	0	0	0	0	0	0	0
Triloculina oblonga	0	0	0	0	0	0	0	0	0	0
Ammottium salsum	0	0	0	0	0	0	0	0	0	0
Reophax cf. R. arcticus	0	0	0	0	0	0	0	0	0	0
Quinqueloculina jugosa	0	0	0	0	0	0	0	0	0	0

Elphidium excavatum	0	0	0	0	0	0	0	0	0	0
Metal Added (mg/L)	**0.09**	**0.09**	**0.9**	**0.9**	**9**	**9**	**90**	**90**	**900**	**900**
Actual Concentration (mg/L)	**0.00709**	**0.00755**	**0.02353**	**0.0241**	**0.2856**	**0.179**	**12.12**	**9.96**	**683.5**	**698.3**
Temperature (Celsius)	**18º**	**18º**	**18º**	**18º**	**18º**	**18º**	**18º**	**18º**	**18º**	**18º**
Salinity (PSU)	**32**	**32**	**32**	**32**	**32**	**32**	**32**	**32**	**32**	**32**
Ovammina opaca	18	28	13	25	17	55	11	8	5	11
Psammophaga sapela	5	0	0	0	4	13	4	2	0	4
Ammonia tepida	12	4	6	4	0	12	0	0	0	0
Haynesina germanica	3	14	66	86	0	5	0	0	0	0
Buliminella elegantissima	0	0	0	0	0	0	0	0	0	0
Miliammina fusca	14	2	0	0	0	0	0	0	0	0
Textularia candeiana	0	0	0	0	0	0	0	0	0	0
Textularia earlandi	0	0	0	0	0	0	0	0	0	0
Textularia palustris	0	0	0	0	0	0	0	0	0	0
Triloculina oblonga	0	0	0	0	0	0	0	0	0	0
Ammottium salsum	0	0	0	0	0	0	0	0	0	0
Reophax cf. R. arcticus	0	0	0	0	0	0	0	0	0	0
Quinqueloculina jugosa	0	0	0	0	0	0	0	0	0	0
Elphidium excavatum	0	0	0	0	0	0	0	0	0	0
Metal Added (mg/L)	**0.09**	**0.09**	**0.9**	**0.9**	**9**	**9**	**90**	**90**	**900**	**900**
Actual Concentration (mg/L)	**0**	**0**	**0**	**0**	**0.103**	**0.2726**	**1.64**	**3.415**	**595.7**	**291**
Temperature (Celsius)	**30º**	**30º**	**30º**	**30º**	**30º**	**30º**	**30º**	**30º**	**30º**	**30º**
Salinity (PSU)	**32**	**32**	**32**	**32**	**32**	**32**	**32**	**32**	**32**	**32**
Ovammina opaca	5	1	15	21	74	28	5	6	0	2
Psammophaga sapela	12	0	6	0	14	18	7	8	0	0
Ammonia tepida	45	16	0	0	35	11	0	0	0	0
Haynesina germanica	13	3	0	0	16	0	0	1	0	0
Buliminella elegantissima	0	0	0	0	0	0	0	0	0	0
Miliammina fusca	22	44	79	33	0	0	0	0	0	1

Textularia candeiana	3	9	0	0	0	0	0	0	0	0
Textularia earlandi	4	7	4	4	0	0	0	0	0	0
Textularia palustris	0	0	0	0	4	0	0	0	0	0
Triloculina oblonga	0	0	0	0	0	0	0	0	0	0
Ammottium salsum	0	0	0	0	0	0	0	0	0	0
Reophax cf. R. arcticus	0	0	0	2	0	0	0	0	0	0
Quinqueloculina jugosa	0	0	0	0	0	0	0	0	0	0
Elphidium excavatum	0	0	0	0	0	0	0	0	0	0
Control										
Metal Added (mg/L)	**N/A**	**N/A**	**N/A**	**N/A**	**N/A**	**N/A**	**N/A**	**N/A**	**N/A**	**N/A**
Actual Nickel (mg/L)	**0.04063**	**0.04243**	**0.02547**	**0.02047**	**0.02021**	**0.02032**	**0.03904**	**0.03803**	**0.03507**	**0.03361**
Actual Zinc (mg/L)	**0.01225**	**0.01153**	**0.00501**	**0.00688**	**0.00403**	**0.00614**	**0.00574**	**0.5174**	**1.068**	**0.00956**
Temperature (Celsius)	**22º**	**22º**	**22º**	**22º**	**22º**	**22º**	**18º**	**18º**	**30º**	**30º**
Salinity (PSU)	**32**	**32**	**12**	**12**	**40**	**40**	**32**	**32**	**32**	**32**
Ovammina opaca	0	0	5	6	0	0	20	20	9	8
Psammophaga sapela	0	0	9	14	0	0	8	11	0	0
Ammonia tepida	46	29	42	40	32	45	17	25	21	29
Haynesina germanica	68	82	45	56	0	15	45	53	11	27
Buliminella elegantissima	0	0	0	0	0	0	0	0	0	0
Miliammina fusca	10	0	0	0	65	51	0	0	63	34
Textularia candeiana	0	0	4	11	17	16	0	4	0	0
Textularia earlandi	0	0	0	5	0	0	8	11	0	0
Textularia palustris	0	0	0	0	0	0	0	0	0	0
Triloculina oblonga	0	0	0	0	0	0	0	0	0	0
Ammottium salsum	0	0	0	0	0	0	0	0	0	0
Reophax cf. R. arcticus	0	0	0	0	4	1	0	0	0	0
Quinqueloculina jugosa	0	0	0	0	0	0	0	0	0	0
Elphidium excavatum	0	0	0	0	0	0	0	0	0	0
Little Duck Key										
Nickel										
Metal Added (mg/L)	**0.074**	**0.074**	**0.74**	**0.74**	**7.4**	**7.4**	**74**	**74**	**740**	**740**

Actual Concentration (mg/L)	**0.1229**	**0.08327**	**0.2325**	**0.2988**	**1.341**	**1.748**	**25.62**	**17.86**	**290.1**	**336.7**
Temperature (Celsius)	**22º**	**22º**	**22º**	**22º**	**22º**	**22º**	**22º**	**22º**	**22º**	**22º**
Salinity (PSU)	**32**	**32**	**32**	**32**	**32**	**32**	**32**	**32**	**32**	**32**
Ammonia tepida	1	0	0	0	0	1	1	0	0	0
Archais angulatus	0	0	0	0	0	0	0	0	0	0
Bolivina lowmani	6	4	5	2	0	0	0	0	0	0
Bolivina pulchella	0	0	0	0	0	0	0	0	0	0
Bolivina striatula	0	0	0	0	0	0	0	0	0	0
Buliminella elegantissima	0	0	0	0	0	0	0	0	0	0
Cibicides spp.	0	0	0	0	0	0	0	0	0	0
Cornuspira planorbis	0	0	0	0	0	0	0	0	0	0
Discorbis mira	0	0	0	0	0	0	0	0	0	0
Elphidium discoidale	0	0	0	0	0	0	2	0	0	0
Elphidium mexicanum	0	0	1	0	1	22	0	0	0	0
Hauerina bradyi	0	0	0	0	0	0	0	0	0	0
Miliolinella circularis	8	0	0	0	2	0	0	0	0	0
Miliolinella subrotunda	0	0	0	0	0	0	0	0	0	0
Nonionoides grateloupi	0	0	0	0	0	0	0	0	0	0
Ovammina opaca	13	0	16	11	3	1	1	0	5	6
Peneroplis pertusus	0	0	0	0	0	0	0	0	0	0
Quinqueloculina agglutinans	0	0	0	0	0	0	0	0	0	0
Quinqueloculina bosciana	0	4	6	3	0	0	0	0	0	0
Quinqueloculina laevigata	0	0	0	0	0	0	0	0	0	0
Quinqueloculina lamarckiana	2	0	0	0	1	0	0	0	0	0
Quinqueloculina poeyana	0	0	0	0	0	1	0	0	0	0
Quinqueloculina polygona	0	0	0	0	0	0	0	0	0	0
Quinqueloculina sabulosa	11	17	12	7	1	0	1	1	0	0
Quinqueloculina seminula	32	11	3	0	1	0	0	1	0	0
Reophax gaussicus	1	17	15	0	1	1	0	0	0	0
Rosalina floridana	0	0	0	0	0	0	0	0	0	0

Rosalina globularis	0	0	0	0	0	0	0	0	0	0
Sorites marginalis	0	0	0	0	0	0	0	0	0	0
Textularia candeiana	6	19	7	6	0	1	0	0	0	0
Textularia earlandi	4	0	2	1	1	0	0	0	0	0
Triloculina oblonga	16	30	6	5	1	0	1	0	2	2
Triloculina rotunda	0	0	0	0	0	0	0	0	0	0
Triloculina tricarinata	0	0	0	0	0	0	0	0	0	0
Metal Added (mg/L)	**0.074**	**0.074**	**0.74**	**0.74**	**7.4**	**7.4**	**74**	**74**	**740**	**740**
Actual Concentration (mg/L)	**0.1095**	**0.09123**	**0.09798**	**0.09704**	**0.1057**	**0.08335**	**0.2051**	**0.2152**	**1.832**	**1.377**
Temperature (Celsius)	**22º**	**22º**	**22º**	**22º**	**22º**	**22º**	**22º**	**22º**	**22º**	**22º**
Salinity (PSU)	**12**	**12**	**12**	**12**	**12**	**12**	**12**	**12**	**12**	**12**
Ammonia tepida	0	0	0	2	0	0	0	0	0	0
Archais angulatus	0	0	0	0	0	0	0	0	0	0
Bolivina lowmani	0	0	0	0	0	0	0	0	0	0
Bolivina pulchella	0	0	0	0	0	0	0	0	0	0
Bolivina striatula	0	0	0	0	0	0	0	0	0	0
Buliminella elegantissima	0	0	0	0	0	0	0	0	0	0
Cibicides spp.	0	0	0	0	0	0	0	0	0	0
Cornuspira planorbis	0	0	0	0	0	0	0	0	0	0
Discorbis mira	0	0	0	0	0	0	0	0	0	0
Elphidium discoidale	0	0	0	0	0	0	0	0	0	0
Elphidium mexicanum	0	0	0	4	6	11	0	0	0	0
Hauerina bradyi	0	0	0	0	0	0	0	0	0	0
Miliolinella circularis	0	0	0	2	1	2	0	0	0	0
Miliolinella subrotunda	0	0	0	0	0	0	0	0	0	0
Nonionoides grateloupi	0	0	0	0	0	0	0	0	0	0
Ovammina opaca	27	35	0	10	6	4	3	7	10	4
Peneroplis pertusus	0	0	0	0	0	0	0	0	0	0
Quinqueloculina agglutinans	0	0	0	0	0	0	0	0	0	0
Quinqueloculina bosciana	0	0	0	2	0	0	0	0	0	0
Quinqueloculina laevigata	0	0	0	3	0	0	0	0	0	0

Quinqueloculina lamarckiana	0	0	0	0	1	0	0	0	0	0
Quinqueloculina poeyana	0	0	0	0	0	0	0	0	0	0
Quinqueloculina polygona	0	0	0	0	0	0	0	0	0	0
Quinqueloculina sabulosa	3	7	0	0	10	11	0	0	0	0
Quinqueloculina seminula	0	0	0	0	0	0	1	0	0	0
Reophax gaussicus	0	0	0	0	0	0	0	0	0	0
Rosalina floridana	0	0	0	0	0	0	0	0	0	0
Rosalina globularis	0	0	0	0	0	0	0	0	0	0
Sorites marginalis	0	0	0	0	0	0	0	0	0	0
Textularia candeiana	0	0	0	0	0	0	0	0	0	0
Textularia earlandi	0	0	0	0	0	0	0	0	0	0
Triloculina oblonga	8	15	0	7	0	5	0	3	1	2
Triloculina rotunda	0	0	0	0	0	0	0	0	0	0
Triloculina tricarinata	0	0	0	0	0	0	0	0	0	0
Metal Added (mg/L)	**0.074**	**0.074**	**0.74**	**0.74**	**7.4**	**7.4**	**74**	**74**	**740**	**740**
Actual Concentration (mg/L)	**0.09273**	**0.07609**	**0.1938**	**0.1994**	**2.113**	**1.376**	**8.52**	**8.875**	**337.5**	**337.9**
Temperature (Celsius)	**22º**	**22º**	**22º**	**22º**	**22º**	**22º**	**22º**	**22º**	**22º**	**22º**
Salinity (PSU)	**40**	**40**	**40**	**40**	**40**	**40**	**40**	**40**	**40**	**40**
Ammonia tepida	0	0	0	0	0	0	0	0	0	0
Archais angulatus	0	0	0	0	0	0	0	0	0	0
Bolivina lowmani	8	5	9	7	0	0	0	0	0	0
Bolivina pulchella	0	0	0	0	0	0	0	0	0	0
Bolivina striatula	0	0	0	0	0	0	0	0	0	0
Buliminella elegantissima	2	0	0	0	0	0	0	0	0	0
Cibicides spp.	0	0	0	0	0	0	0	0	0	0
Cornuspira planorbis	0	0	0	0	0	0	0	0	0	0
Discorbis mira	0	0	0	0	0	0	0	0	0	0
Elphidium discoidale	0	0	0	0	0	0	0	0	0	0
Elphidium mexicanum	3	0	0	0	0	2	0	0	0	0
Hauerina bradyi	0	0	0	0	0	0	0	0	0	0
Miliolinella circularis	0	0	0	0	0	0	0	0	0	0

Miliolinella subrotunda	0	0	0	0	0	0	0	0	0	0
Nonionoides grateloupi	0	0	0	0	0	0	0	0	0	0
Ovammina opaca	37	36	25	35	0	0	0	0	0	1
Peneroplis pertusus	0	0	0	0	0	0	0	0	0	0
Quinqueloculina agglutinans	0	0	0	0	0	0	0	0	0	0
Quinqueloculina bosciana	0	0	0	0	0	0	0	0	0	0
Quinqueloculina laevigata	0	0	0	0	0	0	0	0	0	0
Quinqueloculina lamarckiana	0	0	0	0	0	0	0	0	0	0
Quinqueloculina poeyana	0	0	0	0	0	0	0	0	0	0
Quinqueloculina polygona	0	0	0	0	0	0	0	0	0	0
Quinqueloculina sabulosa	38	49	22	24	10	17	0	0	0	0
Quinqueloculina seminula	0	0	0	0	0	0	0	0	0	0
Reophax gaussicus	22	17	20	9	5	3	1	2	0	0
Rosalina floridana	0	0	0	0	0	0	0	0	0	0
Rosalina globularis	0	0	0	0	0	0	0	0	0	0
Sorites marginalis	0	0	0	0	0	0	0	0	0	0
Textularia candeiana	0	0	12	19	9	14	1	0	0	0
Textularia earlandi	0	0	0	0	0	0	0	0	0	0
Triloculina oblonga	38	52	20	28	58	56	1	0	0	0
Triloculina rotunda	0	0	0	0	0	0	0	0	0	0
Triloculina tricarinata	0	0	0	0	0	0	0	0	0	0
Metal Added (mg/L)	**0.074**	**0.074**	**0.74**	**0.74**	**7.4**	**7.4**	**74**	**74**	**740**	**740**
Actual Concentration (mg/L)	**0.02862**	**0.03387**	**0.2247**	**0.3057**	**0.01804**	**0.02035**	**39.04**	**41.09**	**377.3**	**447.6**
Temperature (Celsius)	**18º**	**18º**	**18º**	**18º**	**18º**	**18º**	**18º**	**18º**	**18º**	**18º**
Salinity (PSU)	**32**	**32**	**32**	**32**	**32**	**32**	**32**	**32**	**32**	**32**
Ammonia tepida	0	0	0	0	0	0	0	0	0	0
Archais angulatus	0	0	0	0	0	0	0	0	0	0
Bolivina lowmani	6	5	6	3	2	4	2	0	0	0
Bolivina pulchella	0	2	2	0	0	0	0	0	0	0
Bolivina striatula	0	0	0	0	0	0	0	0	0	0
Buliminella elegantissima	0	0	0	0	0	0	0	0	0	0

Cibicides spp.	0	0	0	0	0	0	0	0	0	0
Cornuspira planorbis	0	0	0	0	0	0	0	0	0	0
Discorbis mira	0	0	0	0	0	0	0	0	0	0
Elphidium discoidale	0	0	0	0	0	0	0	0	0	0
Elphidium mexicanum	0	0	0	1	0	3	1	0	0	0
Hauerina bradyi	0	0	0	0	0	0	0	0	0	0
Miliolinella circularis	0	0	0	3	3	0	0	0	0	0
Miliolinella subrotunda	0	0	0	0	0	0	0	0	0	0
Nonionoides grateloupi	0	0	0	0	0	0	0	0	0	0
Ovammina opaca	45	51	3	6	3	8	3	3	2	0
Peneroplis pertusus	0	0	0	0	0	0	0	0	0	0
Quinqueloculina agglutinans	5	0	0	0	0	0	0	0	0	0
Quinqueloculina bosciana	0	4	2	0	0	4	0	0	0	0
Quinqueloculina laevigata	0	0	0	0	0	0	0	0	0	0
Quinqueloculina lamarckiana	1	0	0	0	1	0	1	2	0	0
Quinqueloculina poeyana	0	0	0	0	0	0	0	0	0	0
Quinqueloculina polygona	0	0	0	0	0	0	0	0	0	0
Quinqueloculina sabulosa	18	13	1	8	8	13	0	0	0	0
Quinqueloculina seminula	1	4	2	1	0	0	0	0	0	0
Reophax gaussicus	1	5	2	6	3	6	0	0	0	0
Rosalina floridana	0	0	0	0	0	0	0	0	0	0
Rosalina globularis	0	0	0	0	0	0	0	0	0	0
Sorites marginalis	0	0	1	0	0	0	0	0	0	0
Textularia candeiana	8	3	10	16	3	0	0	0	0	0
Textularia earlandi	0	2	4	4	0	0	0	0	0	0
Triloculina oblonga	4	8	5	6	5	7	1	0	0	0
Triloculina rotunda	0	0	0	0	0	0	0	0	0	0
Triloculina tricarinata	0	0	0	0	0	0	0	0	0	0
Metal Added (mg/L)	**0.074**	**0.074**	**0.74**	**0.74**	**7.4**	**7.4**	**74**	**74**	**740**	**740**
Actual Concentration (mg/L)	**0.07007**	**0.07002**	**0.1924**	**0.1751**	**1.307**	**1.239**	**1.86**	**2.791**	**377.4**	**306.2**

Temperature (Celsius)	**30º**	**30º**	**30º**	**30º**	**30º**	**30º**	**30º**	**30º**	**30º**	**30º**
Salinity (PSU)	**32**	**32**	**32**	**32**	**32**	**32**	**32**	**32**	**32**	**32**
Ammonia tepida	0	0	10	13	0	0	0	0	0	0
Archais angulatus	0	0	0	0	0	0	0	0	0	0
Bolivina lowmani	10	3	0	0	3	5	0	0	0	0
Bolivina pulchella	0	0	0	0	0	2	0	0	0	0
Bolivina striatula	0	0	0	0	0	0	0	0	0	0
Buliminella elegantissima	0	0	0	0	0	0	0	0	0	0
Cibicides spp.	0	0	0	0	0	0	0	0	0	0
Cornuspira planorbis	0	0	0	0	0	0	0	0	0	0
Discorbis mira	0	0	0	0	0	0	0	0	0	0
Elphidium discoidale	0	0	0	0	0	0	0	0	0	0
Elphidium mexicanum	27	18	26	25	17	24	0	0	0	0
Hauerina bradyi	0	0	0	0	0	0	0	0	0	0
Miliolinella circularis	3	0	0	0	5	2	0	0	0	0
Miliolinella subrotunda	0	0	0	0	0	0	0	0	0	0
Nonionoides grateloupi	0	0	0	0	0	0	0	0	0	0
Ovammina opaca	5	2	0	0	6	5	1	2	2	3
Peneroplis pertusus	0	0	0	0	0	0	0	0	0	0
Quinqueloculina agglutinans	0	0	0	0	0	0	0	0	0	0
Quinqueloculina bosciana	10	4	0	0	3	5	1	0	0	0
Quinqueloculina laevigata	0	0	0	0	1	0	0	0	0	0
Quinqueloculina lamarckiana	0	0	0	0	0	1	0	0	0	0
Quinqueloculina poeyana	0	0	0	0	0	0	0	0	0	0
Quinqueloculina polygona	0	0	0	0	0	0	0	0	0	0
Quinqueloculina sabulosa	22	17	14	8	5	3	0	0	0	0
Quinqueloculina seminula	3	4	0	0	0	0	0	2	0	0
Reophax gaussicus	24	29	11	14	17	19	0	0	0	0
Rosalina floridana	0	0	0	0	0	0	0	0	0	0
Rosalina globularis	0	0	0	0	0	0	0	0	0	0
Sorites marginalis	2	5	0	0	1	3	1	2	0	0

Textularia candeiana	36	40	30	20	16	12	0	0	0	0
Textularia earlandi	0	0	0	0	2	1	0	0	0	0
Triloculina oblonga	38	35	19	20	9	12	1	4	0	0
Triloculina rotunda	0	0	0	0	0	1	0	0	0	0
Triloculina tricarinata	0	0	0	0	0	0	0	0	0	0
Zinc										
Metal Added (mg/L)	**0.09**	**0.09**	**0.9**	**0.9**	**9**	**9**	**90**	**90**	**900**	**900**
Actual Concentration (mg/L)	**0.04465**	**0.04717**	**0.2505**	**0.2735**	**2.415**	**1.839**	**5.4**	**5.605**	**9.088**	**10.79**
Temperature (Celsius)	**22º**	**22º**	**22º**	**22º**	**22º**	**22º**	**22º**	**22º**	**22º**	**22º**
Salinity (PSU)	**32**	**32**	**32**	**32**	**32**	**32**	**32**	**32**	**32**	**32**
Ammonia tepida	0	0	1	0	0	0	0	0	0	0
Archais angulatus	0	0	0	0	0	0	0	0	0	0
Bolivina lowmani	0	4	2	0	0	0	0	0	0	0
Bolivina pulchella	0	0	0	0	0	0	0	0	0	0
Bolivina striatula	0	0	0	0	0	0	0	0	0	0
Buliminella elegantissima	0	0	0	0	0	0	0	0	0	0
Cibicides spp.	0	0	0	0	0	0	0	0	0	0
Cornuspira planorbis	0	0	0	0	0	0	0	0	0	0
Discorbis mira	0	0	0	0	0	0	0	0	0	0
Elphidium discoidale	0	0	0	0	0	0	0	0	0	0
Elphidium mexicanum	0	0	1	0	0	0	0	0	0	0
Hauerina bradyi	0	0	0	0	0	0	0	0	0	0
Miliolinella circularis	0	5	0	0	0	1	0	0	0	0
Miliolinella subrotunda	0	0	0	0	0	0	0	0	0	0
Nonionoides grateloupi	0	0	0	0	0	0	0	0	0	0
Ovammina opaca	5	0	0	0	0	1	1	0	0	0
Peneroplis pertusus	0	0	0	0	0	0	0	0	0	0
Quinqueloculina agglutinans	0	0	0	0	0	0	0	0	0	0
Quinqueloculina bosciana	4	0	3	2	0	0	0	0	0	0
Quinqueloculina laevigata	0	0	2	0	1	1	1	1	0	0
Quinqueloculina lamarckiana	0	0	0	0	0	0	0	0	0	0

Quinqueloculina poeyana	0	0	0	0	0	0	0	0	0	0
Quinqueloculina polygona	0	0	0	0	0	0	0	0	0	0
Quinqueloculina sabulosa	10	18	2	6	0	0	0	0	0	0
Quinqueloculina seminula	3	5	0	4	0	0	0	1	0	0
Reophax gaussicus	16	12	8	8	0	0	0	0	0	0
Rosalina floridana	0	0	0	0	0	0	0	0	0	0
Rosalina globularis	0	0	0	0	0	0	0	0	0	0
Sorites marginalis	0	0	0	0	0	0	0	0	0	0
Textularia candeiana	0	11	0	1	0	0	0	0	0	0
Textularia earlandi	0	0	3	0	0	0	0	0	0	0
Triloculina oblonga	8	17	0	0	0	0	1	1	0	0
Triloculina rotunda	0	0	0	0	0	0	0	0	0	0
Triloculina tricarinata	0	0	0	0	0	0	0	0	0	0
Metal Added (mg/L)	**0.09**	**0.09**	**0.9**	**0.9**	**9**	**9**	**90**	**90**	**900**	**900**
Actual Concentration (mg/L)	**0**	**0**	**0**	**0**	**0**	**0**	**0**	**0**	**1.263**	**1.375**
Temperature (Celsius)	**22º**	**22º**	**22º**	**22º**	**22º**	**22º**	**22º**	**22º**	**22º**	**22º**
Salinity (PSU)	**12**	**12**	**12**	**12**	**12**	**12**	**12**	**12**	**12**	**12**
Ammonia tepida	0	0	0	0	0	0	0	0	0	0
Archais angulatus	0	0	0	0	0	0	0	0	0	0
Bolivina lowmani	0	0	0	1	0	0	0	0	0	0
Bolivina pulchella	0	0	0	0	0	0	0	0	0	0
Bolivina striatula	0	0	0	0	0	0	0	0	0	0
Buliminella elegantissima	0	0	0	0	0	0	0	0	0	0
Cibicides spp.	0	0	0	0	0	0	0	0	0	0
Cornuspira planorbis	0	0	0	0	0	0	0	0	0	0
Discorbis mira	0	0	0	0	0	0	0	0	0	0
Elphidium discoidale	0	0	0	1	0	0	0	0	0	0
Elphidium mexicanum	0	0	0	0	0	0	0	0	0	0
Hauerina bradyi	0	0	0	0	0	0	0	0	0	0
Miliolinella circularis	0	0	0	2	0	0	0	0	0	0
Miliolinella subrotunda	0	0	0	0	0	0	0	0	0	0

Nonionoides grateloupi	0	0	0	0	0	0	0	0	0	0
Ovammina opaca	34	39	0	0	7	9	0	0	2	2
Peneroplis pertusus	0	0	0	0	0	0	0	0	0	0
Quinqueloculina agglutinans	0	0	0	0	0	0	0	0	0	0
Quinqueloculina bosciana	0	0	0	1	0	0	0	0	0	0
Quinqueloculina laevigata	0	0	0	0	0	0	0	0	0	0
Quinqueloculina lamarckiana	0	0	0	0	0	0	0	0	0	0
Quinqueloculina poeyana	0	0	0	0	0	0	0	0	0	0
Quinqueloculina polygona	0	0	0	0	0	0	0	0	0	0
Quinqueloculina sabulosa	0	3	0	0	1	3	0	0	0	0
Quinqueloculina seminula	0	0	0	0	1	0	0	0	0	0
Reophax gaussicus	0	0	0	0	0	0	0	0	0	0
Rosalina floridana	0	0	0	0	0	0	0	0	0	0
Rosalina globularis	0	0	0	0	0	0	0	0	0	0
Sorites marginalis	0	0	0	0	0	0	0	0	0	0
Textularia candeiana	0	0	0	0	0	0	0	0	0	0
Textularia earlandi	0	0	0	0	0	0	0	0	0	0
Triloculina oblonga	11	9	0	0	2	0	0	0	0	0
Triloculina rotunda	0	0	0	0	0	0	0	0	0	0
Triloculina tricarinata	0	0	0	0	0	0	0	0	0	0
Metal Added (mg/L)	**0.09**	**0.09**	**0.9**	**0.9**	**9**	**9**	**90**	**90**	**900**	**900**
Actual Concentration (mg/L)	**0**	**0**	**0**	**0**	**2.929**	**0.9336**	**4.96**	**5.585**	**8.551**	**11.04**
Temperature (Celsius)	**22º**	**22º**	**22º**	**22º**	**22º**	**22º**	**22º**	**22º**	**22º**	**22º**
Salinity (PSU)	**40**	**40**	**40**	**40**	**40**	**40**	**40**	**40**	**40**	**40**
Ammonia tepida	0	0	0	0	0	0	0	0	0	0
Archais angulatus	0	0	0	0	0	0	0	0	0	0
Bolivina lowmani	10	9	6	1	4	2	0	0	0	0
Bolivina pulchella	0	0	0	0	0	0	0	0	0	0
Bolivina striatula	0	0	0	0	0	0	0	0	0	0
Buliminella elegantissima	0	0	0	0	0	0	0	0	0	0
Cibicides spp.	0	0	0	0	0	0	0	0	0	0

Cornuspira planorbis	0	0	0	0	0	0	0	0	0	0
Discorbis mira	0	0	0	0	0	0	0	0	0	0
Elphidium discoidale	0	0	0	0	0	0	0	0	0	0
Elphidium mexicanum	0	0	5	1	1	0	0	0	0	0
Hauerina bradyi	0	0	0	0	0	0	0	0	0	0
Miliolinella circularis	0	0	0	0	2	1	0	0	0	0
Miliolinella subrotunda	0	0	0	0	0	0	0	0	0	0
Nonionoides grateloupi	0	0	0	0	0	0	0	0	0	0
Ovammina opaca	31	25	0	10	0	0	0	0	0	3
Peneroplis pertusus	0	0	0	0	0	0	0	0	0	0
Quinqueloculina agglutinans	0	0	0	0	0	0	0	0	0	0
Quinqueloculina bosciana	0	0	4	2	3	2	0	0	0	0
Quinqueloculina laevigata	0	0	0	0	0	0	0	0	0	0
Quinqueloculina lamarckiana	0	0	0	0	0	0	0	0	0	0
Quinqueloculina poeyana	0	0	0	0	0	0	0	0	0	0
Quinqueloculina polygona	0	0	0	0	0	0	0	0	0	0
Quinqueloculina sabulosa	35	35	22	32	10	12	0	0	0	0
Quinqueloculina seminula	0	0	0	0	0	0	0	0	0	0
Reophax gaussicus	13	19	14	11	3	7	0	0	0	0
Rosalina floridana	0	0	0	0	0	0	0	0	0	0
Rosalina globularis	0	0	0	0	0	0	0	0	0	0
Sorites marginalis	0	0	0	0	0	0	0	0	0	0
Textularia candeiana	16	9	19	19	6	6	0	0	0	0
Textularia earlandi	0	0	0	0	0	0	0	0	0	0
Triloculina oblonga	36	38	28	25	13	23	0	0	0	4
Triloculina rotunda	0	0	0	0	0	0	0	0	0	0
Triloculina tricarinata	0	0	0	0	0	0	0	0	0	0
Metal Added (mg/L)	**0.09**	**0.09**	**0.9**	**0.9**	**9**	**9**	**90**	**90**	**900**	**900**
Actual Concentration (mg/L)	**0**	**0**	**0**	**0**	**1.271**	**1.174**	**8.415**	**8.385**	**13.44**	**11.82**

Temperature (Celsius)	**18º**	**18º**	**18º**	**18º**	**18º**	**18º**	**18º**	**18º**	**18º**	**18º**
Salinity (PSU)	**32**	**32**	**32**	**32**	**32**	**32**	**32**	**32**	**32**	**32**
Ammonia tepida	0	0	0	0	0	0	0	0	0	0
Archais angulatus	0	0	0	0	0	0	0	0	0	0
Bolivina lowmani	11	8	2	3	0	0	0	0	0	0
Bolivina pulchella	0	2	0	0	0	0	0	0	0	0
Bolivina striatula	0	0	0	0	0	0	0	0	0	0
Buliminella elegantissima	0	0	2	0	0	0	0	0	0	0
Cibicides spp.	0	0	0	0	0	0	0	0	0	0
Cornuspira planorbis	0	0	0	0	0	0	0	0	0	0
Discorbis mira	0	0	0	0	0	0	0	0	0	0
Elphidium discoidale	0	0	0	0	0	0	0	0	0	0
Elphidium mexicanum	0	0	0	0	0	0	0	0	0	0
Hauerina bradyi	0	0	0	0	0	0	0	0	0	0
Miliolinella circularis	0	0	1	2	1	0	0	0	0	0
Miliolinella subrotunda	0	0	0	0	0	0	0	0	0	0
Nonionoides grateloupi	0	0	0	0	0	0	0	0	0	0
Ovammina opaca	3	6	3	5	0	0	2	5	4	1
Peneroplis pertusus	0	0	0	0	0	0	0	0	0	0
Quinqueloculina agglutinans	0	0	0	0	0	0	0	0	0	0
Quinqueloculina bosciana	0	0	0	0	0	0	0	1	0	0
Quinqueloculina laevigata	0	0	0	0	0	0	0	0	0	0
Quinqueloculina lamarckiana	1	0	1	0	0	0	0	0	0	0
Quinqueloculina poeyana	0	0	0	0	0	0	0	0	0	0
Quinqueloculina polygona	0	0	0	0	0	0	0	0	0	0
Quinqueloculina sabulosa	13	13	1	2	0	0	0	0	0	0
Quinqueloculina seminula	2	5	0	0	0	0	2	0	0	0
Reophax gaussicus	6	12	1	2	0	0	0	0	0	0
Rosalina floridana	0	0	0	0	0	0	0	0	0	0
Rosalina globularis	0	0	0	0	0	0	0	0	0	0
Sorites marginalis	0	0	1	0	0	0	0	0	0	0

Textularia candeiana	8	11	4	6	0	0	0	0	0	0
Textularia earlandi	0	0	0	0	0	0	0	0	0	0
Triloculina oblonga	0	0	0	0	0	0	0	0	0	0
Triloculina rotunda	0	0	0	0	0	0	0	0	0	0
Triloculina tricarinata	0	0	0	0	0	0	0	0	0	0
Metal Added (mg/L)	**0.09**	**0.09**	**0.9**	**0.9**	**9**	**9**	**90**	**90**	**900**	**900**
Actual Concentration (mg/L)	**0**	**0**	**0**	**0**	**1.091**	**0.7233**	**2.263**	**3.109**	**4.793**	**3.832**
Temperature (Celsius)	**30º**	**30º**	**30º**	**30º**	**30º**	**30º**	**30º**	**30º**	**30º**	**30º**
Salinity (PSU)	**32**	**32**	**32**	**32**	**32**	**32**	**32**	**32**	**32**	**32**
Ammonia tepida	55	49	1	2	0	1	0	0	0	0
Archais angulatus	0	0	0	0	0	0	0	0	0	0
Bolivina lowmani	16	22	11	12	0	0	0	0	0	0
Bolivina pulchella	0	0	0	0	0	0	0	0	0	0
Bolivina striatula	0	0	0	0	0	0	0	0	0	0
Buliminella elegantissima	0	0	0	0	0	0	0	0	0	0
Cibicides spp.	0	0	0	0	0	0	0	0	0	0
Cornuspira planorbis	0	0	0	0	0	0	0	0	0	0
Discorbis mira	0	0	0	0	0	0	0	0	0	0
Elphidium discoidale	0	0	0	0	0	0	0	0	0	0
Elphidium mexicanum	0	0	0	5	2	1	0	0	0	0
Hauerina bradyi	0	0	0	0	0	0	0	0	0	0
Miliolinella circularis	0	0	0	0	2	0	0	0	0	0
Miliolinella subrotunda	0	0	0	0	0	0	0	0	0	0
Nonionoides grateloupi	0	0	0	0	0	0	0	0	0	0
Ovammina opaca	0	0	5	12	0	1	0	0	1	3
Peneroplis pertusus	0	0	0	0	0	0	0	0	0	0
Quinqueloculina agglutinans	0	0	0	0	0	0	0	0	0	0
Quinqueloculina bosciana	8	9	1	0	1	2	0	0	0	0
Quinqueloculina laevigata	0	0	0	0	0	0	0	0	0	0
Quinqueloculina lamarckiana	0	0	0	0	0	0	0	0	0	0

Quinqueloculina poeyana	0	0	0	0	0	0	0	0	0	0
Quinqueloculina polygona	0	0	0	0	0	0	0	0	0	0
Quinqueloculina sabulosa	52	60	5	6	1	1	0	0	0	0
Quinqueloculina seminula	0	0	0	0	0	0	0	0	0	0
Reophax gaussicus	12	8	5	0	0	0	0	0	0	0
Rosalina floridana	0	0	0	0	0	0	0	0	0	0
Rosalina globularis	0	0	0	0	0	0	0	0	0	0
Sorites marginalis	0	0	0	0	2	1	0	0	0	0
Textularia candeiana	7	5	0	0	0	0	0	0	0	0
Textularia earlandi	0	0	0	0	0	0	0	0	0	0
Triloculina oblonga	18	24	2	19	2	8	1	2	1	2
Triloculina rotunda	0	0	0	0	0	0	0	0	0	0
Triloculina tricarinata	0	0	0	0	0	0	0	0	0	0
Control										
Metal Added (mg/L)	**N/A**	**N/A**	**N/A**	**N/A**	**N/A**	**N/A**	**N/A**	**N/A**	**N/A**	**N/A**
Actual Nickel (mg/L)	**0.04063**	**0.04243**	**0.02547**	**0.02047**	**0.02021**	**0.02032**	**0.01701**	**0.01521**	**0.01628**	**0.01445**
Actual Zinc (mg/L)	**0.00369**	**0.00316**	**0.00349**	**0.00668**	**0.00124**	**0.00628**	**0.00206**	**0.00618**	**0.07291**	**0.00472**
Temperature (Celsius)	**22º**	**22º**	**22º**	**22º**	**22º**	**22º**	**18º**	**18º**	**30º**	**30º**
Salinity (PSU)	**32**	**32**	**12**	**12**	**40**	**40**	**32**	**32**	**32**	**32**
Ammonia tepida	4	0	0	1	0	0	0	2	0	0
Archais angulatus	0	0	0	0	0	0	0	0	0	0
Bolivina lowmani	16	11	0	1	13	0	8	11	18	13
Bolivina pulchella	0	0	0	0	0	0	0	0	0	0
Bolivina striatula	0	0	0	0	0	0	0	0	0	0
Buliminella elegantissima	0	0	0	0	0	0	0	0	0	0
Cibicides spp.	0	0	0	0	0	0	0	0	0	0
Cornuspira planorbis	0	0	0	0	0	0	0	0	0	0
Discorbis mira	0	0	0	0	0	0	0	0	0	0
Elphidium discoidale	0	0	0	0	0	0	0	0	0	0
Elphidium mexicanum	0	3	0	1	6	9	0	4	22	21
Hauerina bradyi	0	0	0	0	0	0	0	0	0	0
Miliolinella circularis	0	3	2	4	0	4	0	0	0	0

Miliolinella subrotunda	0	0	0	0	0	0	0	0	0	0
Nonionoides grateloupi	0	0	0	0	0	0	0	0	0	0
Ovammina opaca	29	14	41	29	39	39	61	48	12	5
Peneroplis pertusus	0	0	0	0	0	0	0	0	0	0
Quinqueloculina agglutinans	0	0	0	0	0	0	0	0	0	0
Quinqueloculina bosciana	2	3	0	0	0	0	3	1	15	0
Quinqueloculina laevigata	0	0	0	0	0	0	0	0	0	0
Quinqueloculina lamarckiana	0	0	0	0	0	0	0	0	0	0
Quinqueloculina poeyana	0	0	0	0	0	0	0	0	0	0
Quinqueloculina polygona	0	0	0	0	0	0	0	0	0	0
Quinqueloculina sabulosa	16	21	8	14	27	17	25	17	34	27
Quinqueloculina seminula	0	5	0	0	27	4	3	0	1	5
Reophax gaussicus	11	0	0	0	0	33	10	5	16	14
Rosalina floridana	0	0	0	0	0	0	0	0	0	0
Rosalina globularis	0	0	0	0	0	0	0	0	0	0
Sorites marginalis	0	0	0	0	0	0	0	0	0	0
Textularia candeiana	0	6	0	0	0	0	6	15	32	28
Textularia earlandi	0	0	0	0	0	0	0	3	0	0
Triloculina oblonga	10	18	10	7	42	33	6	16	47	32
Triloculina rotunda	0	0	0	0	0	0	0	0	0	0
Triloculina tricarinata	0	0	0	0	0	0	0	0	0	0